LRFD Metal Loss and Service-Life Strength Reduction Factors for Metal-Reinforced Systems

DETAILS

105 pages | | PAPERBACK

ISBN 978-0-309-15549-6 | DOI 10.17226/14497

AUTHORS

Kenneth L Fishman; James L Withiam; Transportation Research Board

NATIONAL COOPERATIVE HIGHWAY RESEARCH PROGRAM

NCHRP REPORT 675

LRFD Metal Loss and Service-Life Strength Reduction Factors for Metal-Reinforced Systems

Kenneth L. Fishman
McMahon & Mann Consulting Engineers, P.C.
Buffalo, NY

James L. Withiam
D'Appolonia Engineers
Monroeville, PA

Subscriber Categories
Highways • Bridges and Other Structures • Geotechnology

Research sponsored by the American Association of State Highway and Transportation Officials
in cooperation with the Federal Highway Administration

TRANSPORTATION RESEARCH BOARD

WASHINGTON, D.C.
2011
www.TRB.org

NATIONAL COOPERATIVE HIGHWAY RESEARCH PROGRAM

Systematic, well-designed research provides the most effective approach to the solution of many problems facing highway administrators and engineers. Often, highway problems are of local interest and can best be studied by highway departments individually or in cooperation with their state universities and others. However, the accelerating growth of highway transportation develops increasingly complex problems of wide interest to highway authorities. These problems are best studied through a coordinated program of cooperative research.

In recognition of these needs, the highway administrators of the American Association of State Highway and Transportation Officials initiated in 1962 an objective national highway research program employing modern scientific techniques. This program is supported on a continuing basis by funds from participating member states of the Association and it receives the full cooperation and support of the Federal Highway Administration, United States Department of Transportation.

The Transportation Research Board of the National Academies was requested by the Association to administer the research program because of the Board's recognized objectivity and understanding of modern research practices. The Board is uniquely suited for this purpose as it maintains an extensive committee structure from which authorities on any highway transportation subject may be drawn; it possesses avenues of communications and cooperation with federal, state and local governmental agencies, universities, and industry; its relationship to the National Research Council is an insurance of objectivity; it maintains a full-time research correlation staff of specialists in highway transportation matters to bring the findings of research directly to those who are in a position to use them.

The program is developed on the basis of research needs identified by chief administrators of the highway and transportation departments and by committees of AASHTO. Each year, specific areas of research needs to be included in the program are proposed to the National Research Council and the Board by the American Association of State Highway and Transportation Officials. Research projects to fulfill these needs are defined by the Board, and qualified research agencies are selected from those that have submitted proposals. Administration and surveillance of research contracts are the responsibilities of the National Research Council and the Transportation Research Board.

The needs for highway research are many, and the National Cooperative Highway Research Program can make significant contributions to the solution of highway transportation problems of mutual concern to many responsible groups. The program, however, is intended to complement rather than to substitute for or duplicate other highway research programs.

NCHRP REPORT 675

Project 24-28
ISSN 0077-5614
ISBN 978-0-309-15549-6
Library of Congress Control Number 2011923669

COPYRIGHT INFORMATION

NOTICE

The project that is the subject of this report was a part of the National Cooperative Highway Research Program, conducted by the Transportation Research Board with the approval of the Governing Board of the National Research Council.

The members of the technical panel selected to monitor this project and to review this report were chosen for their special competencies and with regard for appropriate balance. The report was reviewed by the technical panel and accepted for publication according to procedures established and overseen by the Transportation Research Board and approved by the Governing Board of the National Research Council.

The opinions and conclusions expressed or implied in this report are those of the researchers who performed the research and are not necessarily those of the Transportation Research Board, the National Research Council, or the program sponsors.

The Transportation Research Board of the National Academies, the National Research Council, and the sponsors of the National Cooperative Highway Research Program do not endorse products or manufacturers. Trade or manufacturers' names appear herein solely because they are considered essential to the object of the report.

Published reports of the

NATIONAL COOPERATIVE HIGHWAY RESEARCH PROGRAM

are available from:

Transportation Research Board
Business Office
500 Fifth Street, NW
Washington, DC 20001

and can be ordered through the Internet at:

http://www.national-academies.org/trb/bookstore

Printed in the United States of America

THE NATIONAL ACADEMIES

Advisers to the Nation on Science, Engineering, and Medicine

The **National Academy of Sciences** is a private, nonprofit, self-perpetuating society of distinguished scholars engaged in scientific and engineering research, dedicated to the furtherance of science and technology and to their use for the general welfare. On the authority of the charter granted to it by the Congress in 1863, the Academy has a mandate that requires it to advise the federal government on scientific and technical matters. Dr. Ralph J. Cicerone is president of the National Academy of Sciences.

The **National Academy of Engineering** was established in 1964, under the charter of the National Academy of Sciences, as a parallel organization of outstanding engineers. It is autonomous in its administration and in the selection of its members, sharing with the National Academy of Sciences the responsibility for advising the federal government. The National Academy of Engineering also sponsors engineering programs aimed at meeting national needs, encourages education and research, and recognizes the superior achievements of engineers. Dr. Charles M. Vest is president of the National Academy of Engineering.

The **Institute of Medicine** was established in 1970 by the National Academy of Sciences to secure the services of eminent members of appropriate professions in the examination of policy matters pertaining to the health of the public. The Institute acts under the responsibility given to the National Academy of Sciences by its congressional charter to be an adviser to the federal government and, on its own initiative, to identify issues of medical care, research, and education. Dr. Harvey V. Fineberg is president of the Institute of Medicine.

The **National Research Council** was organized by the National Academy of Sciences in 1916 to associate the broad community of science and technology with the Academy's purposes of furthering knowledge and advising the federal government. Functioning in accordance with general policies determined by the Academy, the Council has become the principal operating agency of both the National Academy of Sciences and the National Academy of Engineering in providing services to the government, the public, and the scientific and engineering communities. The Council is administered jointly by both Academies and the Institute of Medicine. Dr. Ralph J. Cicerone and Dr. Charles M. Vest are chair and vice chair, respectively, of the National Research Council.

The **Transportation Research Board** is one of six major divisions of the National Research Council. The mission of the Transportation Research Board is to provide leadership in transportation innovation and progress through research and information exchange, conducted within a setting that is objective, interdisciplinary, and multimodal. The Board's varied activities annually engage about 7,000 engineers, scientists, and other transportation researchers and practitioners from the public and private sectors and academia, all of whom contribute their expertise in the public interest. The program is supported by state transportation departments, federal agencies including the component administrations of the U.S. Department of Transportation, and other organizations and individuals interested in the development of transportation. **www.TRB.org**

www.national-academies.org

COOPERATIVE RESEARCH PROGRAMS

CRP STAFF FOR NCHRP REPORT 675

Christopher W. Jenks, *Director, Cooperative Research Programs*
Crawford F. Jencks, *Deputy Director, Cooperative Research Programs*
Edward T. Harrigan, *Senior Program Officer*
Melanie Adcock, *Senior Program Assistant*
Eileen P. Delaney, *Director of Publications*
Scott E. Hitchcock, *Editor*

NCHRP PROJECT 24-28 PANEL
Field of Soils and Geology—Area of Mechanics and Foundations

Norman D. Dennis, Jr., *University of Arkansas - Fayetteville, Fayetteville, AR* (Chair)
Richard M. Lane, *Pembroke, NH*
Robert A. Gladstone, *Association for Metallically Stabilized Earth, McLean, VA*
Mohammed A. Mulla, *North Carolina DOT, Raleigh, NC*
Robert A. Reis, *California DOT, Sacramento, CA*
Louis D. Taylor, *Michigan DOT, Lansing, MI*
John J. Wheeler, Jr., *New York State DOT, Albany, NY*
Masha B. Wilson, *Nevada Department of Public Safety, Carson City, NV*
Thomas F. Zimmie, *Rensselaer Polytechnic Institute, Troy, NY*
Michael Adams, *FHWA Liaison*
G. P. Jayaprakash, *TRB Liaison*

FOREWORD

By Edward T. Harrigan
Staff Officer
Transportation Research Board

NCHRP Report 675 presents the findings of research conducted to develop metal loss models for metal-reinforced systems that are compatible with the *AASHTO LRFD (Load and Resistance Factor Design) Bridge Design Specifications.* The report will be of immediate interest to engineers in state highway agencies and industry with responsibility for the construction and maintenance of bridges and structures, with particular emphasis on mechanically stabilized earth (MSE) walls.

Transportation agencies use a variety of metal-reinforced systems in geotechnical applications, including soil and rock reinforcements, ground anchors, and tiebacks. These systems support retaining walls and soil and rock slopes, and they stabilize roadway cuts and fills. The precise conditions governing the deterioration of these systems are uncertain, but corrosion is known to have an impact on their service life. Engineers, faced with the task of allocating budgets to rehabilitate aging facilities, need reliable techniques for assessing corrosion and estimating metal loss. Service-life estimates for new systems need to be improved, and consideration of metal loss in their design needs to be consistent with the reliability-based approach adopted in the *AASHTO LRFD Bridge Design Specifications*.

The objectives of this research were to (1) assess and improve the predictive capabilities of existing computational models for corrosion potential, metal loss, and service life of metal-reinforced systems used in retaining structures, highway cuts and fills, and other applications; (2) develop methodology that incorporates the improved predictive models into an LRFD approach for the design of metal-reinforced systems; and (3) recommend additions and revisions to the AASHTO LRFD specifications that incorporate the improved models and methodology. The project was carried out by McMahon & Mann Consulting Engineers, P.C., Buffalo, New York, assisted by subcontractor D'Appolonia Engineers, Monroeville, Pennsylvania.

The report fully documents the research leading to the following key products: (1) metal loss models for estimating sacrificial steel requirements for Type I metal-reinforced systems [mechanically stabilized earth (MSE) reinforcements], for which the AASHTO LRFD specifications include metal loss as a specific part of the design; (2) recommended sampling and testing protocols needed for condition assessment and corrosion monitoring of MSE reinforcements to develop input data for the metal loss models; and (3) an example problem demonstrating analysis and design of an MSE wall using LRFD and the corresponding metal loss models and resistance factors. The report also presents service-life estimates and example calibrations for a Type II metal-reinforced system (specifically, a rock bolt), for which metal loss is not incorporated in the LRFD design calculations.

Three of seven appendices from the contractor's final report not contained in *NCHRP Report 675* may be downloaded from the NCHRP Project 24-28 webpage at http://apps.trb.org/cmsfeed/TRBNetProjectDisplay.asp?ProjectID=727.

AUTHOR ACKNOWLEDGMENTS

The authors gratefully acknowledge assistance and cooperation from various state DOTs and other government agencies, universities, private consultants, and contractors, particularly with respect to data collection activities that comprised such an important part of this project. Caltrans Corrosion Technology Branch, Materials Engineering and Testing Services Unit provided access to sites in California and shared expertise with respect to corrosion monitoring including Messrs. Rob Reis, Doug Parks, Dave Castanon, Rudy Lopez, Joe Shanabrook, Charlie Sparkman, and Rich Sullivan. Ms. Kathryn Griswell, Caltrans Retaining Wall Specialist also assisted, and personnel from Caltrans Districts 1, 4, 7 and 8 assisted with site access and maintaining traffic control. NCDOT personnel including Messrs. Mohammed Mulla, Cecil Jones, Chris Peoples, Kelly Croft, and Dan Smith provided access, information, and assistance as necessary to collect data from sites in North Carolina. Messrs. Robert Burnett, JJ Wheeler Jr., and Joseph DiGregorio from NYSDOT provided access, information, and assistance as necessary to collect data from sites in New York. Messrs. Dennis S. Brown, Thomas Prestach, Kevin Nagy, Glenn Keiper (now with American Geotechnical & Environmental Services, Inc.) provided access, information, and assistance as necessary to collect data on ground anchors at the site along I-99 in Altoona, PA. Mr. Dave Weatherby from Schnabel Foundations, Inc., provided installation details from this site. Messrs. Craig Compton, Dennis R. Dolinar, and Paul K. Stefko facilitated access at the NIOSH SRCM. Mr. Richard Lane, Mr. Dave Merrill, and Ms. Krystle Pelham provided access, information and assistance as necessary to collect data from the site of the Barron Mountain Rock Cut in Woodstock, NH. Prof. Alberto Sagues from the University of South Florida, and Jean Marc Jailloux from Profactal Engineering and Consulting provided data from their corrosion monitoring activities in Florida and France, respectively. The FHWA provided use of their PR monitors for corrosion monitoring at selected sites. Use of the FHWA equipment is greatly appreciated and is also available from the FHWA to state DOTs on an as needed basis.

Project consultants included Prof. Gregory Baecher from the University of Maryland, Mr. Peter Anderson, Reinforced Earth Company (RECO), Dr. Barry Christopher (Consultant), and Mr. Louis Pinto (Consultant). Dr. James L. Withiam, P.E., from D'Appolonia was co-Principal Investigator for the project and other personnel from D'Appolonia including Mr. Vince Gusbar and Dr. Yasser Hegazy contributed to the project. Personnel from McMahon and Mann Consulting Engineers, P.C., including Ms. Suzanne George, and Messrs. Andrew Klettke, James Janora, Richard J. Bojarski, Vince LoVullo, and Andrew McMahon contributed to data collection activities, data analysis, and reliability studies.

CONTENTS

Note: Many of the photographs, figures, and tables in this report have been converted from color to grayscale for printing. The electronic version of the report (posted on the Web at www.trb.org) retains the color versions.

CHAPTER 1

Background

Transportation agencies use a variety of metal-reinforced systems in geotechnical applications, including soil and rock reinforcements, ground anchors, and tiebacks. These systems support retaining walls, bridge abutments, approaches, and highway embankments, and they also stabilize roadway cuts and fills. Corrosion is known to have an impact on service life, and engineers, faced with the task of allocating budgets to rehabilitate aging facilities, need reliable techniques to estimate that remaining service life. Service life estimates for new systems need to be evaluated, and consideration of metal loss in the design needs to be consistent with the reliability-based approach adopted in the *AASHTO Load and Resistance Factor Design (LRFD) Bridge Design Specifications*. NCHRP Project 24-28 addresses these needs by developing a database to document the performance of earth reinforcement systems, and by performing the statistical and reliability analyses necessary to consider service life within the context of reliability-based design.

The objectives of NCHRP Project 24-28 are to (1) assess and improve the predictive capabilities of existing computational models for corrosion potential, metal loss, and service life of metal-reinforced systems used in geotechnical engineering applications; (2) develop methodology that incorporates the improved predictive models into an LRFD approach for the design of metal-reinforced systems; and (3) recommend additions and revisions to the AASHTO LRFD specifications to incorporate the improved models and methodology. Current design specifications (AASHTO, 2009) incorporate metal loss models, but these models have limited application with respect to reinforcement type and fill conditions. Results from this study serve to broaden the recommendations for metal loss modeling, and describe effects of fill quality and reinforcement type on performance and service life.

Earth Reinforcements

For the purpose of this study, metal-reinforced systems are broadly categorized into two types. Type I reinforcements are passive elements used in the construction of metallically reinforced earth structures [i.e., mechanically stabilized earth (MSE)] that may consist of steel strips, welded wire fabric, wire mesh, or soil nails. Type I elements are not prestressed, and load is transferred to the elements as the structure deforms during construction, and throughout its service life. Type II reinforcements are active elements that are prestressed during installation and include ground anchors (strands and bars) and rock bolts. Due to the application of prestress, the loads in active systems are controlled and involve more certainty compared to passive systems. In general, Type II reinforcements consist of relatively high-strength steel and a higher level of corrosion protection compared to Type I reinforcements. A significant difference between element types is that Type I elements are often designed by including sacrificial steel to account for metal loss due to corrosion, whereas Type II elements do not include sacrificial material and the durability of the corrosion protection system controls the design life.

Details of Type I Reinforcements

Most steel reinforcements for MSE structures are hot-rolled steel strips, welded wire grids, or bar-mat grids manufactured from cold-drawn wire as depicted in Figure 1. Standard sizes of reinforcements, steel grades, and details of galvanization have evolved, and current practices differ from those employed prior to approximately 1978. Type I reinforcements are manufactured from mild steel and, currently, steel strips are manufactured from ASTM A-572, Grade 65 steel. Prior to 1978 steel strips were manufactured from Grade 36 steel, described by ASTM A-446. Grids are manufactured from Grade 80 cold-drawn wire in accordance with ASTM A-82, and deformed welded wire is sometimes used, as described by ASTM A-496. Bar mats are often configured with between two and five longitudinal wires, whereas welded wire mesh may have 10 or more longitudinal wires per unit.

Most often the reinforcements include hot-dip galvanizing for corrosion protection that is applied in accordance with ASTM A-123 for wire- or strip-type reinforcements. Minimum

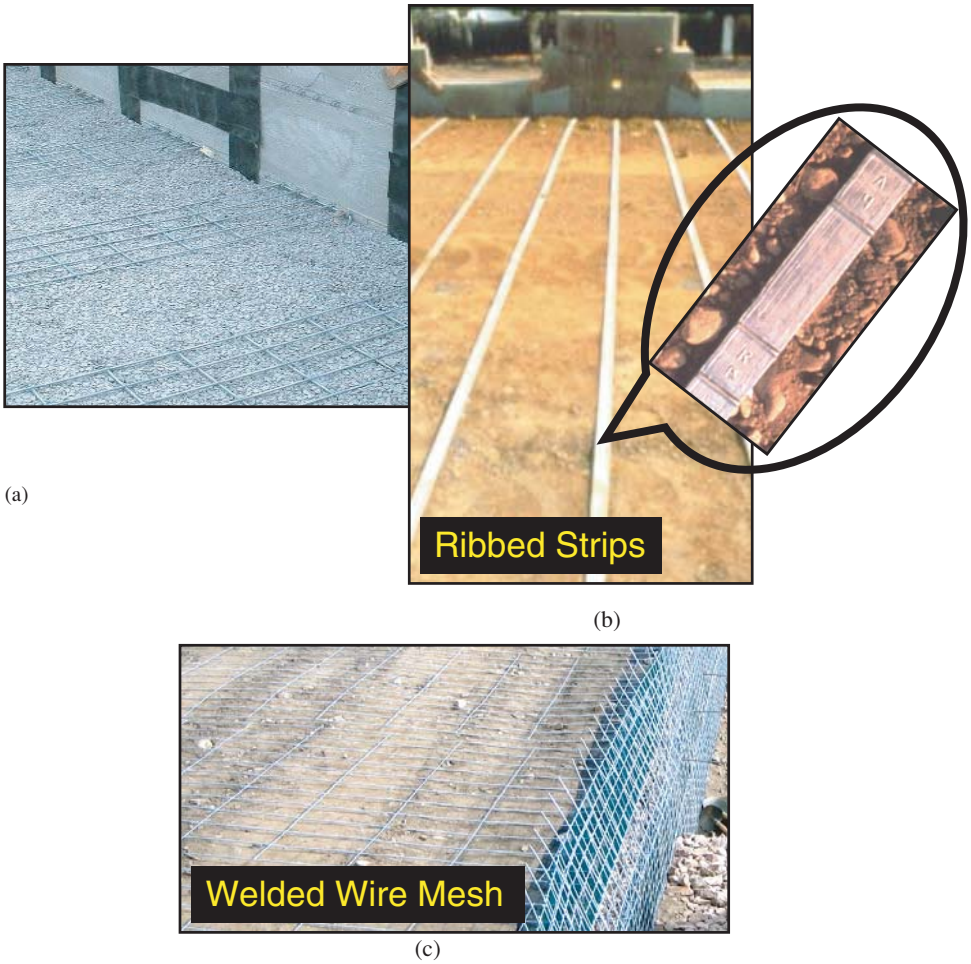

Figure 1. Examples of metallic reinforcements used in MSE construction: (a) bar-mat grid reinforcements, (b) hot-rolled steel strip reinforcements, and (c) welded-wire grid reinforcements.

requirements for thickness of zinc coating depend on the thickness and size of the reinforcements. AASHTO specifications require a minimum of 86 μm per side for MSE reinforcements, as described in ASTM A-123. However, for reinforcements installed prior to 1978 and galvanized in accordance with ASTM A-525 or A-641, the specified initial thickness of zinc coating was less than the current specifications of 86 μm and ranged between 17 μm and 30 μm.

The hot-dip process provides good coverage of zinc along the surface, but the distribution of thickness is difficult to control. Thus, the mean thickness of the zinc coating necessarily exceeds the AASHTO minimum requirements of 86 μm. This ensures a low probable occurrence of a spot with less than the minimum requirement. From the standpoint of reliability analyses it is important to recognize that zinc thickness is a variable. Sagues et al. (1998) and Rossi (1996) report measurements of zinc coating thickness from frequent intervals along the lengths of a limited number of strip-type reinforcement samples. These data reflect a mean zinc coating thickness of approximately 150 μm. However, these data are very limited and more data describing the variation of the thickness of zinc coating are needed to obtain a reasonable distribution of measurements.

Soil nails are steel bars with diameters ranging between 1 and 1.5 inches that are inserted into a 4-inch to 12-inch diameter drill hole and surrounded by grout. Often Grade 60 deformed, reinforcing steel bars are employed for soil nails but high strength prestressing steel bars (e.g., Grade 150) are sometimes used. Soil nails may be galvanized or epoxy coated and sometimes are encapsulated similar to the corrosion protection systems described for Type II reinforcements in the next section. However, there are several new developments in soil nails that may not be fully encapsulated, if at all, including self-drilling and self-grouted nails, screwed-in nails, and dynamically inserted nails (i.e., inserted using a nail gun or sonic method).

Details of Type II Reinforcements

Type II reinforcements include ground anchors and rock bolts. Key features of these systems, summarized in Table 1, are described in this section. More complete details of these reinforcements, including descriptions of components, materials, installation details, and performance issues can be found in USACOE (1980), International Federation for Prestressing (FIP) (1986), *NCHRP Web Document 27* (D'Appolonia et al., 2001), Kendorski (2003), and Sabatini et al. (1999).

Tensioned elements of the system include bar and strand components. The steel grade and level of prestress employed in these systems are relevant to the type of corrosion problems that may occur, and prediction of service life. Bar elements are available in a variety of steel grades ranging from Grade 60 to 160. Strand elements are manufactured from Grade 250 and 270 high-strength steel and generally consist of seven wire strands with six wires wrapped around a seventh wire called the "king wire." Wire tension systems using the button head anchorage of BBRV (Birkinmaier, Brandistini, Ros, and Vogt) and Prescon have also been used, but are not as popular as strands. These systems use a set of parallel wires, rather than strands, as reinforcing elements.

Ground anchors include an anchored or "bonded" zone and a free length or "unbonded" zone. The bonded zone is anchored to the soil or rock with cement grout. Current guidance documents [Post Tensioning Institute (PTI), 2004; Sabatini et al., 1999] recommend incorporating corrosion protection measures into the design of ground anchors. Corrosion protection measures include the use of coatings, protective sheaths, grouting, encapsulation, and electrical isolation. Use of portland cement-based grout provides limited corrosion protection as a barrier, and by fostering a passive film layer due to its high alkalinity.

Recent installations employ Class I or Class II corrosion protection systems as recommended by PTI (2004). For Class I protection the anchor is encapsulated (often referred to as double corrosion protection) and, for Class II, the anchor is protected by grout (often referred to as single corrosion protection). The free lengths of the anchors are protected by grease and plastic sheaths, and a trumpet head assembly surrounds the reinforcements behind the bearing plate. Double corrosion protection is recommended for ground anchors in aggressive ground conditions and permanent installations. Products on the market today offer systems that comply with the current standards. However, many of the older installations do not incorporate details that meet today's standards, or may have been installed without any corrosion protection beyond the passivation of the grouted portion of the tensioned elements.

Rock bolts are installed with either mechanical anchorages (e.g., expansion shell, split wedge), or are grouted into rock using portland cement or resin grout. The anchorage may either be concentrated near the end point of a mechanical device or by the short length of grout near the end of the bolt; or the bolt may be fully grouted with the pullout resistance distributed along the length of the bonded zone.

Older style rock bolts with mechanical anchorages may have no corrosion protection. Portland cement or resin grouted rock bolts are surrounded by grout, but the bolts heads are often not encapsulated. There is also the possibility of voids along the grouted length. Rock bolt installations may also be similar to ground anchors with a free length and a bonded zone, but trumpet head assemblies are not always installed, leaving the area behind the head of the rock bolt exposed.

Durability and Performance Issues for Earth Reinforcements

Durability of earth reinforcements is controlled by backfill characteristics, site conditions, climate, steel type (galvanized or not), and details of project construction and in-service operations. Weatherby (1982), FIP (1986), Briaud et al. (1998), D'Appolonia et al. (2001), Withiam et al. (2002), and Elias et al. (2009) describe factors that contribute to corrosion potential of earth reinforcements and measurement of the relevant electrochemical parameters for soils and groundwater. In general, "minimum" resistivity (ρ_{min}), pH, chemical composition including the presence of organics, porosity, and groundwater level are the factors that most affect the corrosiveness of the underground environment. Generally, ground conditions

Table 1. Summary of Type II reinforcements.

Type of Metal Tensioned Systems	Tendon Type	Anchorage Type	Corrosion Protection
Ground anchors	Strands or bars	Cement grout in bonded zone	More recent permanent installations use Class I or Class II Protection (PTI, 2004); older systems may have no protection other than grout cover.
Rock bolts	Usually bars, but could be strands	Mechanical, resin grout, or cement grout	Epoxy coating, galvanized, grout cover, older installations may have none

are considered aggressive if one or more of the following conditions are detected (PTI, 2004; Elias et al., 2009):

- pH < 4.5 for steel; or
- 4.5 > pH > 10 for galvanized elements;
- ρ_{min} < 2000 Ω-cm;
- presence of sulfides, sulfates, or chlorides; and
- presence of organics.

Metal loss and service life models are correlated with underground conditions, particularly with respect to electrochemical properties of soil and groundwater. The National Bureau of Standards (NBS) commissioned a study to observe metal loss from steel and galvanized specimens that were buried under a variety of soil conditions for more than 50 years. Based on the results from the NBS study, Romanoff (1957) proposed the following power law to predict rates of corrosion of buried metal elements:

$$x = kt^n \tag{1}$$

where
x is loss of thickness per side or loss of radius,
k and n are constants, and
t is time (years).

Equation (1) applies to uniform-type corrosion and may also consider localized- or pitting-types of corrosion, but does not consider more complex forms of corrosion, including hydrogen embrittlement or stress corrosion cracking (SCC) as described by Fontana (1986), FIP (1986), and Sabatini et al. (1999). Equation (1) reflects observations that the corrosion rate is generally higher during the first few years and attenuates with respect to time (i.e., n is < 1). This is due to the steel surface becoming "passivated" from stable corrosion by-products that adhere to the surface and formation of a passive film layer. Equation (1) serves as the basis for several models used to estimate service life and associated sacrificial steel requirements. These models differ in terms of the data sets (e.g., fill conditions) used to regress the model parameters, and the time frame over which metal loss is considered. Note that in Equation (1) "x" describes metal loss that may include zinc and steel for galvanized elements. However, other metal loss equations presented in this report use "X" to denote loss of steel subsequent to zinc deletion for galvanized elements. Metal loss models for Type I and Type II reinforcements are discussed separately with due consideration given to differences in site conditions, construction details, and metal type (e.g., use of galvanized reinforcements for Type 1 reinforcements).

Type I Reinforcements

Based on research conducted over the past several decades (e.g., King, 1978; Darbin et al., 1988; Elias, 1990) values for the constants k and n are identified depending on metal type (e.g., galvanized or plain steel) and for fill conditions representative of MSE construction. Linearized versions of Equation (1) have been adopted as a conservative approach to extrapolate observations of metal loss over limited time frames and for design recommendations (Rehm, 1980; Jackura et al., 1987; Elias, 1990; AASHTO, 2009).

Darbin et al. (1988) and Elias (1990) proposed equations, having the same form as Equation (1), to estimate steel loss for plain steel and galvanized elements, respectively. These models are developed using measurements of corrosion from elements buried in fill representative of MSE construction. The following models apply to galvanized and plain steel reinforcements, respectively:

For galvanized elements:

$$\text{if } t_f > \left(\frac{z_i}{25}\right)^{1.54} \text{ then } \quad X(\mu m) = 50\left(\frac{\mu m}{yr}\right) \times t_f^{0.65}(yr) - 2 \times z_i(\mu m)$$

$$\text{if } t_f \le \left(\frac{z_i}{25}\right)^{1.54} \text{ then } \quad X(\mu m) = 0 \tag{2}$$

For plain steel elements:

$$X(\mu m) = 80\frac{\mu m}{yr} \times t_f^{0.8} \tag{3}$$

where X is loss of steel (base metal) in units of μm, and t_f is service life in years. For Equation (2) loss of base steel occurs subsequent to depletion of the zinc coating, and z_i is the initial zinc thickness. Equation (2) is applicable to the range of fill conditions representative of MSE wall construction that exhibit ρ_{min} greater than 1000 Ω-cm. Data reviewed for Equation (3) are based on the NBS data set for plain steel and include a wider range of fill conditions.

The service life of earth reinforcements is related to the remaining tensile capacity and not necessarily the maximum pit depth. This is because pit penetrations have a limited impact on the overall remaining cross section. Rather than measuring and modeling pit depths, metal loss models and measurements of corrosion rates for earth reinforcements are averaged over the surface area of the reinforcement. Thus, metal loss is idealized as uniformly distributed over the surface. A factor of 2 is commonly applied to this uniform corrosion rate to consider the actual loss of tensile strength capacity (Elias, 1990; Jackura et al., 1987); in other words, the loss of tensile strength is twice that anticipated based on the average loss of section. Although the factor of 2 is often taken as a constant, Smith et al. (1996) describes how the local factor may vary with respect to reinforcement shape. Equations (2) and (3) include a factor of 2 to consider the maximum metal loss and associated loss of tensile strength.

Equation (2) considers that loss of zinc is uniform with $x = 25t^{0.65}$, but a factor of 2 is applied to the steel corrosion rate to consider the maximum metal loss after zinc is consumed as $X = 50t^{0.65}$.

Although corrosion rates for both galvanized and plain steel clearly vary exponentially with respect to time, a number of models (including the AASHTO model) approximate loss of steel using linear extrapolation for the purpose of design. These models assume that the rate of zinc consumption is higher in the first few years and then levels off to a steady but significantly lower rate. Once the galvanized zinc coating is depleted, it is assumed that the base carbon steel corrodes at the carbon steel rate. This is a conservative assumption that does not consider that the insoluble by-product of zinc corrosion continues to protect the underlying steel (Rehm, 1980). Calibration of LRFD resistance factors for galvanized reinforcements assumes that the steel cross section is not consumed before the zinc coating, which serves as the sacrificial anode protecting the base steel. Since the zinc layers do not contribute to the tensile strength of the reinforcements, strength loss is also delayed until the zinc is consumed, and loss of steel section is described according to Equation (4). In general the thickness of steel, *X,* consumed per side over the design life, t_f, may be computed as

$$X(\mu m) = (t_f(yrs.) - C(yrs.)) \times r_s \frac{\mu m}{yr} \quad (4)$$

where C is the time for zinc depletion $\left(C = t_1 + \frac{(z_i - r_{z1} \times t_1)}{r_{z2}} \right)$, which is computed based on the initial zinc thickness, z_i, the initial corrosion rate for zinc, r_{z1}, the subsequent zinc corrosion rate, r_{z2}, and the duration for which r_{z1} prevails (t_1–usually taken as 2 to 3 years). The corrosion rate of the base steel subsequent to zinc depletion is r_s.

Rehm (1980), Jackura et al. (1987) and Elias (1990) propose models for estimating metal loss of galvanized reinforcements in fill conditions applicable to MSE construction. Details of these other models are described in Appendix A and are referred to as the Stuttgart or Caltrans Interim models. These models consider fill conditions that are more severe relative to the potential for corrosion compared to the AASHTO requirements, and are sometimes, but not always, associated with correspondingly higher corrosion rates. Table 2 is a summary of the different fill conditions, model parameters and corresponding estimates of zinc life, and estimates of steel loss considering a 75-year service life.

Considering a service life of 75 years and an initial zinc thickness z_i, equal to 86 μm per side, the steel loss computed with the Darbin equation [Equation (2)] is 655 μm per side. For a 75-year design life, and z_i equal to 86 μm, the AASHTO, Stuttgart-high salt, and Caltrans Interim-select models yield estimates of steel loss close to that computed with the Darbin model. Differences between these models include the data sets that are used to regress model parameters (i.e., corrosion rates). This demonstrates that the current AASHTO model uses corrosion rates that are applicable to fill conditions that are more severe relative to those allowed by the specifications; in other words, the AASHTO model is conservative. For fill conditions that are considered marginal by AASHTO standards, due to higher salts contents (models below the double line in Table 2), considerably higher steel losses are estimated.

A complete comparison of steel losses computed with the models above the double line in Table 2 as a function of service life is presented in Figure 2. Comparisons with the Darbin model shown in Figure 2 imply that the factor of 2 described by Elias (1990) is implicit in the piecewise linear models from Stuttgart, AASHTO, and Caltrans.

Table 3 summarizes the AASHTO-recommended metal loss model for design of MSE structures (AASHTO, 2009) and

Table 2. Summary of piecewise linear metal loss models for galvanized reinforcements.

Model	Electrochemical Parameters Considered[1]				Metal Loss Parameters			Steel Loss/Side t_f = 75 yrs.	
	pH	ρ_{min} Ω-cm	Cl^- ppm	SO_4 ppm	r_{z1}[2] μm/yr	r_{z2} μm/yr	r_s μm/yr	C[3] yrs.	X[4] μm
Stuttgart-mildly corrosive	4.5 to 9	>1,000	<20	<50	6	2	9	39	324
Caltrans Interim-select[5]	>7	>1,000	<500	<2,000	NA	NA	13	20	715
AASHTO-mildly corrosive	**5 to 10**	**>3,000**	**<100**	**<200**	**15**	**4**	**12**	**16**	**708**
Stuttgart-high salt, saturated	4.5 to 9	>1,000	<50	<500	17[2]	2	12	20	654
Caltrans Interim-neutral	>7	>1,000	<500	<2,000	NA	NA	28	10	1820
Caltrans Interim-acidic	<7	>1,000	<500	<2,000	NA	NA	33	10	2145
Caltrans Interim-corrosive	>7	< 1,000	<500	<2,000	NA	NA	71	6	4899

[1]Electrochemical parameters considered for design by Caltrans have been updated since the Interim models were proposed in 1987. See Appendix A for details.
[2]Applies to the first 2 years except for the Stuttgart high salt model where r_{z1} applies to the first 3 years.
[3]C is the time to zinc deletion (i.e., initiation of steel loss) assuming z_i is 86 μm.
[4]X is the steel loss per side for a 75-year service life.
[5]Caltrans select fill is clean gravel with less than 25% passing the No. 4 sieve and less than 5% fines.

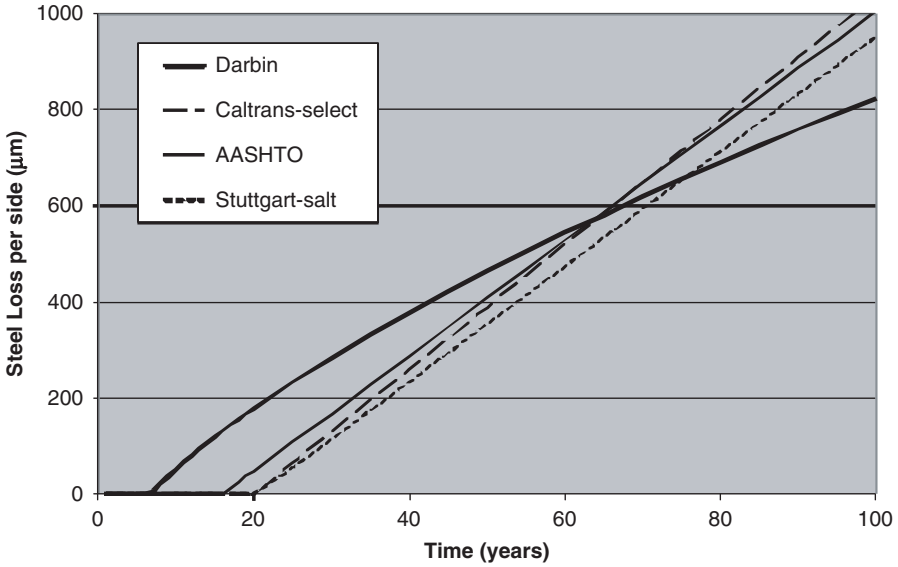

Figure 2. Comparison of metal loss models.

the corresponding fill material requirements. The fill requirements are intended to control corrosion potential with fills that are between noncorrosive and "mildly" corrosive.

Based on the information in Table 3, the steel loss per side (X) in μm/yr for a given service life, t_f, and initial thickness of zinc coating, z_i, is computed as

$$X(\mu\text{m}) = 12\frac{\mu\text{m}}{yr} \times \left(t_f - 2\,yr - \frac{(z_i - 30\,\mu\text{m})}{4\frac{\mu\text{m}}{yr}} \right) yr \qquad (5)$$

The AASHTO model does not give any guidance for corrosion rates or metal loss modeling of plain steel (i.e., not galvanized) reinforcements or for fills that do not meet the stringent electrochemical requirements. A significant effort was devoted in this project to documenting the performance of in-service reinforcements and to verifying the reliability of the AASHTO (and other) models used in MSE structure design.

The frequency and distribution of samples for assessment of electrochemical parameters need to be given careful consideration. The number of samples required increases when evaluating more aggressive or marginal backfill materials, and when more confidence is needed for design (Withiam et al., 2002; Hegazy et al., 2003). Existing data involving frequent sample intervals at sites with poor conditions depict a wide scatter in results (Whiting, 1986; Fishman et al., 2006). For moderate to large sized projects, with fill sources that are expected to be relatively nonaggressive relative to corrosion (i.e., mildly corrosive soils meeting AASHTO criteria), Table 4, taken from Elias et al. (2009), can be used to determine the number of samples that should be taken from each source and evaluated for electrochemical parameters. More samples should be retrieved if marginal quality reinforced fills are being contemplated for construction (not recommended), or when undertaking performance evaluations at sites with poor reinforced fill conditions. In addition to the mean values used for design [i.e., the mean of the minimum resistivity (ρ_{min}) values obtained from each test], the distribution and variability of the measurements is of significant interest from the standpoint of reliability-based design (LRFD).

Table 4 places restrictions on the allowable standard deviations (σ) of the resistivity and salt content (see comment 3) measurements. If these standard deviations are exceeded, then the sampling should be repeated. If the standard deviation, computed using the total numbers of samples, is still outside the limits of Table 4, then the backfill source should not be used for MSE wall fill. If resistivity less than 3,000 Ω-cm is obtained from any test, obtain additional samples in the vicinity of this sample location to identify if there are specific areas wherein the material is unsuitable.

Stockpiles should be sampled from the top, middle, and bottom portions and an excavator with a bucket should be

Table 3. AASHTO metal loss model and backfill requirements.

Metal Loss Model		Backfill Requirements	
Component type (age)	Loss (μm/yr)	pH	5 to 10
		Minimum resistivity	≥3,000 Ω-cm
Zinc (<2 yrs), r_{z1}	15	Chlorides	<100 ppm
Zinc (>2 yrs), r_{z2}	4	Sulfates	<200 ppm
Steel (after zinc), r_s	12	Organic content	<1%

Table 4. Recommended sampling protocol for electrochemical testing of MSE wall fill (Elias et al., 2009).

Range of ρ_{min} (Ω-cm)	General Description	Preconstruction		During Construction	Comments
		No. Samples	$\sigma_{resistivity}$ (Ω-cm)	Sample Interval (yd^3)	
>10,000	Crushed rock and gravel, <10% passing No. 10 sieve	1 / 3[1]	NA	NA	**1.** pH outside the specified limits is not allowed for any sample. **2.** Backfill sources shall be rejected if ρ_{min} measured for any sample is less than 700 Ω-cm, Cl^- > 500 ppm or SO_4 > 1,000 ppm. **3.** For materials with ρ_{min} < 5,000 Ω-cm, σ for Cl^- and SO_4 shall be less than 100 ppm and 200 ppm, respectively.
5,000 to 10,000	Sandy gravel and sands	3 / 6[1]	<2,000	4,000 / 2,000[1]	
<5,000	Silty sands and clayey sand, screenings	5 / 10[1]	<1,000	2,000 / 1,000[1]	

[1] Number of resistivity tests / number of tests for pH, Cl^-, and SO_4.

used to remove material from approximately 2 feet beyond the edge of the stockpile. Particular emphasis on sampling needs to be placed at sites where different reinforced fill sources and/or types are being considered, and each source should be sampled as described in Table 4.

Differences in the electrochemical properties of the soil fill can adversely affect corrosion rates and contribute to more severe and localized occurrences of metal loss. In instances where more easily compacted (e.g., open-graded) material is placed adjacent to the wall face, significant differences in the soil fill conditions may exist with respect to position along the reinforcements. For cases where reinforcements are not electrically isolated (e.g., metallic facing), variations of backfill types along the height of the wall may also have a significant effect on corrosion rates of metallic reinforcements.

Type II Reinforcements

Since the integrity of the corrosion protection system is known to have a significant effect on service life, condition assessment must focus on obtaining information on the system's integrity. Properly installed grease and sheathing, and protection at the anchor head assembly, can provide substantial benefits on service life. Equation (1) and corresponding parameters from Table 5 should be applied to those systems where protection is questionable; otherwise corrosion cannot occur. For high strength steel reinforcements, corrosion processes may also include hydrogen embrittlement or SCC. Equation (1) does not apply to these types of corrosion processes and, for these cases, the end of service is considered to be when the corrosion protection is compromised.

Equation (1) is applied to estimate metal loss of Type II reinforcements assuming that attack from the surrounding environment is immediate and unaffected by the presence of a corrosion protection system or grout cover surrounding the reinforcements. Corrosion protection measures include the use of coatings, protective sheaths, passivation with grout, and encapsulation. Thus, the estimated metal loss is applicable to unprotected portions of the installation and is a conservative estimate for portions of the reinforcements that are passivated by grout or otherwise protected from corrosion.

The appropriate parameters for use in estimating metal loss are based on the corrosiveness index of the surrounding earth. According to the recommendations described in Withiam et al. (2002), the parameters "*k*" and "*n*" for use in Equation (1) are adjusted relative to soil/rockmass conditions as summarized in Table 5. The constant "*n*" is taken as one for simplicity and considering the relatively short time frame (<20 years) inherent to most of the observations used to develop the table. Ground conditions in Table 5 are described as average, corrosive, or highly corrosive based on electrochemical characteristics of the surrounding material that may be soil, rock joint infill, or groundwater. Average conditions and corrosive conditions refer to relatively neutral (pH > 5) and ρ_{min} greater than 2,000 Ω-cm, or 700 Ω-cm < ρ_{min} < 2,000 Ω-cm, respectively. Highly corrosive conditions are acidic (pH < 4),

Table 5. Recommended parameters for service life prediction model for Type II reinforcements (Withiam et al., 2002).

Parameter	Ground Conditions		
	Average	Corrosive	Highly Corrosive
k (μm)	35	50	340
n	1.0	1.0	1.0

correspond to $\rho_{min} < 700$ Ω-cm, or have very high chloride content (> 500 ppm).

The estimated service life of unprotected rock reinforcement systems in moderately aggressive ground conditions is approximately 50 years (Kendorski, 2003), but may be much lower for very aggressive ground conditions, and particularly for high strength steel subject to low pH environments (Withiam et al., 2002).

Test Protocol and Measurement Techniques

Recommended practices for corrosion monitoring and condition assessment of Type I and Type II reinforcements were developed from previous studies including FHWA Demonstration Project 82, *Durability/Corrosion of Soil Reinforced Structures* (Elias, 1990), and *NCHRP Report 477: Recommended Practice for Evaluation of Metal-Tensioned Systems in Geotechnical Applications,* (Withiam et al., 2002). These studies evaluated application of test techniques at a number of selected field sites and developed recommended practices for corrosion monitoring and condition assessment.

Measurement Techniques

Early corrosion monitoring practices involved exhuming and examining samples of reinforcements for evidence of corrosion, including loss of cross section. The practice of exhuming in-service reinforcements is limited to reinforcements that are accessible and usually near the surface of the structure. However, special inspection elements may be placed and later extracted from various positions along the wall face including the top, middle, and bottom of the wall (Jackura et al., 1987). Corrosion rate may be estimated from weight loss and thickness measurements, provided the original thickness or weight and composition (e.g., zinc thickness) of the reinforcements are known. Corrosion rate decays with time (Romanoff, 1957), and a catalog of measurements made at different times is required to assess the rate of metal loss with respect to time.

Less invasive techniques employing nondestructive electrochemical tests such as measurement of half-cell potential and linear polarization resistance (LPR) were implemented for corrosion monitoring of MSE walls beginning in the later 1980s (Lawson et al., 1993; Elias, 1990) and are also applied to Type II reinforcements (Withiam et al., 2002). With these techniques, a large number of samples are monitored and frequent measurements may be collected.

Half-Cell Potential

The half-cell potential, E_{corr}, is the difference in potential between the metal element and a reference electrode. A copper/copper sulfate reference electrode (CSE) is commonly used to monitor earth reinforcements. Results from the test can provide a comparison between metallic elements at different locations at the same site and identify the presence of different metals, for example, zinc or iron. Coupons or dummy reinforcements assist in interpretation of half-cell potential measurements. Plain steel, galvanized steel, and zinc coupons may provide baseline measurements for comparison.

Linear Polarization Resistance

LPR measurements are used to observe the instantaneous corrosion rate. Lawson et al. (1993), Elias (1990, 1997), Berkovitz and Healy (1997), and Elias et al. (2009) describe that application of the LPR technique to MSE reinforcements and application to Type II reinforcements is similar. Polarization resistance is measured from the response to an impressed current and the corrosion rate is computed via the Stern-Geary equation (Stern and Geary, 1957). The surface area of the test element must be known since the Stern-Geary equation is based on the corrosion current density, which is measured in terms of current per unit surface area. The measured resistance, PR′, is actually the sum of the interface and soil resistance ($PR' = PR + R_s$) with a correction for soil resistance often necessary (Elias, 1990).

Sonic Echo Test Measurements

The sonic echo method (impact test) is used for evaluating cracking of grouts, fracture of tendons, and loss of section or loss of prestress for Type II reinforcements (Rodger et al., 1997). The end of the reinforcement is impacted using a hammer or air gun, which generates elastic compression waves with relatively low frequency content. The waves are reflected by changes in geometry or conditions along the length of the reinforcement, including the ends of the elements, transitions from free to bonded zones, and irregularities that may be encountered along the length. Gong et al. (2005) and Liao et al. (2008) describe application of the sonic echo test to evaluate the length and integrity of soil nail installations.

Ultrasonic Test Measurements

The ultrasonic test method is a good technique for evaluating grout condition, fracture of elements, and abrupt changes in the element cross section for Type II reinforcements. The method has many of the features of the sonic echo technique, except that the transmitted signal contains relatively higher frequencies.

An ultrasonic transducer is acoustically coupled to the exposed end of the test element. Grease is used as an acoustic couplant. The time taken for sound pulses, generated at regular

intervals, to pass through the specimen and return, is measured. Return pulses may be either from a single reflection at a discontinuity, or from multiple reflections between a discontinuity and the end of the specimen. The patterns of the received pulses and the arrival times can provide valuable information about the nature of a defect, and of the integrity of the material being tested.

Performance Database

An important component of this research is to organize and incorporate performance data from earth reinforcements into a database. The database is analyzed to assess the reliability of current models for estimating metal loss and service life. The New York State Department of Transportation (NYSDOT) (Wheeler, 2002b), the Colorado Department of Transportation (CDOT) (Hearn et al., 2004), the Association for Metallically Stabilized Earth (AMSE, 2006), the Kentucky Transportation Research Cabinet (Beckham et al., 2005), the Ohio Department of Transportation (Timmerman, 1990), and the National Park Service (Anderson et al., 2009) have all developed databases for retaining walls. In general, these databases follow a format and protocol consistent with that employed by the FHWA mandated Bridge Management System (Hearn et al., 2004). These databases were considered and used as a basis to develop the framework for the performance database developed as part of NCHRP Project 24-28. The database developed for this project provides input necessary for statistical analysis of performance data, reliability analysis, and calibration of resistance factors for reliability-based design (i.e., LRFD).

The AMSE has compiled an inventory documenting details of MSE walls constructed in the United States over the past 35 years (AMSE, 2006). The majority of walls constructed with grid reinforcements serve as retaining walls, but approximately one-third of the walls with strip reinforcements serve as part of a bridge structure (abutment or wing walls). Approximately half of the walls in the AMSE inventory are located in the western region of the United States, within an arid climate where backfill sources are alkaline. Approximately 80% of the fill materials included in the AMSE database have a pH of between 6.5 and 8 (slightly acidic to slightly alkaline) and $\rho_{min} > 10{,}000\ \Omega$-cm. This is similar to data collected in France [Terre Armée International (TAI), 1977] indicating that approximately half of the walls included in the French survey had $\rho_{min} > 10{,}000\ \Omega$-cm and 90% had pH values between 6 and 8.5. Thus, a large portion of the inventory is constructed with fill material that meets AASHTO requirements by a wide margin, and may be considered "high quality fill."

Compared to steel grid-type reinforcements, which are used predominantly within the western region of the United States, use of strip reinforcements is more uniformly distributed geographically. Approximately 40% of the walls constructed with strip reinforcements are located in the more temperate southern climates, where soils are normally slightly acidic.

Load and Resistance Factor Design (LRFD)

LRFD is a reliability-based design method by which loads and resistances are factored such that:

$$\sum \gamma_i Q_{ni} \le \phi R_n \tag{6}$$

where

- Q_{ni} are nominal (i.e., computed) loads from sources that may include earth loads, surcharge loads, impact loads, or live loads;
- γ_i is the load factor for the i^{th} load source;
- R_n is the nominal (i.e., computed) resistance; and
- ϕ is the resistance factor and is usually less than 1.

Load and resistance factors are applied such that the associated probability of the load exceeding the resistance is low. The limit state equation corresponding to Equation (6) is

$$g(R,Q) = R - Q_i = \lambda_R R_n - \sum \lambda_{Qi} Q_{ni} > 0 \tag{7}$$

where

- g is a random variable representing the safety margin;
- R is a random variable representing "measured or actual" resistance;
- Q is a random variable representing "measured or actual" load;
- Q_i are random variables for "measured or actual" loads from various sources that may include earth loads, surcharge loads, impact loads, or live loads; and
- λ_R and λ_{Qi} are bias factors defined as the ratio of measured (actual) to nominal (computed) values of resistance and load, respectively.

Figure 3 depicts the limit state equation described by Equation (7) and the area beneath the tail to the left of $g = 0$ is the probability that $g < 0$ will occur, p_f (i.e., $p_f = P[g|R, Q] < 0$). This area is related to the reliability index, β, which is defined as the number of standard deviations between the mean value of $g(R, Q)$ and the origin of the $g(R, Q)$ function.

Table 6 describes the relationship between β and p_f. In general, $\beta = 0$ corresponds to a 50% probability of occurrence and the probability of occurrence is inversely proportional to β. The objective of LRFD is to find values for load and resistance factors, γ_i and ϕ, to achieve a target reliability index, β_T, corresponding to an acceptable probability of occurrence, p_f.

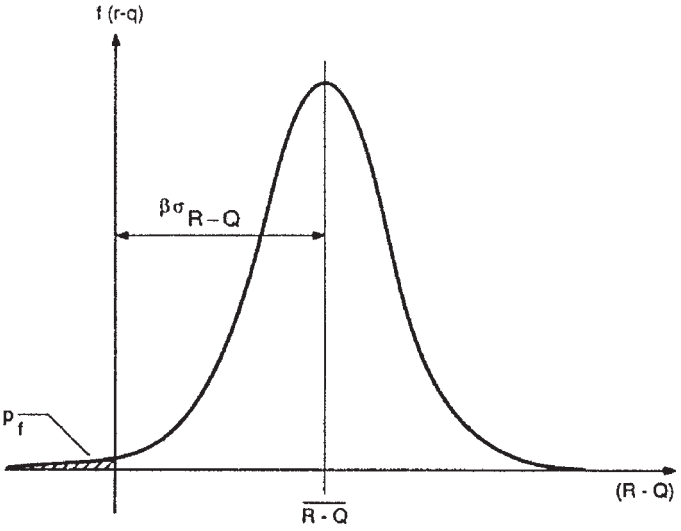

Figure 3. Statistical model of limit state equation.

Resistance Factors for Design of Earth Reinforcements

Reliability-based calibration of the strength reduction factor for LRFD modeling is focused on the design of MSE wall systems, since the AASHTO LRFD specifications for MSE walls include metal loss as an explicit part of the design. Ground anchor systems described in the AASHTO specifications incorporate a Class I corrosion protection system, therefore metal loss is not incorporated into the design calculations. Current AASHTO specifications include resistance factors for the structural resistance of ground anchors that consider variations inherent to steel manufacturing and fabrication. The value of ϕ varies depending on steel type as 0.9 for mild steel (ASTM A-615) and 0.8 for high-strength steel tendons (ASTM A-722). The AASHTO specifications do not specifically address design calculations in support of rock-bolt installations. To address this need, service life estimates and example calibrations of resistance factors for rock bolts are also included in this report.

The current AASHTO (2009) *LRFD Bridge Design Specifications* for design of MSE walls include resistance factors for the yield limit state that are calibrated with respect to safety factors that prevailed for the former allowable stress-based design (ASD). Table 7 is a summary of resistance factors for the yield limit state as presented in the current AASHTO specifications. The ASD employed safety factors of 1.8 (i.e., 1/0.55) or 2.1 (i.e., 1/0.48) relative to yield of strip-type reinforcements or grid-type reinforcements, respectively. The higher safety factor for grid reinforcing members corresponds to a lower resistance factor and is intended to ensure that no individual wire is stressed to more than $0.55F_y$. This compensates for interior longitudinal elements that carry higher load compared to exterior elements due to load transfer through the transverse members of the bar mat. The safety factor of 2.1, and corresponding resistance factor of 0.65, is appropriate for bar mats with four or more longitudinal elements but should be higher for elements with only three longitudinal elements. However, this point is not addressed in the current AASHTO specifications.

Table 6. Relationship between β and p_f.

Reliability Index (β)	Probability of occurrence (p_f)
2.0	2.275×10^{-2}
2.5	6.210×10^{-3}
3.0	1.350×10^{-3}
3.5	2.326×10^{-4}
4.0	3.167×10^{-5}
4.5	3.398×10^{-6}
5.0	2.867×10^{-7}

D'Appolonia (2007) assessed strength reduction factors for the yield limit state via reliability-based calibration, but did not consider metal loss from corrosion as a variable. This project extends these studies to consider variability of metal loss and the impact that this has on computed levels of reliability using existing design methodologies and methods for computing the load transferred to the reinforcements. Calibration of the resistance factors uses load factors from the AASHTO LRFD specifications and calibration methodology recommended by Allen et al. (2005). The resistance factor is calibrated with respect to a target reliability index, β_T, (i.e., probability of occurrence), which accounts for the redundancy of the system and load redistribution inherent to the yield limit state.

Probability of Occurrence (Exceeding Yield) for Existing Construction

Generally, MSE wall systems are prefabricated, resulting in distinct reinforcement and reinforcement spacing. Thus, reinforcement yield resistance is available in discrete increments determined by the distinct size of the reinforcement and reinforcement spacing selected for the project. Reinforcement sizes and spacings are selected based on particular design locations, often near the base of the wall; and unless the wall is very tall, these dimensions are held constant throughout. Therefore, yield resistance is not optimized with respect to the yield limit state, and for many reinforcement locations, there is a large disparity between reinforcement loads and resistance. D'Appolonia (2007) studied this case using data that included measurements of reinforcement load that could be compared with the available yield resistance. Essentially, the results reported by D'Appolonia describe the probability of occurrence for as-built conditions, rather than for a conceptual design for which yield resistance is optimized with respect to the limit state.

Table 7. Resistance factors for yield resistance for MSE walls with metallic reinforcement and connectors from Table 11.5.6-1, AASHTO (2009).

Reinforcement Type	Loading Condition	Resistance Factor
Strip reinforcements[1]	Static loading	0.75
	Combined static/earthquake loading	1.00
Grid reinforcements[1,2]	Static loading	0.65
	Combined static/earthquake loading	0.85

[1] Apply to gross cross section less sacrificial area. For sections with holes, reduce gross area in accordance with AASHTO (2009) Article 6.8.3 and apply to net section less sacrificial area.
[2] Apply to grid reinforcements connected to rigid facing element, for example, a concrete panel or block. For grid reinforcements connected to a flexible facing mat or that are continuous with the facing mat, use the resistance factor for strip reinforcements.

Results from Monte Carlo simulations of the limit state function and comparison with closed form solutions as reported by D'Appolonia indicate that the probability of occurrence for as-built conditions is very low, corresponding to $\beta > 3.5$ and $p_f < 0.0001$. These results are insensitive to metal loss and do not depend on the choice of resistance factor. This leads to the conclusion that reinforcement yield is very unlikely given the as-built conditions of MSE walls, and the yield limit state does not appear to have a significant impact on performance.

The D'Appolonia model assumes that the difference between yield resistance and reinforcement load is randomly distributed. In reality this is not the case. For example, the difference may be much smaller for reinforcements located near the base of the wall or other locations that may govern the required yield resistance. Furthermore, for tall walls there may be a number of locations where yield resistance is selected to meet a given load. Thus, locally, the probability of occurrence may be much higher than that predicted by D'Appolonia.

Alternatively, this report describes reliability-based calibration for resistance factors considering that the yield limit state function is explicitly applied at every reinforcement location. Thus, the potential for overdesign is not directly included in the analysis; however, a target reliability index, β_T of 2.3 corresponding to $p_f = 0.01$, is adopted considering the large redundancy inherent to the system (Allen et al., 2005). Considering as-built conditions, the resistance factors computed by this technique are conservative, although they are in the range of those incorporated into AASHTO (2009) as shown in Table 7.

CHAPTER 2

Research Approach

Tasks

The research approach includes nine tasks and the project was conducted in two phases. Tasks 1 through 5 were included in Phase I, and Phase II includes Tasks 6 through 9. Results from Phase I were described in the project interim report that was submitted in April 2007, and this report includes results from Phase II. A brief description of tasks from Phase I is summarized to help place the approach and results from Phase II into context.

Task 1—Literature Review and Survey

Task 1 consists of a review of existing literature and a survey of owners, designers, and contractors to (1) identify existing data on the past performance of metallic reinforcements; (2) trace the development of corrosion potential, metal loss and service life models that form the basis for the existing AASHTO specifications and FHWA recommendations; (3) document information relative to existing installations; and (4) solicit information regarding existing sites and planned construction/deconstruction where access to reinforcements could be gained for field studies, including opportunities to exhume reinforcement samples for observation and testing.

Task 2—Prepare Performance Database

Task 2 consists of (1) developing and populating a database using existing performance data identified in Task 1, (2) collecting information regarding the existing inventory of metallic earth reinforcements, and (3) studying attributes of the performance data and comparing attributes of the general population to those from sites with performance data.

Task 3—Estimate Reliability of Service-Life Models

Task 3 consists of analyzing the results from Tasks 1 and 2 to estimate the reliability and utility of promising models for predicting the corrosion potential, metal loss, and service life of metal-reinforced systems in geotechnical applications.

Task 4—Develop Work Plan for Field Investigation

Task 4 consists of preparing detailed plans for a comprehensive field investigation to evaluate the performance of earth reinforcement systems. This plan addresses some of the deficiencies in the performance database identified in Task 2. These deficiencies include limitations with respect to geographic distribution, range of fill characteristics, spatial and temporal variations, and corrosion rate measurements for Type II reinforcements.

Task 5—Submit Interim Report

Task 5 consists of preparing an interim report summarizing the results, conclusions, and recommended work plans developed during Tasks 1 to 4. This report was submitted to and approved by NCHRP in April 2007.

Task 6—Implement Field Investigation

Task 6 consists of implementing the workplan developed in Task 4 and approved in Task 5.

Task 7—Identify Target Reliability Index for LRFD

Using the data from Tasks 2, 3 and 6, statistical properties are computed to describe the variability of factors that affect metal loss and service life estimates of in-ground metallic reinforcement systems. This includes (1) reevaluation of the prediction model(s) to assess its accuracy and precision to estimate metal loss caused by corrosion and (2) development of appropriate resistance factors for use in LRFD that account for metal loss caused by corrosion. Calibration of the resistance factors uses load factors from the AASHTO LRFD specifications

and calibration methodology recommended by Allen et al. (2005). The resistance factors consider the nominal metal loss used in design and the redundancy of the design and load redistribution inherent to the identified limit states.

The reliability index (β) for other systems that are vulnerable to metal loss (unprotected soil nails and rock bolts) will also be considered and compared to the β_T values used in design.

Task 8—Recommend Revisions to AASHTO LRFD Specifications

Based on the results from Task 7, revisions to the current AASHTO LRFD specifications used in the design of metal-tensioned systems were reviewed and recommended. In particular, resistance factors for design of MSE walls are recommended that take into account the estimated metal loss over the service life of the installation. Metal loss parameters will be updated as appropriate for galvanized and plain steel reinforcements, while taking into consideration different backfill characteristics.

Task 9—Submit Final Report

This final report summarizes the findings of, draws conclusions from, and documents the research products, including

- A performance database documenting the attributes and metal loss observed for a variety of metal-tensioned systems used in geotechnical applications, including the additional results from field studies conducted in Task 6.
- Updated metal loss models that consider targeted levels of confidence, sources of error, and different types of elements and site conditions.
- Recommended revisions to the current AASHTO LRFD specifications, including updated resistance factors for the design of MSE walls and other earth reinforcements.
- Discussion of deficiencies in present knowledge and recommendations for future work.

Test Protocol

Berkovitz and Healey (1997) and Elias et al. (2009) describe test protocols and procedures for sampling and testing Type I reinforcements. Withiam et al. (2002) present a recommended practice resulting from NCHRP Project 24-13 for condition assessment and service life modeling of Type II reinforcements. These procedures, protocols, and recommended practices were followed in the course of this research. Appendix B describes salient details of test procedures, sampling, data analysis, and interpretation for Type I and Type II reinforcements. In general, the protocols include (1) assessing the site and installation conditions; (2) sampling and testing backfill, groundwater, and in situ earth materials; (3) performing nondestructive testing (NDT) supplemented with visual observations; and (4) comparing results with expectations for service life models (Fishman et al., 2005).

NDT applied to Type I reinforcements includes measurement of half-cell potential and LPR. Half-cell potential measurements are useful to probe the surface and assess if corrosion has occurred and whether or not zinc coating remains on the surface of galvanized reinforcements. LPR is useful to estimate corrosion rate at an instant in time. Single measurements do not provide enough information and a sampling strategy is incorporated into the test protocol to consider random, spatial, and temporal variations in measurements.

Additional NDT applied to Type II reinforcements includes impact and ultrasonic tests. Impact test results are useful to diagnose loss of prestress, assess grout quality, and indicate if the cross section is compromised from corrosion or from a bend or kink in the element. Ultrasonic test results are useful for obtaining more detailed information about the condition of elements within the first few feet from the proximal end of the element.

Calibration of Resistance Factors for LRFD

The procedure for reliability-based calibration of resistance factors for LRFD is as follows (Allen et al., 2005):

1. Consider limit state equation for yield of reinforcements.
2. Statistically characterize the data upon which the calibration is based.
3. Select a target reliability index.
4. Use reliability theory to compute resistance factors.

Factors that impact the extent to which variability of metal loss affects probability of occurrence need to be included in the reliability-based calibration. To help identify these factors, Figure 4 illustrates how the steel incorporated into the design of a reinforcement cross section can be interpreted to include

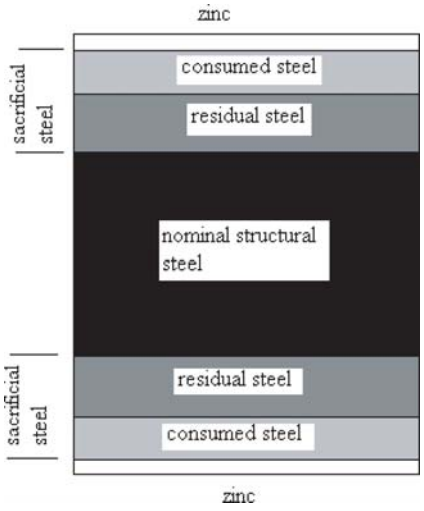

Figure 4. Idealized reinforcement cross section.

three components: (1) steel needed to resist the applied load without yielding (nominal structural steel), (2) steel loss from corrosion (consumed steel), and (3) residual steel that was intended to serve as sacrificial steel, but not actually consumed by corrosion. Residual steel contributes to the reinforcement resistance, and consequently to the bias inherent to the design. Differences between the metal loss model used in design and the prevailing corrosion rates determine the amount of residual steel at the end of the service life. Prevailing corrosion rates depend on the electrochemical properties of the fill, making fill quality an important factor to include in the calibration. Reinforcement size is also important because the significance of residual steel becomes less as the cross-sectional area of the reinforcement increases. In consideration of these factors, the reliability-based calibration is performed in terms of the following design parameters:

- service lives of 50, 75 and 100 years;
- different reinforcement dimensions for strips 3 mm, 4 mm, 5 mm and 6 mm, or wire diameters for grids W7, W9, W11, W14; and
- different backfill conditions (not all meet AASHTO specifications).

Yield Limit State

Loss of cross section affects the yield resistance of MSE reinforcements and is incorporated into the LRFD procedure in terms of the yield limit state equations. The yield limit state is reached when the reinforcement tension exceeds the yield resistance. Therefore, calculation of loads and yield resistance contribute to the yield limit state equations.

Reinforcement loads may be computed via several different methods including the coherent gravity method, tieback wedge method, structure stiffness method, or the simplified method (Berg et al., 2009). Most metallic reinforcements are considered to be relatively inextensible, and, traditionally, loads have been computed via the coherent gravity method; however, the structure stiffness method and the simplified method have also been applied. For the purpose of this study the coherent gravity and simplified methods are considered and used to compute the load bias for the calibration of resistance factor. Reinforcement loads are computed based on the horizontal stress carried by the reinforcements computed as

$$\sigma_H = K\sigma_v + \Delta\sigma_H \tag{8}$$

where

σ_H is the horizontal stress at any depth in the reinforced zone,
K is the coefficient of lateral earth pressure,
σ_v is the factored vertical pressure at the depth of interest, and
$\Delta\sigma_H$ is the supplemental factored horizontal pressure due to external surcharges.

The main differences between the simplified and the coherent gravity methods are with respect to the determination of K and computation of σ_v (Berg et al., 2009). The manner in which reinforcement loads are computed affects the load bias used in the calibration of resistance factor. Allen et al. (2001 and 2005) and D'Appolonia (2007) assessed the load bias for metallic MSE reinforcements using the simplified and coherent gravity methods of analysis, respectively. We have used the load bias from these references to calibrate resistance factors for LRFD.

The maximum reinforcement tension is computed from σ_H based on the spacing of the reinforcements as

$$T_{\max} = \sigma_H S_V \tag{9}$$

where

$T_{\max}$ is the maximum reinforcement tension at a given level per unit width of wall and
S_V is equal to the vertical spacing of reinforcements.

Equations (8) and (9) describe the demand placed on the reinforcements; the capacity is the yield resistance of the reinforcements computed as

$$R = \frac{F_y A_c}{S_H} \tag{10}$$

where

R is resistance per unit width of wall,
F_y is the yield strength of the steel,
A_c is the cross-sectional area of the reinforcement at the end of the service life, and
S_H is the horizontal spacing of the reinforcements.

For strip-type reinforcements:

$$A_c = bE_c \tag{11}$$

For steel grid-type reinforcements:

$$A_c = n \times \pi \times \frac{D^{*2}}{4} \tag{12}$$

where

b is the width of the reinforcements,
E_c is the strip thickness corrected for corrosion loss;
$E_c = (S - \Delta S)$ for $\Delta S < S$, and 0 for $\Delta S \geq S$,
S is the initial thickness,
ΔS is the loss of thickness (both sides) from corrosion,
n is the number of longitudinal bars/wires, and
D^* is the diameter of the bar or wire corrected for corrosion loss;
$D^* = D_i - \Delta S$ for $\Delta S < D_i$, and 0 for $\Delta S \geq D_i$, where D_i is the initial diameter.

For galvanized reinforcements:

$$\Delta S = 2 \times r_s \times (t_f - C) \qquad \text{For } C < t_f$$
$$\Delta S = 0 \qquad \text{For } C \geq t_f \tag{13a}$$

$$C = 2\,yrs + \frac{(z_i - 2 \times r_{z1})}{r_{z2}} \tag{13b}$$

where

r_s is the corrosion rate of steel after zinc has been consumed,
t_f is the intended service life,
C is the time to initiation of steel loss,
z_i is the zinc initial thickness per side,
r_{z1} is the initial corrosion rate for zinc, and
r_{z2} is the corrosion rate for zinc after the first two years.

For plain steel reinforcements:

$$\Delta S = 2 \times r_s \times t_f \tag{14}$$

Variables for the resistance calculation include F_y, A_c, r_s, r_{z1}, r_{z2}, and z_i. The spacings of the reinforcements (S_H and S_V) are considered to be constants. Using the statistics and observed distribution for measurements of corrosion rate, the bias of the remaining strength is computed and used as input for the reliability-based calibration of resistance factor. The bias is computed as

$$\lambda_R = \frac{F_y^* A_c^*}{F_y A_c} \tag{15}$$

The denominator includes nominal values used in design; A_c is based on the metal loss model recommended by AASHTO for design of metallic MSE reinforcements, and F_y is the nominal yield strength. The statistics of the observed corrosion rates from the database described in Chapter 3 are used to describe the variable A_c^*, and the statistics for F_y^* are taken from Galambos and Ravindra (1978) and Bounopane et al. (2003). Bounopane et al. consider yield strengths to be normally distributed with mean 1.05 times the nominal and COV = 0.1.

Resistance Factor Calibration

Monte Carlo simulations are employed to compute the relationship between the reliability index, β, and resistance factor, ϕ. The Monte Carlo simulation method is used because the approach is more adaptable and rigorous compared to other techniques, and it has become the preferred approach for calibrating load and resistance factors for the LRFD specifications (Allen et al., 2005; D'Appolonia, 2007). The simulations are performed in terms of a given load factor, γ, load bias, λ_Q, and resistance bias, λ_R. The Monte Carlo technique utilizes a random number generator to extrapolate the limit state function, g, for calibration of yield resistance. Random values of g are generated using the mean, standard deviation, and the distribution (e.g., normal, lognormal, or Weibull) of the load bias and the resistance bias. The extrapolation of g makes estimating β possible for a given combination of γ and ϕ. A value of γ is adopted that is compatible with the static earth load calculations (AASHTO, 2009). A range of ϕ values is assumed and estimated values of β (by iteration) are checked against a value of 2.3 as used in previous LRFD calibrations (Allen et al., 2005; D'Appolonia, 2007). Monte Carlo simulations were facilitated by the Lumenaut software package (Lumenaut, 2007), which performs Monte Carlo simulations through a link with Microsoft Excel.

The vertical pressure due to the weight of the reinforced soil zone (σ_v in Equation 8) is assigned load type "EV" as described by Berg et al. (2009). AASHTO (2009) specifies γ equal to 1.35 for EV at the strength limit state, therefore, γ = 1.35 is adopted for calibration of the resistance factor similar to D'Appolonia Engineers (2007) and Berg et al. (2009). The load bias depends on use of the simplified or coherent gravity method and may depend on reinforcement type (strip or grid) as described by Allen et al. (2001), Allen et al. (2005), and D'Appolonia (2007). Results from these studies demonstrate that the load bias has a lognormal distribution, mean, and standard deviation as summarized in Table 8.

Resistance bias is computed using Equations (10) to (15), nominal values for yield strength and remaining cross section, the yield strength variation, and the mean, standard deviation, and distribution from observations of metal loss archived in the performance database. Thus, the resistance bias depends on the nominal strength, which depends on the metal loss model used in design, as well as the manner in which observations of corrosion rate and metal loss are extrapolated to render the estimated remaining strength at the end of service.

Monte Carlo simulations were performed using these values for load bias and load factor, and several different scenarios were considered. Different scenarios treat metal loss as deterministic or variable, and contrast "as built" versus

Table 8. Mean (μ) and standard deviation (σ) of lognormal load bias.

Parameter	Strip		Grid	
	Simplified Method[1]	Coherent Gravity Method[2]	Simplified Method[1]	Coherent Gravity Method[2]
μ_{λ_Q}	0.973	1.294	0.973	1.084
σ_{λ_Q}	0.449	0.499	0.449	0.737

[1]Allen et al. (2005).
[2]D'Appolonia (2007).

Lumenaut Simulation Report

Output Cell:	Simple!$B$9	**Workbook:**	ɔ 75 yrs 4mm Simple p-10000 0.85.xls
Output Name:	g	**Date:**	7-Aug-09
Iterations:	10000	**Time:**	10:10:29 AM

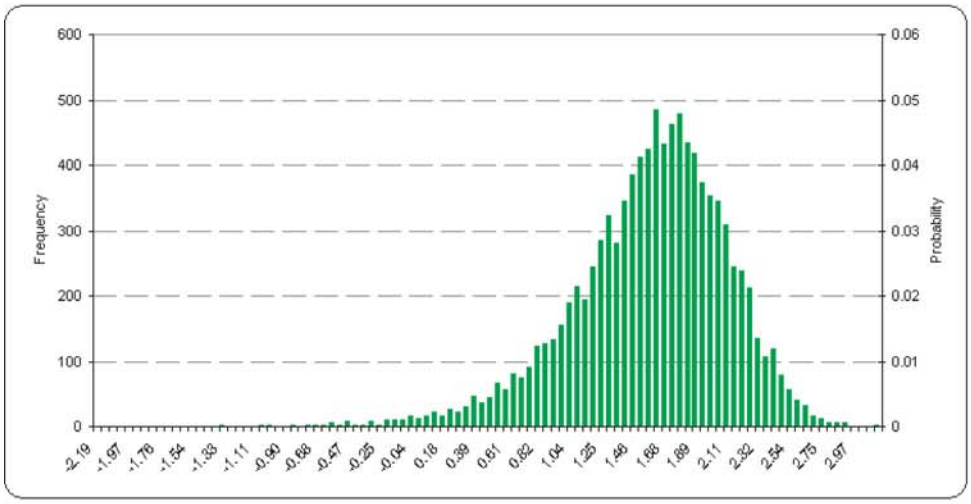

Percentile	Min to Max
0%	-2.239322412
10%	0.874284512
20%	1.170341287
30%	1.353907141
40%	1.497322296
50%	1.61591604
60%	1.73764129
70%	1.856778793
80%	1.998045861
90%	2.177293693
100%	3.128517542

Percentile	Max to Min
100%	3.128517542
90%	2.177293693
80%	1.998045861
70%	1.856778793
60%	1.73764129
50%	1.61591604
40%	1.497322296
30%	1.353907141
20%	1.170341287
10%	0.874284512
0%	-2.239322412

Mean	1.55957141
Median	1.615902211
Mode	N/A
Stand. Deviation	0.5374818
Variance	0.288886686
Mean Std. Error	0.005374818
Range	5.367839954
Range Min	-2.239322412
Range Max	3.128517542
Skewness	-0.900825859
Kurtosis	2.102930424

Lumenaut Simulation Input

Cell Name:	Load Bias
Cell:	Simple!$B$5
Distribution:	Lognormal
Mean	0.973
Stand. Dev.	0.45
Min:	0.15
Max:	5.38

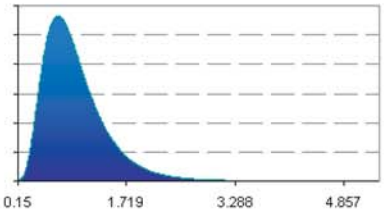

Cell Name:	Resistance Bias
Cell:	Simple!$B$6
Distribution:	Normal
Mean:	1.597
Stand. Dev.	0.1877
Min:	0.85
Max:	2.35

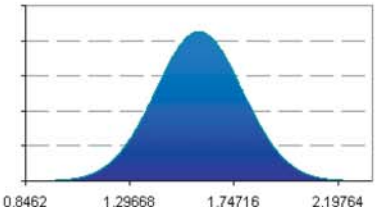

Figure 5. Monte Carlo simulation example showing input and output reports.

design conditions. For each scenario different aspects of the design, including reinforcement size and service life, are considered and 10,000 iterations are performed to arrive at the distribution of the limit state function.

The Monte Carlo analysis for calibration of resistance factor computes values for the limit state function, $g = R - Q$, considering the uncertainty of R and Q, and renders the probability that $g < 0$. The variables R and Q can be related to nominal values as $Q = Q_n \times \lambda_Q$, and based on the LRFD equation [Equation (6)], $R = \lambda_R \times R_n = \dfrac{\lambda_R \times \gamma_Q \times Q_n}{\phi}$. The analysis proceeds by selecting a value for Q_n; a value of unity is used for convenience. The Monte Carlo analysis then computes a range of values for g, using randomly generated values for λ_R and λ_Q based on their statistics, and a trial value of ϕ. The Lumenaut software outputs the results of the iterations in the form of a histogram and corresponding intervals are summarized in a table. Figure 5 is an example output from a typical Monte Carlo simulation for computing β based on a trial selection of ϕ. The top graph is a histogram depicting the distribution of g from results of the Monte Carlo simulation. The probability that $g < 0$ may be computed by sorting and ranking these results and computing the cumulative probability at $g = 0$. The table beneath the histogram summarizes the statistics associated with g and the figures at the bottom of the page describe the statistics and associate distribution provided as input (in this case for λ_R and λ_Q).

A worksheet, including the actual results from the 10,000 iterations, is also generated. The g values are then sorted and ranked in an ascending order and the cumulative probability at each g is calculated. Figure 6 shows a typical result depicting the standardized normal variable (z) versus randomly generated g. The reliability index, β is equal to ($-z$) at $g = o$. For the example shown in Figure 6, β is equal to 2.27 corresponding to p_f = 1.15E-02. The analysis is repeated with different trial values for ϕ until the probability that $g < 0$ corresponds to the target reliability index. Appendix E includes details similar to Figures 5 and 6 in support of all Monte Carlo simulations described in this report.

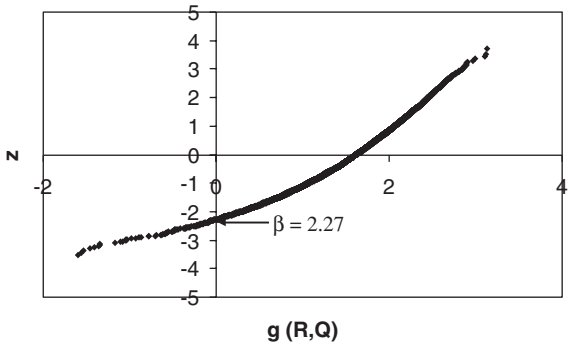

Figure 6. Typical Monte Carlo result from resistance factor calibration.

McVay et al. (2000) proposed representing design efficiency as the ratio of resistance factor and mean bias (ϕ/λ_R). This measure of efficiency accompanies computed resistance factors to avoid the misconception that high resistance factors are correlated with the economy of a design method. Paikowski (2004) demonstrates that this ratio is systematically higher for methods that predict more accurately, regardless of the bias. Using different models for the nominal resistance in the denominator of Equation (15) may lead to different values of the mean bias (λ_R) and corresponding resistance factors (ϕ), but if the COVs are the same, the resulting efficiency factors are identical. Higher efficiency factors are only obtained with methods that produce a lower COV with respect to the computed bias. This may be accomplished by improving the quality and quantity of measured or estimated resistance, the models and methods used to represent and extrapolate the data, or both.

If the metal loss is assumed to be deterministic, the only variable (i.e., not a constant) describing the tensile strength remaining at the end of service condition corresponds to yield strength, F_y. Thus, the bias for remaining tensile strength is considered as normally distributed with mean equal to 1.05 and standard deviation of 0.105 (Bounopane et al., 2003). These results are presented to serve as a baseline to assess the impact that variations in metal loss have on the computed values for ϕ.

The calibration is performed to identify the resistance factor corresponding to β of approximately 2.3 ($p_f \approx 0.01$). Resistance factors, summarized in Table 9, are rounded to the nearest increment of 0.05.

These results may be compared to the current AASHTO specifications where ϕ is specified as 0.75 for strip-type reinforcements and 0.65 for grids that are attached to a rigid wall facing. These factors are the same for the simplified and coherent gravity methods in the current edition of the specifications. It appears that the current AASHTO specifications implicitly consider some variation with respect to estimated sacrificial steel requirements for galvanized reinforcements. This is in spite of the fact that the resistance factors are not determined from a reliability-based calibration, but are calibrated with respect to safety factors corresponding to the earlier specifications for ASD.

Table 9. Resistance factors considering deterministic metal loss model.

Type	Simplified/Coherent
Strip	0.55/0.45
Grid	0.50/0.35

CHAPTER 3

Findings and Applications

As part of Tasks 1, 2 and 6 for this project, performance data were collected and archived from sites located in the northeastern, mid-Atlantic, southeastern, southwestern, and western United States consistent with details of the existing inventory. Data are included from 170 sites located throughout the United States and Europe. Table 10 updates the summary similar to Berkovitz (1999) of statewide practice and MSE corrosion monitoring programs that have been implemented by State DOTs. These programs have produced data that have been archived into the performance database.

In general, the database is self-contained yet structured such that it can be ported to other existing databases. The database is formatted using Microsoft Access, which is linked to a geographic information system (GIS) (ArcView) platform to provide visual and spatial recognition of data. The organization and structure of the various tables and data fields are updated, as necessary, to accommodate different types of information that are identified from available data sets. For example, observations of reinforcement performance and condition may be based on NDT, direct physical measurement, or visual observations, and these data types are archived accordingly. Drop down lists and check boxes are implemented to facilitate mining or querying of the database. Separate databases have been developed for MSE reinforcements (Type I), and for ground anchors, rock bolts, and soil nails (Type II). The Type II database is similar to the Type I database, but some data fields are different to address corrosion protection measures, different subsurface conditions, and types of monitoring techniques that are specific to the Type II systems.

Information within the shell of the database is distributed amongst seven distinct tables comprising a total of 150 data fields. The tables are divided into categories of information similar to those employed in other databases that are based on the FHWA Bridge Management Inventory. The database includes the following tables:

- Project,
- Walls/Structure,
- Reinforcements,
- Backfill/Subsurface,
- Observation Points,
- NDT Results, and
- Direct Observations.

Microsoft Access data forms were created to facilitate data entry and examples of these forms are included in Appendix C. Tables are related with a one-to-many relationship using "project number" as a key parameter. Other relationships may also be created, but currently all other tables are considered to be a sub-form to the project form, which serves as the master form. Thus, a project may have a number of walls or backfills. A wall may have numerous observation points, and a number of observations, including NDT or direct physical observations, may be associated with each observation point. For example, the project in Las Vegas, Nevada, described by Fishman et al. (2006) includes three walls; Wall #1 has 15 monitoring stations, Wall #2 has six, and Wall #3 has four. Each monitoring station includes two in-service reinforcements wired for monitoring (NDT) and at least two coupons: one plain and one galvanized. Also, direct physical measurement of section loss is performed on 18 samples retrieved from six of the monitoring stations (i.e., three reinforcements exhumed from six of the stations). These data are all organized into separate tables that are linked to the Las Vegas, Nevada, entry from the project table. Relationships are also defined between backfill, wall, reinforcements, monitoring stations, and results tables.

Each project is associated with a point that is displayed on a map within ArcView as shown in Appendix C. ArcView-mapped points are also linked to the Microsoft Access tables so pertinent information for each project can be displayed next to each point when selected by the user. In this way, the geographic distribution of performance data, as well as specific attributes for each site can be displayed within a GIS platform. Thus, the user may associate the

Table 10. Summary of state DOT MSE wall corrosion assessment programs.

State	Description	References
California	Have been installing inspection elements with new construction since 1987, and have been performing tensile strength tests on extracted elements. Some electrochemical testing of in-service reinforcements and coupons has also been performed. LPR and EIS tests were performed on inspection elements at selected sites as part of NCHRP Project 24-28 and results compared with direct physical observations on extracted elements.	Jackura et al. (1987), Elias (1990), Coats et al. (1990), Coats et al. (2003- Draft Report)
Florida	Program focused on evaluating the impact of saltwater intrusion, including laboratory testing and field studies. Coupons were installed and reinforcements were wired for electrochemical testing and corrosion monitoring at 10 MSE walls. Monitoring has continued since 1996.	Sagues et al. (1998, and 2000), Berke and Saques (2009)
Georgia	Began evaluating MSE walls in 1979 in response to observations of poor performance at one site located in a very aggressive marine environment incorporating an early application of MSE technology. Exhumed reinforcement samples for visual examination and laboratory testing. Some in situ corrosion monitoring of in-service reinforcements and coupons at 12 selected sites using electrochemical test techniques was also performed.	McGee (1985), Deaver (1992)
Kentucky	Developed an inventory and performance database for MSE walls. Performed corrosion monitoring including electrochemical testing of in-service reinforcements and coupons at five selected sites.	Beckham et al. (2005)
Nevada	Condition assessments and corrosion monitoring of three walls at a site with aggressive reinforced fill and site conditions. Exhumed reinforcements for visual examination and laboratory testing; performed electrochemical testing on in-service reinforcements and coupons. A total of 12 monitoring stations were dispersed throughout the site providing a very good sample distribution.	Fishman et al. (2006)
New York	Screened inventory and established priorities for condition assessment and corrosion monitoring based on suspect reinforced fills. Two walls with reinforced fill known to meet department specifications for MSE construction are also included in program as a basis for comparison. Corrosion monitoring uses electrochemical tests on coupons and in-service reinforcements.	Wheeler (1999, 2000, 2001, 2002a and 2002b)
North Carolina	Initiated a corrosion evaluation program for MSE structures in 1992. Screened inventory and six walls were selected for electrochemical testing including measurement of half-cell potential and LPR. This initial study included in-service reinforcements, but coupons were not installed. Subsequent to the initial study, NCDOT has installed coupons and wired in-service reinforcements for measurement of half-cell potential on MSE walls and embankments constructed since 1992. LPR testing was also performed at approximately 30 sites in cooperation with NCHRP Project 24-28.	Medford (1999)
Ohio	Concerned about the impact of their highway and bridge deicing programs on the service life of metal reinforcements. Performed laboratory testing on samples of reinforced fill but did not sample reinforcements or make in situ corrosion rate measurements.	Timmerman (1990)
Oregon	Preliminary study including 1) a review of methods for estimating and measuring deterioration of structural reinforcing elements, 2) a selected history of design specifications and utilization of metallic reinforcements, and 3) listing of MSE walls that can be identified in the ODOT system.	Raeburn et al. (2008)

Note: EIS = electrochemical impedance spectroscopy.

data with geographic location and view all of the performance data and pertinent information associated with that location.

Type I—Measured Corrosion Rates

Consistent with the data needs for reliability analysis and calibration of strength reduction factors for LRFD, the following studies were performed:

1. Collection of data on comparison of LPR and weight loss measurements using data available from the existing literature augmented with additional data collected from this project. These data are useful to discern any bias with respect to LPR measurements that should be considered in the reliability analysis.
2. Study of the relationship between corrosion rate and resistivity of reinforced fill materials. Resistivity is known to have a significant impact on corrosivity, however, data

comparing measured corrosion rates to resistivity measurements include a lot of scatter. Some of the scatter may be due to spatial and temporal differences between measurement of corrosion rate and sampling and testing of reinforced fill materials. However, the study is useful to demarcate threshold levels of resistivity wherein corrosion rates may be significantly affected and to define ranges within which particular metal loss models may apply.

3. Study of the effect of climate/region on measured corrosion rates considering data from different geographic regions associated with different climates, and construction and maintenance practices. The purpose of this study is to further evaluate if data should be partitioned into regions for the purpose of reliability analysis.
4. Partitioning the data into sites that incorporate reinforced fill materials meeting AASHTO requirements, and considering metal loss or corrosion rate as a function of time. The purpose of this study is to evaluate the robustness of available metal loss models and the probability of exceeding metal loss rates used in design.
5. Observation of trends for marginal fills that do not meet AASHTO criteria for reinforced fills. The purpose of this study is to make recommendations on the appropriate parameters for modeling metal loss and the reliability of metal loss estimates for a selected range of resistivity; for example, between 1,000 Ω-cm and 3,000 Ω-cm.

Detailed results from these studies are included in Appendix D. Data are grouped by quality of reinforced fill, age of sample, and reinforcement type. Figures 7 and 8 summarize the statistics (mean and COV) from these data groups for galvanized and plain steel reinforcements, respectively. Reinforcement type does not appear to have a significant impact on corrosion rates, but lower COVs are realized when data are partitioned into groups defined by reinforcement type.

The best results in terms of lower COV are from galvanized reinforcements between 2 and 16 years old, where the COVs range between approximately 30% and 60%. Higher COVs are realized for younger reinforcements (<2 years old) and reinforcements that are older than 16 years. This may be due to variations in the time it takes for the zinc surface to become passivated for younger reinforcements, and the variation of remaining zinc on the surface of older reinforcements. Data are more scattered (i.e., have higher COVs) considering fill materials that do not meet AASHTO requirements (ρ_{min} < 3,000 Ω-cm), and this is may be because, although a low value of ρ_{min} is indicative of the potential for higher corrosion rates, this potential may not be realized if the moisture content is kept low, and moisture content and degree of saturation exhibit significant variability.

More scatter is evident for plain steel reinforcements. This may be due to the tendency for galvanized surfaces to undergo more uniform corrosion compared to plain steel; also, steel may be more sensitive to changes in environment over the range of conditions for which measurements were obtained.

Bias of LPR Measurements

Figure 9 depicts observations of corrosion and metal loss with respect to age of the reinforcements for fill conditions meeting the AASHTO criteria described in Table 3. Observations included in Figure 9 are via LPR measurements from sites located in the northeastern, mid-Atlantic, southeastern,

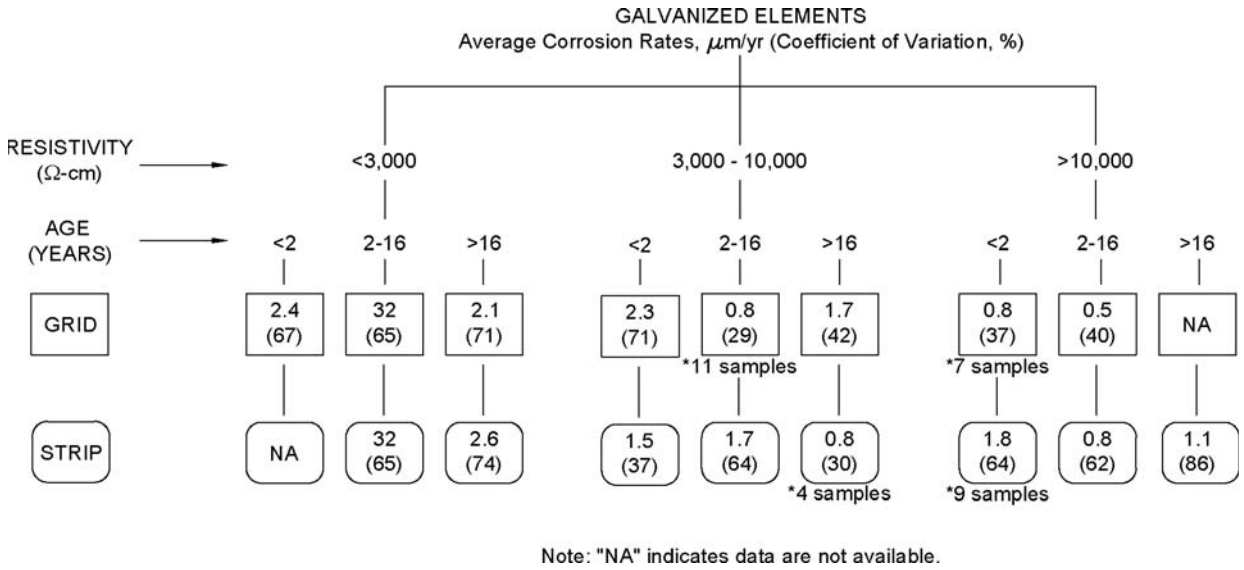

Figure 7. Summary of statistics for galvanized reinforcements (= limited samples).*

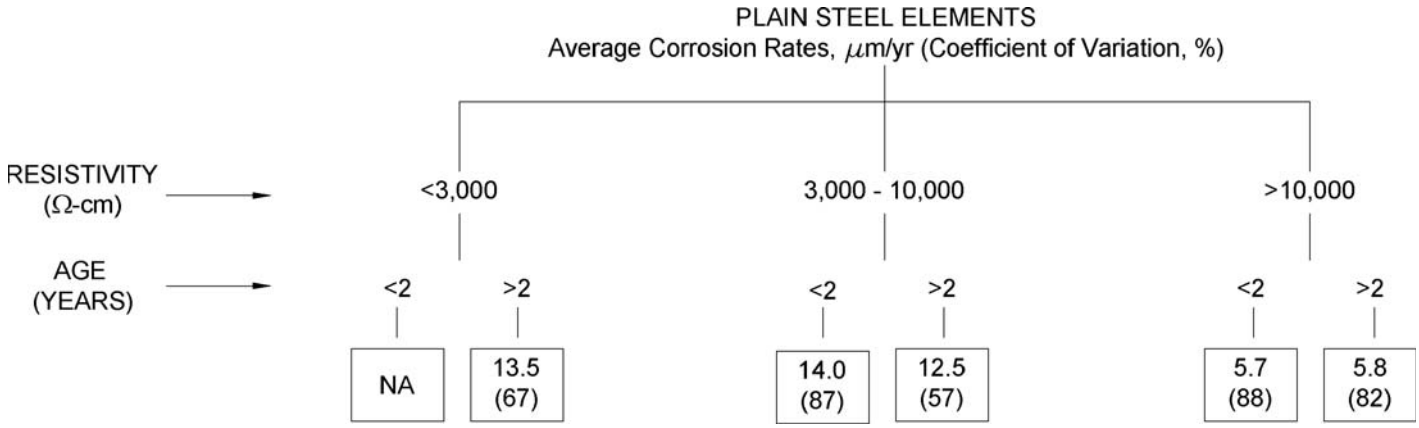

Figure 8. Summary of statistics for plain steel reinforcements (NA indicates data are not available).

southwestern, and western United States, and from weight-loss measurements from reinforcements that were exhumed from sites in Europe (Darbin et al., 1988). Since LPR measurements render corrosion rate at an instant in time, these data must be extrapolated to estimate metal loss. Metal loss is computed as the product of the measured corrosion times the age of the reinforcement, adjusted for higher corrosion rates assumed to occur during the first 2 years of service. Except for younger reinforcements that are less than 2 years old, it is assumed that 30 μm of zinc per side is lost during the first 2 years, and the measured corrosion rate is considered to be constant thereafter. This assumption is less significant considering older reinforcements.

Figure 9 includes approximately 404 data points from LPR measurements and 50 weight-loss measurements. Weight-loss and LPR measurements are not from the same samples, and the samples are from different sites. However, all fills meet electrochemical requirements similar to AASHTO. These data are useful to demonstrate that metal loss extrapolated from LPR measurements are in the same range as those observed directly via weight-loss measurements. Metal losses computed from LPR appear to be equal to or higher than those from weight-loss measurements. Thus, the methodology of using LPR measurements to estimate metal loss appears to be conservative (at least for the range of corrosion rates depicted in Figure 9).

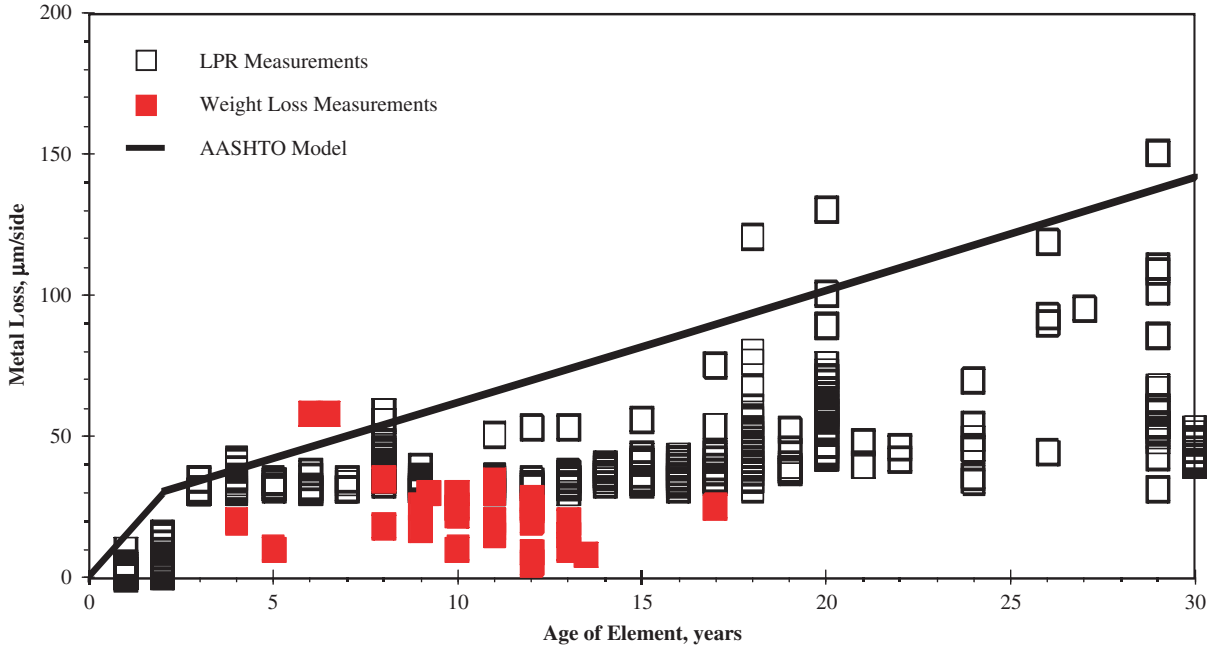

Figure 9. Comparison of LPR and weight loss measurements for galvanized elements in fill materials that meet AASHTO criteria.

For the purpose of this comparison it is assumed that all samples in Figure 9 are still coated with zinc. Thus, for the AASHTO model, the corrosion rate remains constant after 2 years (4 μm/yr). The AASHTO model appears to be a good upper limit for metal loss throughout the experience period and most of the data points lie well below the envelope described by the AASHTO model (note that many of the data points in Figure 9 overlap one another). Many of these data represent metal loss that is less than half of what is computed with the AASHTO model. This is consistent with the analysis of metal loss and corrosion rate measurements reported by Gladstone et al. (2006).

Appendix B includes data for which LPR measurements are directly compared with visual observations. Much of these data are from elements extracted during fieldwork for Task 6 performed in cooperation with Caltrans. These data demonstrate that the ratio of maximum metal loss (i.e., loss of tensile strength) to average corrosion rate or metal loss from LPR measurements ranges from 1.2 to 4.8 with a mean of 2.4. This factor appears to be inversely proportional to severity of corrosion and tends to range between 2 and 3 when more severe loss of cross section is observed.

For galvanized elements, corrosion rates via LPR correlate best with the percentage of zinc remaining on the surface. When more than 70% of the surface is covered by zinc, corrosion rates measured via LPR reflect the rate of zinc loss. However, there may be instances in which localized corrosion of steel may not be reflected in the LPR measurement of corrosion rate. This is more of an issue at sites with relatively poor or marginal quality fill materials where metal loss is less uniform and localized loss of zinc is observed. In general, corrosion rates from LPR measurements are consistent with observations of maximum metal loss considering a factor between 2 and 3 relates the average to the maximum metal loss. This is consistent with the factor of 2 commonly used to relate loss of tensile strength to uniform corrosion losses, as discussed by Elias (1990).

Trends

Data were analyzed to identify trends from corrosion rate measurements with respect to spatial and temporal variations, climate, environment (marine vs. non-marine), and fill characteristics described in terms of electrochemical parameters (ρ_{min}, pH, Cl^-, SO_4) and organics content. Details of results from data analysis and identification of trends are described in Appendix D and in the interim report that was submitted for the project in April 2007.

Spatial Variations

Consideration is given to elevation (top vs. bottom) and distance from the wall face (front vs. back). One would expect to observe increased corrosion near the top of the wall and near the wall face due to the potential for infiltration of storm water and relatively higher levels of oxygen within the fill at these locations. However, the majority of the data as described in the interim report indicates that location does not have a significant effect on measured corrosion rates. Data from one site in New York exhibits higher corrosion rates for samples located near the face compared to the backside of the reinforced fill. Data from several sites in California, where inspection elements were placed along three rows at vertical spacing of 10 feet, suggest that increased corrosion activity may occur near the top of the walls. Given the limited amount of data and lack of a clear trend, spatial variability is considered to be random for the purpose of the reliability analysis and calibration of resistance factor.

Temporal Variations

The effect of time on corrosion rates is apparent in the data. For galvanized reinforcement and fill materials that meet AASHTO requirements for electrochemical parameters, on average, lower corrosion rates are realized from samples with ages between 2 and 16 years compared to those that are younger than 2, or older than 16 years. This is due to the attenuation of corrosion rate with respect to time, and the possibility that higher corrosion rates prevail as zinc is consumed from galvanized samples. Although the upper bound of corrosion rate measurements for galvanized reinforcements less than 2 years old is close to 15 μm/yr, which is the rate included in the AASHTO model for young (<2 years old) galvanized steel reinforcements, the mean of the measurements in this time frame is only about twice as high as measurements obtained after 2 years of service. Higher corrosion rates measured after 16 years of service may be due to zinc loss and exposure of base steel; however, the measured corrosion rates are much lower than those measured for plain black steel.

Corrosion rates for plain steel attenuate with respect to time, but not as rapidly as those for galvanized elements. This is consistent with corrosion rate models that are based on Equation (1). The Darbin model, Equation (2), applies an exponent of 0.65 to the time factor to describe metal loss of galvanized reinforcements and Elias (1990) applies an exponent of 0.8 in Equation (3) to describe metal loss of plain steel elements. A higher exponent reflects a lower attenuation of corrosion rate with respect to time. These temporal variations were considered in the reliability analysis and calibration of resistance factor.

Corrosion rates do not necessarily attenuate when fill materials are of marginal quality (i.e., do not meet AASHTO criteria), indicating that a less favorable environment (e.g., high in chlorides) interferes with the formation and sustenance of a passive film layer.

Climate

Four regions within the United States were considered including the northeastern, southeastern, high plains and western states. These regions are distinguished by differences in climate, availability of suitable fill materials, use of deicing salts, and prevalence of reinforcement type. For galvanized reinforcements no significant differences were observed. Mean corrosion rates ranged between approximately 1 μm/yr and 2 μm/yr, with slightly higher means observed for the northeastern and western regions. Because there does not appear to be a significant effect of climate on measured corrosion rates, measurements from different regions are combined to evaluate the effects of backfill character, time, and reinforcement type on corrosion rates and observations of metal loss for galvanized reinforcements. Thus, data from all the regions were used to generate statistics for galvanized reinforcements used in the reliability analysis and calibration of resistance factor.

More significant variations were observed relative to corrosion rates for plain steel reinforcements. Mean corrosion rates for plain steel ranged between approximately 3 μm/yr and 20 μm/yr, with much higher corrosion rates observed for the western region. However, climate may not be the only factor, as the western states tend to use fill materials with less favorable electrochemical parameters (higher salt contents) compared to other regions including the Northeast and Southeast. These different fill conditions were considered for the reliability analysis and calibration of resistance factors. Thus, the statistics for these different climates were considered separately for plain steel reinforcements.

Environmental Conditions (Marine vs. Non-marine)

Data from coastal/marine environments, that come from locations near the coast, but are not submerged or in direct contact with saltwater, were separated from non-marine environments. Marine environments did not have a significant impact on the performance of galvanized reinforcements, however, there was a significant effect observed for plain steel reinforcements. These data demonstrate that plain steel reinforcements should not be used in marine environments. Effects on corrosion rate from use of deicing salts were not apparent in the data.

Effect of Backfill Character

The electrochemical properties of reinforced fill have a profound effect on corrosion rates, and resistivity appears to have the strongest influence, although a few data from sites with low pH (pH<4) also exhibit very high corrosion rates. Figure 10 depicts observed corrosion rates from galvanized reinforcements versus measurements of resistivity from samples of fill that are most often taken from stockpiles prior to construction. Figure 10 incorporates 489 data points from 53 sites distributed amongst the states of California, Florida, Kentucky, North Carolina, Nevada, and New York. Reinforcement ages range from 1 to 30 years with an average of 13. Therefore, data points in Figure 10 generally depict corrosion rates for zinc, particularly for $\rho > 3{,}000$ Ω-cm.

Figure 10 depicts scatter that is significantly higher considering lower levels of fill resistivity. This may be due to the variability of fill conditions at sites that are characterized as having lower quality fill, uncertainty regarding the correlation between sources of samples and fill placed during construction, and the possibility that zinc may be consumed in less than 10 years when $\rho < 3{,}000$ Ω-cm. On average, observations from sites with fill resistivities less than 3,000 Ω-cm are approximately an order of magnitude higher than observations from sites with fill resistivity greater than 3,000 Ω-cm. Observations from sites with fill resistivities between 3,000 and 10,000 Ω-cm have average corrosion rates slightly higher than those associated with resistivity greater than 10,000 Ω-cm. Based on these data a power law was regressed to achieve the "best fit" with the data rendering the following equation, which

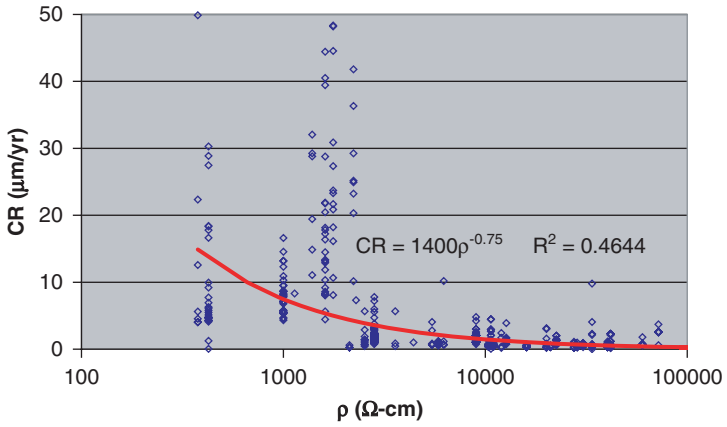

Figure 10. Observed corrosion rates versus fill resistivity for galvanized reinforcements (CR = corrosion rate).

Table 11. Computed corrosion rates for galvanized reinforcements at selected resistivities.

ρ (Ω-cm)	CR (μm/yr)
1,000	7.9
3,000	3.5
10,000	1.4
20,000	0.8

is limited to galvanized reinforcements that are less than 20 years old:

$$CR \approx 1400\rho^{-0.75} \quad (16)$$

Table 11 is a summary of corrosion rates computed with Equation (16) for selected resistivities. The corrosion rate computed at ρ = 3,000 Ω-cm is consistent with the AASHTO model for corrosion of zinc after 2 years in service (i.e., 4 μm/yr) and the corrosion rates computed at ρ = 10,000 Ω-cm and 20,000 Ω-cm are consistent with the statistics presented in Figure 7.

It also appears that corrosion rates for galvanized reinforcements are not necessarily lower than plain steel considering fill materials with low ρ_{min}. This is not surprising because it is well known that zinc does not perform better than steel for all environments.

Reliability analyses and resistance factor calibrations were performed on data groups according to selected ranges of fill resistivity, including 1,000 Ω-cm < ρ_{min} < 3,000 Ω-cm; 3,000 Ω-cm ≤ ρ_{min} < 10,000 Ω-cm; and ρ_{min} ≥ 10,000 Ω-cm. Due to the relatively high variability, marginal fills (with 1,000 Ω-cm < ρ_{min} < 3,000 Ω-cm) should be used with extreme caution. Considerably more effort is needed to sample and test these materials to reliably characterize them and select appropriate corrosion rates for use in design (Elias et al., 2009). Use of marginal material is not recommended, but guidance is developed to demonstrate the issues and level of effort required to properly manage the risk that is involved when used. Walls with fill material closer to the 3,000 Ω-cm range may become more prevalent depending on whether or not recommendations from NCHRP Project 24-22 are adopted in practice.

Metal Loss Models and Reliability

AASHTO Model—Galvanized Reinforcements

Figures 11(a) and 11(b) compare corrosion rates measured via the LPR technique to the AASHTO metal loss model (see Table 3). Figure 11(a) includes 150 data points and Figure 11(b) includes 257 data points documenting the performances of galvanized reinforcements within good and high quality fills, respectively. The highest rates of corrosion are observed from elements that are equal to or less than 2 years old, but these higher rates are less than half of the rate of 15 μm/yr included in the AASHTO model. The mean corrosion rate during the first 2 years is approximately twice the mean corrosion rate measured from elements older than 2 years.

When reinforcements are greater than 2 years old, the means of the observed corrosion rates are less than half of those anticipated on the basis of the AASHTO model. Due to the low rate of zinc loss, most of the observations reflect corrosion rates prior to depletion of the zinc coating. However, zinc may have been depleted when corrosion rates, observed from elements more than 16 years old, are greater than 4 μm/yr. This applies to two points each for Figures 11(a) and 11(b) where the average rates of steel loss for good and high quality fill may be inferred as approximately 6 μm/yr and 4 μm/yr, respectively. Considering a factor of 2 to relate observations of average (uniform) metal loss to tensile strength suggests that steel losses of 12 μm/yr and 8 μm/yr may be used to model corrosion rates for steel after zinc has been depleted from galvanized reinforcements, considering good and high quality fills, respectively.

The AASHTO model is used to compute the nominal metal loss and corresponding sacrificial steel for the calibration of resistance factors when considering galvanized elements in both good and high quality fills. A Monte Carlo analysis was performed to assess the probability that metal loss in excess of the nominal amount may occur (p_f). This analysis uses the means and standard deviations of the observations as described in Figure 7. A lognormal distribution was also assumed to describe the variations in measurements, and the validity of this assumption is verified as described in Appendix E. Because the majority of observations reflect corrosion rates for zinc, these measurements are best suited of estimating zinc life. Results from the Monte Carlo analysis render a 99% probability that zinc coating with an initial thickness of 86 μm will last 15 years considering good quality fill, and 32 years considering high quality fill. Thus, good quality fill supports zinc life similar to 16 years as predicted by the AASHTO model for z_i = 86μm, and the zinc life appears to be twice as long with high quality fill. The increased zinc life for high quality fill is due to the lower observed corrosion rates evident in Figure 11(b).

Steel loss, *X,* is assumed to commence subsequent to zinc depletion. The mean steel loss is assumed to occur at a rate of 12 μm/yr with a COV of approximately 0.66. Table 12 presents reinforcement ages corresponding to p_f equal to 0.01 and 0.05, and the probability that the sacrificial steel will not be consumed for the intended design life (75 or 100 years).

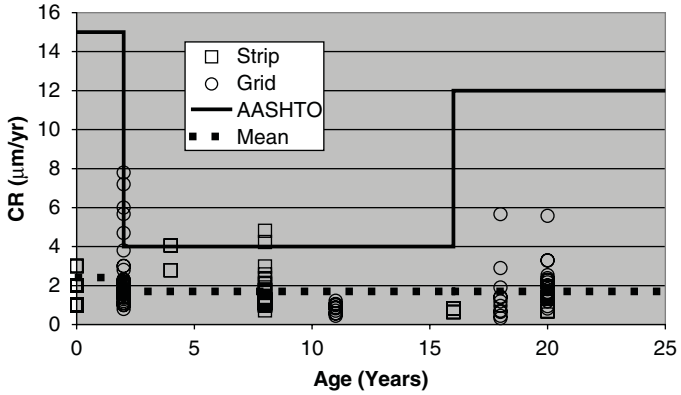

Figure 11(a). Corrosion rates vs. time and comparison with the AASHTO model for galvanized elements within good quality fill.

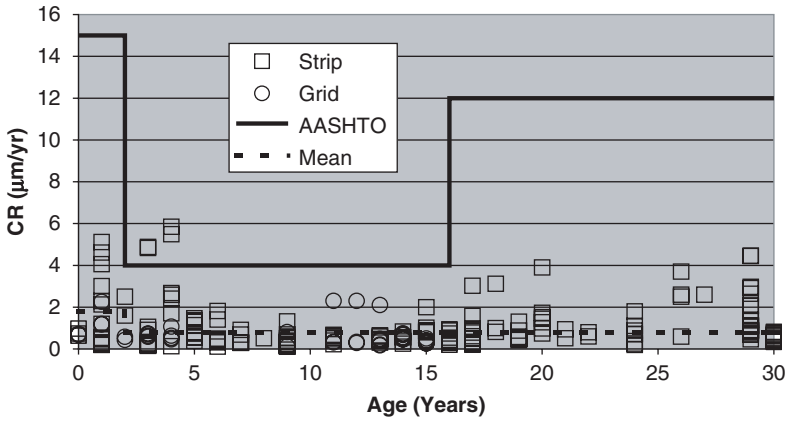

Figure 11(b). Corrosion rates vs. time and comparison with the AASHTO model for galvanized elements within high quality fill.

Based on the results in Table 12 it appears that the probability of sacrificial steel being consumed within design lives of 75 or 100 years is approximately 10% with good quality fill and 1.5% with respect to high quality fill (i.e., probabilities of 90% and 98.5% that design lives may be exceeded with good or high quality fills, respectively).

Plain Steel Reinforcements

Figures 12(a) and 12(b) compare corrosion rates measured via the LPR technique to the Elias and Stuttgart metal loss models proposed for design. Figure 12(a) includes 53 data points and Figure 12(b) includes 70 data points documenting the performances of plain steel reinforcements within good and high quality fills, respectively. Compared to data for galvanized reinforcements, the data for plain steel reinforcements are less ambiguous because only the presence of one metal type along these surfaces needs to be considered; whereas either zinc, steel or both may be present along the surfaces of galvanized reinforcements. Measured corrosion rates plotted in Figures 12(a) and 12(b) were multiplied by a factor of 2 to reflect higher rates of localized corrosion inherent to the behavior of buried steel elements. Significant attenuation of mean observed corrosion rates with respect to time is not

Table 12. Occurrence of sacrificial steel consumption for galvanized reinforcements.

Fill Quality	t_{design} (years)	X (μm)	$p_f = 0.01$ (years)	$p_f = 0.05$ (years)	p_f @ t_{design}
Good	75	708	54	69	0.075
	100	1,008	65	84	0.116
High	75	708	75	102	0.010
	100	1,008	86	118	0.022

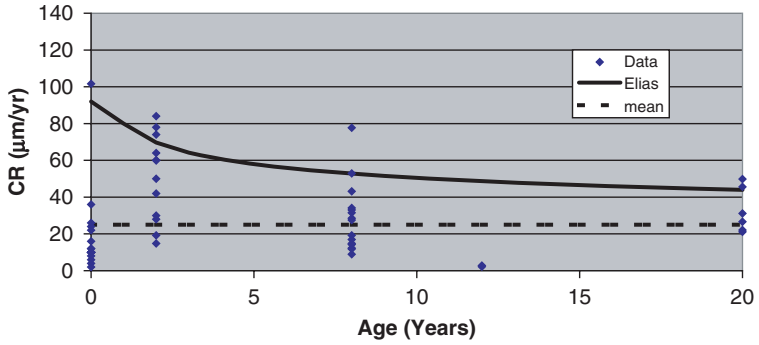

Figure 12(a). Corrosion rates vs. time and comparison with the Elias model for plain steel elements within good quality fill.

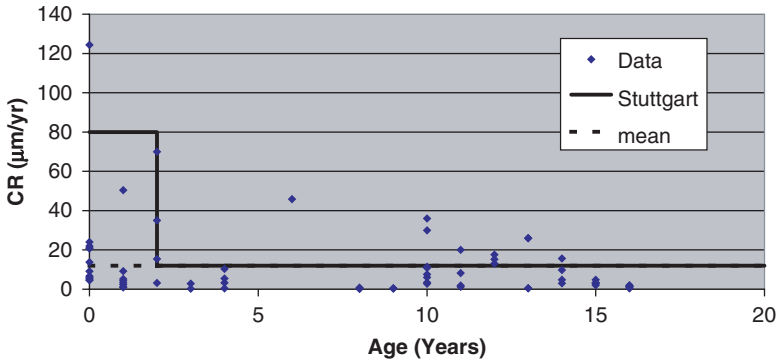

Figure 12(b). Corrosion rates vs. time and comparison with the Stuttgart model for plain steel elements within high quality fill.

observed. However, more scatter is evident in these data compared to galvanized reinforcements [Figures 11(a) and 11(b) compared to Figures 12(a) and 12(b)].

The Elias model described by Equation (3), and the Stuttgart model as described in Appendix A, are considered for design of plain steel reinforcements and the calibration of resistance factors considering good and high quality fill conditions, respectively. Given the nonlinear form of Equation (3) (Elias model) the differences between the mean of the observed corrosion rates and the Elias model, depicted in Figure 12(a), are inversely proportional to age/design life. Considering a design life of 50 years, the Elias model renders a mean corrosion rate (averaged over 50 years) of 37 µm/yr, compared to the observed mean of 25 µm/yr based on measurements obtained from reinforcements with ages spanning 20 years. The mean of observed corrosion rates from reinforcements within high quality fill is similar to the Stuttgart model (12 µm/yr) for plain steel reinforcements that are older than 2 years. Higher rates are used in the Stuttgart model for the first 2 years of service; however, this is not very important considering a service life of 75 years.

A Monte Carlo analysis was performed to assess the probability that metal loss in excess of the nominal amount may occur (p_f). This analysis uses the means and standard deviations of the observations as described in Figure 8. A lognormal distribution was also assumed to describe the variations in measurements and the validity of this assumption is verified as described in Appendix E. Design lives of 50 and 75 years are considered for plain steel reinforcements within good and high quality fills, respectively. Given the uncertainty associated with variations of observed performance, and lack of data from reinforcements older than 20 years, estimations of sacrificial steel requirements for longer service lives are considered dubious. Table 13 summarizes results from the Monte Carlo simulations of service life. Due to the higher variance inherent to the observed performances, probabilities of exceeding estimated metal losses are higher for plain steel reinforcements than for galvanized reinforcements (Table 12 compared to Table 13). This will be reflected in relatively lower calibrated resistance factors used to achieve the same overall probability that MSE designs will meet the intended service life.

Table 13. Occurrence of sacrificial steel consumption for plain steel reinforcements.

Fill Quality	t_{design} (years)	X (μm)	$p_f = 0.01$ (years)	$p_f = 0.05$ (years)	p_f @ t_{design}
Good	50	1,829	25	35	0.16
High	75	1,036	20	33	0.31

Marginal Quality Fill

Figure 13 compares corrosion rates measured via the LPR technique to the metal loss model proposed for design [Jackura et al. (1987) and described subsequently with Equation 17(a)]. These figures include approximately 200 data points documenting the performances of galvanized reinforcements within marginal quality fill. Performance data were obtained from 11 sites distributed amongst California, Nevada, New York, and North Carolina. Much higher scatter is evident in these data compared to corrosion rates observed from good and high quality fills. Higher scatter may be attributed to uncertainties with respect to fill resistivity. Samples, corresponding to these 11 sites, were collected from different locations or sources (stockpiles) but the destinations of these fills relative to specific locations within MSE wall constructions are unknown. Furthermore, characteristics including salt content are not homogeneous and can vary spatially with corresponding variations in the related resistivity.

Often results from five to 10 resistivity measurements are available and used to represent fill conditions for a particular site. These measurements depict a range with some measurements above 3,000 Ω-cm, and some below 1,000 Ω-cm. This is significant because resistivities neighboring 1,000 Ω-cm appear to be a threshold, and substantially higher corrosion rates are realized at resistivities below this threshold. Thus, although a site may be classified as having marginal quality fill, depending on location within the fill and the actual sources used during construction, there may be locations that have resistivity higher than 3,000 Ω-cm, or less than 1,000 Ω-cm. This is reflected in large scatter in the data as depicted in Figure 13 where measured corrosion rates obtained from a particular site on the same day may vary from less than 4 μm/yr to more than 25 μm/yr.

Due to the paucity of data between 2 and 10 years of service, statistics are generated for the first 2 years of service (μ = 2.4 μm/yr and σ = 1.6 μm/yr) and after 10 years of service (μ = 4.6 μm/yr and σ = 6.3 μm/yr). These statistics demonstrate that the corrosion rates for marginal quality fill are approximately two to three times higher than those observed from good quality fills.

A Monte Carlo simulation was performed to estimate zinc life assuming a lognormal distribution of corrosion rates. There are no data from reinforcements between the ages of 2 and 10 years so the statistics from reinforcements less than or equal to 2 years old are assumed to apply until the reinforcements have been in service for 10 years. Results from the Monte Carlo analysis render a 99% probability that zinc coating with an initial thickness of 86 μm will last 10 years considering marginal quality fill. This compares with 16 years and 32 years for galvanized reinforcements within good and high quality fills, respectively. Thus, the use of marginal quality fills appears to have a significant effect on zinc life, and zinc life is approximately 60% of that expected with good quality fills.

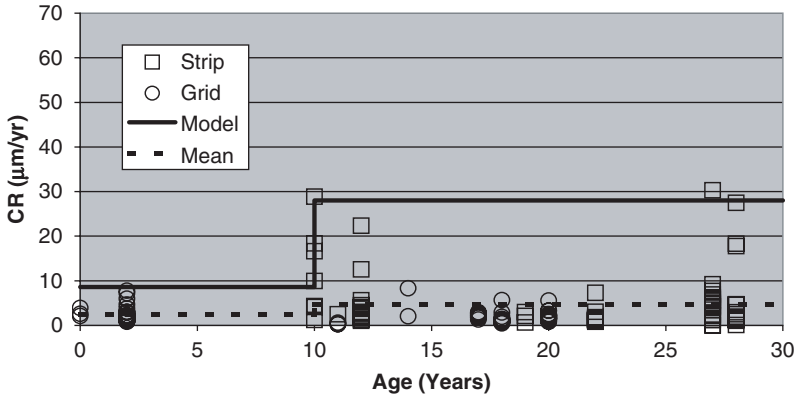

Figure 13. Corrosion rates vs. time and comparison with the Jackura model for galvanized elements within marginal quality fill.

Due to the high scatter inherent to these data and uncertainties with respect to fill properties, conservative assumptions are made regarding zinc life and corrosion rates of base steel subsequent to zinc deletion. For the purpose of estimating service life, zinc life is assumed to be constant and equal to 10 years (with $z_i = 86$ μm) and the observed corrosion rate of steel subsequent to zinc depletion is taken as 32 μm/yr with standard deviation of 21 μm/yr and a lognormal distribution. The corrosion rate of steel is based on observations from galvanized reinforcements after 8 years of service with the lower corrosion rates (i.e., < 4 μm/yr) culled from the data as described in Appendix E.

The model used to compute nominal sacrificial steel requirements for design is similar to the recommendations described by Jackura et al. (1987) for "neutral" fill with ρ > 1,000 Ω-cm and salt contents limited as described in Table 2 (Caltrans-Interim model). This model assumes that steel is exposed on the surface of galvanized reinforcements ($z_i = 86$ μm) after 10 years of service and that the base steel will corrode at an average rate of 28 μm/yr subsequent to zinc depletion.

Two different metal loss models are studied to illustrate how this affects the reliability of service life estimates. The first model (Model I) is from Jackura et al. (1987) for "neutral" fill and the second model (Model II) is a similar form, but with double the corrosion rate for steel as follows:

$$\text{Model I}: X(\mu\text{m}) = (t_{design} - 10)\, years \times 28 \frac{\mu\text{m}}{year} \tag{17a}$$

$$\text{Model II}: X(\mu\text{m}) = (t_{design} - 10)\, years \times 56 \frac{\mu\text{m}}{year} \tag{17b}$$

A Monte Carlo analysis was performed to assess the probability that metal loss in excess of the nominal amount may occur (p_f). This analysis uses the means and standard deviations of the observations as described in the preceding paragraphs and as depicted in Figure 7. A lognormal distribution was also assumed to describe the variations in measurements and the validity of this assumption is verified as described in Appendix E. Design lives of 50 years are considered for galvanized steel reinforcements within marginal quality fills. Given the uncertainty associated with variations of observed performance, and lack of data from reinforcements older than 25 years, estimations of sacrificial steel requirements for longer service lives are considered dubious. Table 14 summarizes results from the Monte Carlo simulations of service life when nominal sacrificial steel requirements are estimated with Models I and II.

Table 14 shows that the probabilities of sacrificial steel consumption are significantly affected by the nominally computed sacrificial steel requirements (i.e., the amount of sacrificial steel estimated for a 50-year design life according to Model I or Model II). In principal, different resistance factors computed with different nominal models should offset the differences in nominal sacrificial steel requirements, rendering similar design as long as the COVs of the different bias distributions are also similar. Resistance factors will be calibrated in the next section that will render the probability that reinforcements will be overstressed during their design life to be similar, independent of the metal loss model that is selected (i.e., resistance factors may be calibrated for each model to render the same p_f). The effect of the different models on steel requirements is illustrated in the design example presented in Appendix F.

Calibration of Resistance Factors

Galvanized Reinforcements

Data included in Appendix D include observations from galvanized reinforcements and coupons, and from plain steel (i.e., not galvanized) elements. In-service reinforcements and coupons are placed in the same fill conditions but have very different dimensions, and coupons may be placed at both front and back locations with respect to the wall face. Data from in-service reinforcements and coupons were compared, and, on the basis of this comparison, the decision was made to include them in one data set, thus enhancing the quantity of data within each partition.

Metal loss is considered in the resistance factor calibration where the bias of remaining strength (i.e., ratio of measurements to nominal value used in design) is computed as Equation (15). The nominal remaining strength used in design and in the denominator of Equation (15) is computed as described in Equations (10) through (14) with values of r_{z1}, r_{z2}, and r_s from the metal loss model recommended by AASHTO for assessing metal loss of galvanized reinforcements, and described in Tables 2 and 3. Since the oldest MSE walls are approximately 40 years old, direct measurements of remaining strength after

Table 14. Occurrence of sacrificial steel consumption for galvanized steel reinforcements in marginal quality fill.

Design Model	t_{design} (years)	X (μm)	$p_f = 0.01$ (years)	$p_f = 0.05$ (years)	p_f @ t_{design}
Model I	50	1,120	18	24	0.44
Model II	50	2,240	28	40	0.11

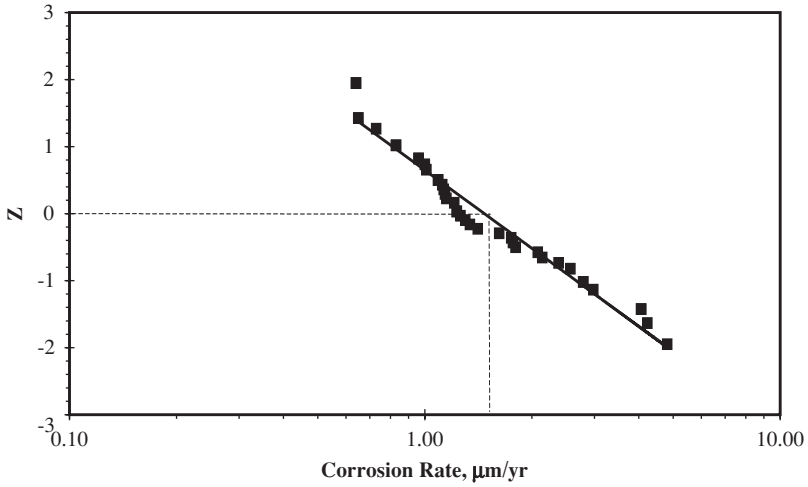

Figure 14. Probability plot depicting lognormal distribution for data describing corrosion rates of galvanized reinforcements within good quality fill.

a service life of 75 or 100 years are not available. Therefore corrosion rate measurements must be extrapolated to estimate "measurements" of remaining strength used in the numerator of Equation (15). The extrapolation also employs equations similar to Equations (10) through (14), but with corrosion rates r_{z1}, r_{z2}, and r_s from the observed performance of reinforcements during service. This approximation is considered conservative due to the likely attenuation of corrosion rate with respect to time. The corrosion rates used to extrapolate metal loss are considered constants over prescribed time intervals, and are higher than those expected to prevail at the end of service.

Figures 14 and 15 are examples of inputs and intermediate results from the calibration exercise. Tables 15 to 18 summarize the final results from the calibration. The following list describes the steps involved in the calibration process and generation of resistance factors using the Monte Carlo Technique:

a) Generate statistics from observations for corrosion rates including the mean (μ), standard deviation (σ), and the shape of the probability density function (pdf). It is important to select the correct shape of the pdf to represent the data. Probability plots similar to the one depicted in Figure 14 are used to check the match between the empirical

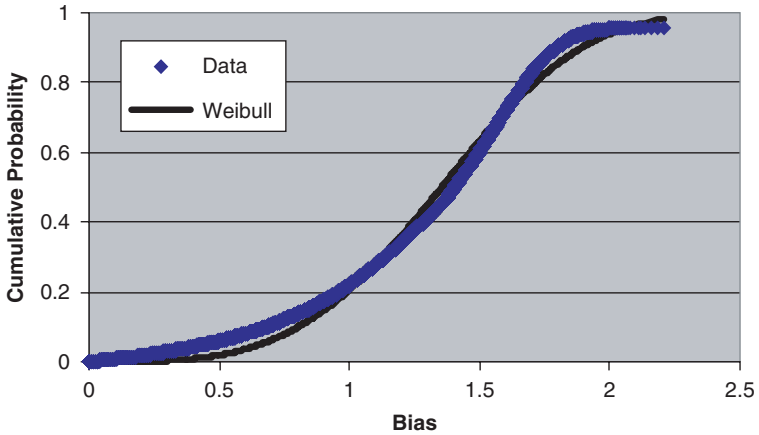

Figure 15. Typical plot showing Weibull distribution $\left(f(x)=1-e^{-\left(\frac{x}{\alpha}\right)^{\beta}}\right)$ ***for bias; galvanized strip reinforcement with S = 4 mm, t_f =75 years; α = 1.5, β = 1.6 corresponding to mean = 1.35 and standard deviation = 0.42.***

Table 15. Summary of ϕ for conservative steel model.

Reinforcement Type	Design Life	Reinforcement Thickness	ϕ Simple/Coherent
Strip	75 years	4 mm	0.45/0.35
		5 mm	0.45/0.35
		6 mm	0.50/0.40
	100 years	4 mm	0.25/0.15
		5 mm	0.30/0.20
		6 mm	0.25/0.20

data frequencies and the theoretical pdf. Probability grids similar to Figure 14 are generated for each variable used to describe corrosion rates and metal loss. In most cases lognormal distributions were found to fit well with the observed corrosion rates.

b) Extrapolate metal loss to the end of the selected service life using the statistics of observed corrosion rates and corresponding assumptions regarding the trends of corrosion rates with respect to time.
c) Compute the remaining tensile strength, T_{rem}, and the statistics of the resistance bias, λ_R, via Monte Carlo simulations. The distribution of λ_R is modeled with a pdf. The bias distributions were modeled with either normal, lognormal, or Weibull distributions. Probability plots similar to the one depicted in Figure 15 are prepared to check the match between the empirical data frequencies and the theoretical pdf.
d) Compute β and corresponding p_f for an assumed value of ϕ.
e) Iterate on ϕ to converge to the desired target reliability index, β_T. Tables 15 to 18 summarize the resistance factors, ϕ, that converge to β_T for the different cases considered (e.g., galvanized reinforcements in good or high quality fill).

As shown in Figure 7 and discussed in the previous section, the statistics of corrosion rate measurements are different for fill materials that are considered good enough to meet AASHTO electrochemical requirements (good fill), and those that exceed AASHTO requirements by a wide margin (high quality fill). Therefore, resistance factors are calibrated with respect to fill quality (i.e., good fill and high quality fill).

Table 16. Effect of z_i on computed ϕ; S = 4 mm, t_f = 75 years.

z_i (μm)	λ_R		ϕ
	μ	σ	
86	1.35	0.42	0.35
150	1.54	0.26	0.65

Table 17. Summary of ϕ for the zinc residual steel model.

Reinforcement Type	Design Life	Reinforcement Thickness/Size	ϕ Simple/Coherent
Strip	75 years	4 mm	0.70/0.65
		5 mm	0.65/0.55
		6 mm	0.65/0.55
	100 years	4 mm	0.55/0.50
		5 mm	0.60/0.50
		6 mm	0.65/0.50
Grid	75 years	W7	0.60/0.50
		W9	0.60/0.50
		W11	0.60/0.50
		W14	0.55/0.50
	100 years	W7	0.55/0.45
		W9	0.55/0.45
		W11	0.55/0.45
		W14	0.55/0.45

Good Quality Fill

Good quality fill meets AASHTO requirements for electrochemical and mechanical properties, and has ρ_{min} in the range of 3,000 Ω-cm and 10,000 Ω-cm. The statistics for reinforcements that are between 2 and 16 years, shown in Figure 7, are considered representative of the life of the zinc coating. Thus, the corrosion rate for zinc is assumed to be constant with respect to time with a mean rate of 1.7 μm/yr (r_{z1} and r_{z2}) and standard deviation of 1.09 μm/yr. The distribution is modeled as lognormal based on the probability plot depicted in Figure 14. The data shown in Figure 14 plot close to a straight line with a coefficient of correlation, $R^2 = 0.96$. Probability plots, similar to Figure 14, depicting the distributions used for other corrosion rate measurements described in this report are included in Appendix E.

Given the average rate of zinc loss (1.7 μm/yr), and since measurements were made on reinforcements that are less

Table 18. Summary of ϕ considering high quality fill.

Reinforcement Type	Design Life	Reinforcement Thickness/Size	ϕ Simple/Coherent
Strip	75 years	4 mm	0.85/0.70
		5 mm	0.75/0.65
		6 mm	0.70/0.60
	100 years	4 mm	1.0/0.85
		5 mm	0.85/0.70
		6 mm	0.75/0.65
Grid	75 years	W7	0.75/0.65
		W9	0.70/0.60
		W11	0.65/0.55
		W14	0.65/0.55
	100 years	W7	0.90/0.75
		W9	0.80/0.70
		W11	0.80/0.65
		W14	0.75/0.60

than 30 years old, very few measurements are available to describe the corrosion of steel after zinc has been consumed from a galvanized reinforcement. Two different assumptions are applied as described by Elias (1990) that either (1) consider the base steel to corrode at the same rate as plain black steel (i.e., not galvanized) or (2) assume that the base steel will corrode at a rate similar to that prevailing as zinc is finally consumed (i.e., corrosion rate does not change abruptly after zinc is consumed). In addition, "measured" corrosion rates for steel were multiplied by 2 to render loss of tensile strength from LPR measurements.

A conservative model for steel consumption assumes that the base steel corrodes at the same rate as plain steel (i.e., not galvanized) after the sacrificial zinc layer is consumed. Most of the data used for corrosion rates of plain steel embedded in fill materials meeting current AASHTO guidelines are from plain steel coupons installed at MSE sites located in California, New York, and Florida. The statistics of this data set render a mean corrosion rate and standard deviation of 27 μm/yr and 18 μm/yr, respectively; and the distribution can be approximated as lognormal.

A resistance bias is computed for different sizes of strip-type reinforcements (4 mm, 5 mm, and 6 mm) and both 75- and 100-year service lives. The bias tends to decrease with respect to increase in reinforcement size, and is higher considering longer service life. The mean resistance bias, $\lambda_{R,}$ ranges between 1.2 and 1.5 with COV approximately 40% and a distribution that is approximated as a Weibull distribution (Vardeman, 1994). Figure 15 is a typical plot showing the distribution of the computed bias.

Resistance factors are calibrated using the computed statistics for resistance bias and load bias from the literature. Table 15 summarizes the results of the resistance factor calibration applicable to the conservative steel loss estimate. The resistance factors do not vary significantly with respect to reinforcement size but are lower when considering longer service life. Resistance factors of approximately 0.45 and 0.25 apply to 75- and 100-year service lives, respectively. Resistance factors calibrated using the coherent gravity model are slightly lower. The efficiency factor is approximately 0.38 for a design life of 75 years and 0.2 for a design life of 100 years.

Additional calibrations were performed to investigate the effect of initial zinc thickness on the computed resistance factors. Table 16 compares results obtained with z_i equal to 86 μm and 150 μm per side. The comparison considers 4-mm-thick galvanized strip reinforcements, a design life of 75 years, and the same statistics for metal loss (i.e., zinc and steel) as described for galvanized reinforcements with the conservative steel model. The load bias used in the calibration corresponds to the coherent gravity method. In each case the computed resistance bias has a Weibull distribution similar to that shown in Figure 15. The computed resistance factor for $z_i = 150$ μm is 0.65 and compared to the case with $z_i =$ 86 μm, this result is closer to the current AASHTO specifications ($\phi = 0.75$). In this case z_i has a significant effect on the computed ϕ, which demonstrates that zinc thickness is an important variable to include in resistance factor calibrations. However, data on initial zinc thickness are needed to properly characterize the inherent variation and to incorporate the statistics into a reliability analysis. Use of $z_i = 86$ μm corresponds to the minimum requirement and is a conservative approach to modeling initial zinc thickness.

The zinc residual model for steel consumption considers that the corrosion rate of the base steel is affected by the presence of zinc residuals. Zinc residuals passivate the steel surface and include a zinc oxide film layer adhered to the metal surface and zinc oxides within the pore spaces of the surrounding fill. There are very few measurements describing corrosion rates of base steel after zinc has been consumed. A few observations may be applicable from the data set collected in Europe (Darbin et al., 1988) wherein zinc is consumed relatively rapidly (i.e., within a few years) and from measurements made on walls in the United States that are approaching 30 years of age. Rapid zinc consumption from some of the earlier sites in Europe is due to a relatively thin zinc coating ($z_i = 30$ μm) and moderately corrosive reinforced fill materials. A review of these data renders corrosion rates for steel that are close to 12 μm/yr. This is the metal loss model recommended by AASHTO and is adopted as a basis for comparison with calibrations performed by extrapolating measured corrosion rates with the conservative steel model. Similar to other data sets, a COV of 60% and a lognormal distribution is used to describe the variation.

The calibration was performed for both strip- and grid-type reinforcements. The mean of the resistance bias is approximately 1.4 with COV approximately 20% and a distribution that is approximately normal. Table 17 is a summary of the resistance factors calibrated with metal loss measurements extrapolated with the zinc residual model for steel loss. These resistance factors are significantly higher than those obtained with the conservative steel model (Table 15) and are in the range of 0.60 to 0.70 for strip-type reinforcements, and 0.50 to 0.60 for grids. The efficiency ratio for this case is approximately 0.5 and represents an improvement compared to the case in which metal loss measurements are extrapolated via the conservative steel model.

High Quality Reinforced Fill (ρ > 10,000 Ω-cm)

High quality reinforced fills have $\rho_{min} > 10{,}000$ Ω-cm and corrosion rates corresponding to these conditions were observed from sites in Florida (Sagues et al., 1998; Berke and Sagues, 2009) and North Carolina. These data render mean and standard deviation of corrosion rates for the zinc coating

of 0.8 μm/yr and 0.5 μm/yr, respectively, for strip-type reinforcements, and 0.5 μm/yr and 0.2 μm/yr, respectively for grid-type reinforcements. Corrosion rates observed from plain steel coupons older than 16 years correspond to mean and standard deviation values of 11.5 μm/yr and 9.4 μm/yr, and these parameters are used to represent the loss of base steel subsequent to depletion of the zinc coating for this case. Both of these distributions are modeled as lognormal. The mean of the corresponding resistance bias is computed as ranging from 1.4 to 2.0 with COV approximately 10%. The bias distribution is approximately normal considering a 75-year service life, but is better represented by a Weibull distribution considering a 100-year service life.

Table 18 is a summary of the resistance factors calibrated with metal loss measurements from sites with high quality reinforced fill. These resistance factors are equal to or higher than those currently specified by AASHTO (see Table 7). The efficiency ratio for this case is approximately 0.5. Changing the initial zinc thickness from 86 μm to 150 μm per side did not have a dramatic effect on the computed resistance factors compared to the case with good quality backfill and the conservative steel model. This is because the resistance factors computed with z_i = 86 μm considering high quality fill are closer to one.

The resistance factors summarized in Tables 17 and 18 correspond to the target reliability index ($\beta_T = 2.3$ corresponding to $p_f = 0.01$). However, other values of ϕ corresponding to different levels of reliability are also of interest. Table 19 compares the relationship between resistance factors and reliability in terms of β and p_f, for different scenarios involving good or high quality fill, and strip or grid-type reinforcements. Table 19 considers typical galvanized strip reinforcements with $S = 4$ mm and grids with W11 longitudinal wires. On the basis of data depicted in Table 19, alternative approaches may be contemplated for selecting resistance factors for design rather than calibrating to achieve a target reliability index.

For example, consider applying the resistance factors as they stand in the current version of the AASHTO specifications (AASHTO, 2009), where $\phi = 0.75$ and 0.65 for strip- and grid-type reinforcements, respectively. Thus, for designs with strip-type reinforcements the probability (p_f) that stress in excess of yield will occur before the end of the intended design life is 0.005 and 0.015, respectively for construction employing high quality and good quality fill. Similarly, for designs with grid-type reinforcements, p_f would correspond to 0.008 and 0.018. Thus, MSE walls designed in accordance with current AASHTO specifications, and constructed with high quality fills, have a more favorable p_f compared to the target of 0.01. Based on the statistics of the current inventory described by AMSE (2006), this exceptional performance applies to approximately 80% of MSE walls in the existing inventory. The remaining 20%, constructed with good quality fill, are associated with a lower level of performance, and a p_f that is nearly twice the target valued of 0.01.

Verification of Monte Carlo Analysis

Results from the Monte Carlo simulations used to calibrate resistance factors are verified via comparison incorporating alternative formulations for computing resistance bias and closed-form solutions for reliability index. Although the closed-form solutions are limited to particular distributions of the bias variables, they render estimates for comparison and illustrate the effect of incorporating more realistic distributions via Monte Carlo simulations. In general, the verification study is performed as follows:

Step 1. Select a design life and compute the distribution of metal loss using the service life model described by Sagues et al. (2000).

Step 2. Compute the bias of the remaining cross-sectional area, λ_{Ac}, as the ratio of remaining cross section based

Table 19. Comparison of relationship between ϕ and β for different fill quality.

ϕ	Strip Reinforcements (S = 4 mm)				Grid Reinforcements (W11)			
	High Quality Fill		Good Quality Fill		High Quality Fill		Good Quality Fill	
	β	p_f	β	p_f	β	p_f	β	p_f
0.55	3.12	0.001	2.73	0.003	2.99	0.0014	2.49	0.006
0.60	2.97	0.0015	2.64	0.004	2.63	0.004	2.24	0.012
0.65	2.93	0.002	2.42	0.008	2.41	0.008	2.09	0.018
0.70	2.72	0.003	2.30	0.010	2.13	0.016	1.93	0.026
0.75	2.56	0.005	2.17	0.015	2.11	0.017	1.79	0.036
0.80	2.48	0.006	2.04	0.020	1.96	0.025	1.69	0.045
0.85	2.27	0.011	1.91	0.028	1.80	0.035	1.52	0.063
0.90	2.19	0.014	1.80	0.036	1.67	0.047	1.39	0.082

ϕ calibrated for target reliability index $\beta_T = 2.3$ corresponding to $p_f = 0.01$.

ϕ based on current AASHTO specifications (AASHTO, 2009).

on metal loss measurements to the remaining cross section based on nominal metal loss used in design.

Step 3. Compute the bias of the remaining tensile strength, λ_R, as the product of the random variables including the bias of remaining cross section determined in Step 2, and the bias for yield strength.

Step 4. Compute β as a function of resistance factor using the bias of remaining tensile strength determined in Step 3 and available closed-form solutions.

Sagues Formulation

Sagues et al. (2000) formulated a probabilistic deterioration model for service life forecasting of galvanized soil reinforcements. This formulation is based on the following assumptions, which are the same as those employed in the Monte Carlo simulations:

- The distribution of corrosion loss over all elements in the structure mirrors the overall distribution of corrosion measured in the field;
- During the early life of the structure, the corrosion rate distribution reflects that of the galvanized elements;
- Loss of base steel is initiated after the zinc coating is consumed;
- The highest rate of metal loss takes place in the region of maximum reinforcement stress, and the service life of a given element is over when the sacrificial steel in the highest stressed region is consumed; and
- Corrosion rates are constant with time.

The resulting formula to compute the probability that metal loss, X, exceeds a given threshold, X', is given by

$$P\left[X > X' \middle| t_f, z_i, r_z, \sigma_z, r_s, \sigma_s\right] = \int_{r_0}^{\infty} f_z(r_z)\left(1 - F_s\left(\left(X'\right)/\left(t_f - z_i/r_z\right)\right)\right)dr_z \qquad (18)$$

where

P is probability;
X is loss of steel defined by t_f, z_i, r_z, σ_z, r_s, σ_s;
X' is a given amount of steel loss;
t_f is service life;
z_i is the initial zinc thickness;
r_z is the mean zinc corrosion rate;
σ_z is the standard deviation of zinc corrosion rate;
r_s is the mean steel corrosion rate;
σ_s is the standard deviation of steel corrosion rate;
$r_0 = z_i/t_f$ and is the lowest rate of zinc corrosion for which base steel will be consumed within t_f;
$f_z(r_z)$ is the pdf representing zinc corrosion rates, r_z; and
F_s is the cumulative density function (cdf) representing steel corrosion rates.

Equation (18) was programmed into an Excel spreadsheet and the integration performed numerically. The numerical integration was performed in increments between 0.1 and 0.01 times r_0. In most cases convergence to within E-06 was achieved within 100 increments. The numerical integration was performed for a range of X and the corresponding probabilities of exceedance computed for a given service life. For each value of X the bias of the remaining cross section (strip-type reinforcement) is computed as

$$\lambda_{Ac} = \frac{\left(S - 2\times X\right)}{\left[S - 2\times 12\times\left(t_f - C\right)\right]} \qquad (19)$$

wherein the AASHTO metal loss model (Eq. 5) is used in the denominator to compute nominal remaining cross section. A mean and standard deviation were determined from the distribution of the computed bias to describe the variation of λ_{Ac}. The bias of the remaining tensile strength was then computed as:

$$\lambda_R = \lambda_{Ac} \times \lambda_{Fy} \qquad (20)$$

where λ_{Fy} is the bias of the yield stress. Assuming that λ_{Fy} and λ_{Ac} are uncorrelated and their statistics are known, the mean and standard deviation of λ_R could be computed using well known relationships between functions of random variables as described by Baecher and Christian (2003).

Closed-Form Solutions for Reliability Index

For a specific limit state and a single load source, the reliability index (β) and the resistance factor (ϕ) can be related using the following formula (Allen et al., 2005), which assumes that the load and resistance bias both have normal distributions:

$$\beta = \frac{\left(\frac{\gamma_Q}{\phi_R}\right)\lambda_R - \lambda_Q}{\sqrt{\left(\mathrm{COV}_R\left(\frac{\gamma_Q}{\phi_R}\right)\lambda_R\right)^2 + \left(\mathrm{COV}_Q\lambda_Q\right)^2}} \qquad (21)$$

where

β = reliability index (dimensionless),
γ_Q = load factor (dimensionless),
ϕ_R = resistance factor (dimensionless),
λ_Q = mean of load bias (dimensionless),
λ_R = mean of resistance bias (dimensionless),
COV_Q = coefficient of variation of load bias (dimensionless), and
COV_R = coefficient of variation of resistance bias (dimensionless).

In the case of lognormal distributions for load and resistance bias:

$$\beta = \frac{\ln\left[\frac{\gamma_Q \lambda_R}{\phi_R \lambda_Q}\sqrt{\left(1+\mathrm{COV}_Q^2\right)/\left(1+\mathrm{COV}_R^2\right)}\right]}{\sqrt{\ln\left[\left(1+\mathrm{COV}_Q^2\right)\left(1+\mathrm{COV}_R^2\right)\right]}} \quad (22)$$

For a given load factor and known load and resistance statistics, Equations (21) and (22) are satisfied for selected values of resistance factors, rendering related pairs of reliability indices and resistance factors. From the computed pairs of β versus ϕ_R, resistance factors can be selected corresponding to the targeted level of reliability.

Table 20 presents selected results and compares resistance factors computed via Monte Carlo simulations to those computed via the Sagues service life model and closed-form solutions for β. The load bias used in these analyses refers to the coherent gravity method and is a lognormal distribution (D'Appolonia, 2007). A Weibull or normal distribution is used to describe the variation of λ_R.

Results are presented for two cases: (1) where the probability density function (pdf) for λ_R used in the Monte Carlo simulation is normal, and (2) where the pdf is described with a Weibull function. Because the closed-form solutions only consider probability density functions to be normal or lognormal this comparison demonstrates the importance of properly capturing the distribution of the pdf in the analysis, and the need for numerical simulations (i.e., Monte Carlo simulations). Table 20 demonstrates that when λ_R is normally distributed, the comparisons between the Monte Carlo simulations and the closed-form solutions are very good. Note that since the distribution of load bias is lognormal, the closed-form solution, assuming a normal distribution for both λ_R and λ_Q, does not always give the best results, even when λ_R is normally distributed.

Alternatively, when λ_R is described with the Weibull function, the closed-form solutions, which consider the distribution to either be normal or lognormal, do not necessarily compare very well with the results from the more robust Monte Carlo simulations. Therefore, numerical analyses (e.g., Monte Carlo simulations) are necessary to properly model the distribution of λ_R.

Plain Steel Reinforcements

Resistance factor calibrations are performed considering the use of plain steel (i.e., not galvanized) reinforcements. The purpose of these calibrations is to define design parameters that are appropriate for plain steel reinforcements and demonstrate the advantage of using galvanized reinforcements. Since the use of plain steel reinforcements has been limited, most of the data from the performance of plain steel reinforcements are from coupons placed at sites where galvanized in-service reinforcements are employed. The few examples where plain steel reinforcements have been used in the United States are for grid-type reinforcements, as plain steel strip-type reinforcements are not readily available. Therefore, the calibration is performed for grid-type reinforcements. The calibration is performed considering reinforced fill quality that meets AASHTO criteria for electrochemical properties, and both good and high quality fill are considered.

Good Quality Fill

Based on the summary of statistics from corrosion rate measurements depicted in Figure 8, a mean corrosion rate and standard deviation of 25 μm/yr and 14 μm/yr, respectively, represent the statistics for plain steel grid-type reinforcements within good quality fill, and the distribution can be approximated as lognormal. The resistance bias is computed for different sizes of grid-type reinforcements (W7, W9, W11, and W14). The AASHTO metal loss model only applies to galva-

Table 20. Summary of comparison between closed-form solutions and Monte Carlo simulations.[1]

Reinforced Fill Quality w/Details of Steel Loss Model	Life (yrs)	Thickness (mm)	Monte Carlo		Closed-Form	
					Normal	Lognormal
			pdf λ_R	ϕ	ϕ	ϕ
Good w/Zinc Residuals	75	4	Normal	0.60	0.55	0.60
Good w/Conservative Steel	75	15	Normal	0.45	0.50	0.50
High Quality Fill	75	5	Normal	0.65	0.55	0.65
Good w/Conservative Steel	75	4	Weibull	0.35	NA[2]	0.25
Good w/Conservative Steel	75	6	Weibull	0.40	0.10	0.35
High Quality Fill	100	4	Weibull	0.85	NA[2]	0.55

[1] Coherent gravity method applied to galvanized strip type reinforcements with assumed initial zinc thickness of 86 μm. β_T =2.3 was used to compute ϕ.
[2] NA means a result is not available because $\beta > 2.3$ could not be achieved using the closed-form solution.

Table 21. Summary of ϕ considering plain steel reinforcements and good quality fill material.

Reinforcement Type	Design Life	Reinforcement Thickness/Size	ϕ Simple/Coherent
Grid	50 years	W7	0.25/0.20
		W9	0.30/0.25
		W11	0.35/0.25
		W14	0.40/0.35

Table 22. Summary of ϕ considering plain steel reinforcements and high quality fill material.

Reinforcement Type	Design Life	Reinforcement Thickness/Size	ϕ Simple/Coherent
Grid	75 years	W7	0.20/0.20
		W9	0.30/0.20
		W11	0.35/0.25
		W14	0.35/0.30

nized reinforcements, therefore, the nominal metal loss model used in the denominator of Equation (15) is based on data collected by the National Bureau of Standards for plain steel in fill materials similar to those typically used in the construction of MSE and described by Eq. (3). The analysis is limited to a 50-year service life since the sacrificial steel requirements considering 75- and 100-year service lives are considered to be impractical. Thus, a shorter service life is considered appropriate when using plain steel as opposed to galvanized reinforcements. The mean of the resistance bias, λ_R, tends to decrease with respect to increase in reinforcement size and ranges between 1.4 and 1.9 with COV between 30% and 40%, and a distribution that is approximately normal.

Table 21 summarizes the results of the resistance factor calibration. The resistance factors tend to increase with respect to reinforcement size and are approximately 0.1 to 0.15 lower than those computed for galvanized reinforcements with the conservative steel model and longer service lives as depicted in Table 15. The efficiency ratio (ϕ/λ_R) for this case is approximately 0.2, which is also lower than the efficiency ratio computed for galvanized reinforcements

High Quality Fill (ρ > 10,000 Ω-cm)

Based on the summary of statistics from corrosion rate measurements depicted in Figure 8, a mean corrosion rate and standard deviation of 12 μm/yr and 9.6 μm/yr, respectively, represent the statistics for plain steel grid-type reinforcements within high quality fill, and the distribution can be approximated as lognormal. The resistance bias is computed for different sizes of grid-type reinforcements (W7, W9, W11, and W14). For this case, the nominal metal loss model used in the denominator of Eq. (15) is based on the Caltrans-Select model (Jackura et al., 1987) described in Table 2, corresponding to r_s = 13 μm/yr. Given the more favorable sacrificial steel requirements compared to the previous case, the analysis considers service lives of 75 years. The mean of the resistance bias, λ_R, tends to decrease with respect to increase in reinforcement size and ranges between 1.1 and 1.2 with COV between 30% and 35%, and a distribution that is approximately normal.

Table 22 summarizes the results of the resistance factor calibration. The resistance factors tend to increase with respect to reinforcement size and range between 0.25 and 0.35. The efficiency ratio (ϕ/λ_R) for this case is approximately 0.25.

Marginal Fill Quality

Resistance factors are calibrated considering the use of fill that does not meet AASHTO criteria for electrochemical parameters as described in Table 3. Fill with pH in the range of five to seven, but with ρ_{min} between 1,000 Ω-cm and 3,000 Ω-cm is referred to as marginal quality fill. This calibration is performed considering the use of galvanized reinforcements and a 50-year service life.

Based on the analysis of the observed corrosion rates for marginal fill, and the paucity of data for reinforcements less than 10 years old, extrapolations of metal loss assume that the zinc coating will survive 10 years. Corrosion rate measurements are available from six sites located in California that appear to reflect corrosion rates of base steel subsequent to depletion of the zinc coating. A mean corrosion rate and standard deviation of 32 μm/yr and 21 μm/yr, respectively, and a lognormal distribution are used to describe the statistics of these measurements. These statistics appear to be conservative compared to corrosion rates observed from plain steel elements that are more than 10 years old at the time of measurement as described in Appendix E.

Computations of resistance bias and corresponding calibrations of resistance factors are performed considering nominal requirements for sacrificial steel computed with Models I and II as described by Equations (17a) and (17b). These calculations consider z_i = 86 μm, a design life (t_{design}) equal to 50 years, and grid reinforcements with W20 size longitudinal wires. Results from these computations are presented in Table 23 in terms of the statistics of the resistance bias and corresponding calibrations of resistance factors.

As expected, the bias associated with Model I is less than Model II, but the COVs are nearly the same. Due to the differences in the bias, the resistance factor calibrated for Model I is also less than that associated with Model II. However, because the COVs of the bias are similar the calibrated resistance factors render the same design efficiency, ϕ/λ_R, for each case. Similar design efficiencies result in similar design details for a given MSE geometry, load case, design life, and so on. An example problem is presented in Appendix F that demonstrates that

Table 23. Resistance bias and calibration of ϕ considering construction with marginal quality fill.

Model	λ_R[1]	σ_R[1]	COV λ_R[1]	ϕ	β	p_f	ϕ/λ_R
I [Eq. (17a)]	1.01	0.29	0.29	0.30	2.37	0.009	0.297
II [Eq. (17b)]	1.63	0.46	0.28	0.50	2.26	0.011	0.301

[1] Normally distributed.

this is indeed the case. The results from this exercise demonstrate how changing the metal loss model used in design will not effect a change in design if the resistance factors are properly calibrated. The best way to achieve a more efficient design is to improve the COV of the bias. This may be achieved by using models that do a better job of capturing the behavior (e.g., capture trends that may be related to space, time, fill characteristics, and site conditions) and by improving the quality and quantity of performance data.

Type II—Condition Assessment

For Type II reinforcements, installation details have an effect on the vulnerability of the system to the surrounding environment and corresponding susceptibility to corrosion, and on our ability to probe the elements and interpret data from NDT. Relevant details include steel type, corrosion protection measures, drill hole dimensions, bond length, free/stressing length, total length, date of installation, level of prestress, grout type, and use of couplings. For rock bolts, the grout surrounding the reinforcement is often the only corrosion protection afforded to the reinforcements. More complex installation details are incorporated into ground anchorages that include elaborate corrosion protection measures, as described by PTI (2004). Construction details, durability of different material components, and workmanship associated with the corrosion protection system affect the service life and durability of ground anchorages. Generally speaking, rock bolts are more susceptible to metal loss from corrosion compared to ground anchorages. For these reasons, results from condition assessment and analysis of data relative to rock bolt and ground anchor installations are distinct.

Table 24 is a summary of sites with Type II reinforcements that were included in the fieldwork conducted as part of Task 6, and where measurements of corrosion rate and information on the condition of the reinforcements were obtained. Six of the installations described in Table 24 are rock bolts, and three are ground anchorages. Reinforcement age ranges from 8 to 43 years when monitoring was conducted (2007–2008). A variety of site conditions prevail, but in general, the sites provide an environment that is slightly acidic with pH ranging between four and six, and fairly conductive with resistivities less than 10,000 Ω-cm. One exception to this is the National Institute for Occupational Safety and Health (NIOSH) Safety Research Coal Mine (SRCM), which presents a more aggressive environment relative to corrosion.

Grout type is an especially important detail as the extent and type of grout surrounding an element affects the vulnerability of the system to corrosion. Portland cement-based grout is alkaline and protects the steel reinforcement by passivating the surface as well as providing a barrier to moisture and oxygen. Half-cell potential measurements, depicted in Figure 16, are useful to assess if the steel surface is passivated, or if corrosion is occurring. The alkalinity of the portland cement grout tends to shift the potential at the surface of a steel reinforcement to a more positive value. A half-cell potential greater than −200 mV relative to a CSE indicates the surface of the steel reinforcement is passivated. Figure 16 depicts the means and ranges of half-cell potential measurements from sites listed in Table 24. In general, sites with resin-grouted reinforcements exhibit half-cell potentials less than −200 mV, which on average range between approximately −400 mV and −700 mV. Reinforcements surrounded with portland cement grout exhibit half-cell potentials greater than −200 mV (maximum values). Although there are some notable exceptions, in general, these data serve to demonstrate the effectiveness of portland cement grout to protect steel earth reinforcements.

The best demonstration of the effectiveness of portland cement grout to passivate the steel reinforcements is with respect to the dam tie-downs wherein the steel wires are surrounded by portland cement grout within a concrete gravity dam. The fully grouted steel bar tendons at the Barron Mountain Rock Cut are generally passivated, but there are some elements of the population for which the grout protection appears to be compromised. The degree of protection afforded to the strands behind the anchor plate at the reaction blocks along the I-99 17th Street exit ramp in Altoona, PA, do not appear to be protected by grout and this will be discussed later in this section when describing the integrity of ground anchor installations. The half-cell potentials with respect to the restressable anchors at the same site in Altoona, PA, are lower because measurements reflect conditions along the surface of the galvanized trumpet head, and, in contrast to steel, zinc is not passivated by alkalinity.

For resin grout installations, relatively high half-cell potentials indicate that corrosion may have occurred, but these

Table 24. Summary of sites with Type II reinforcements evaluated during Phase II.

Site	Highway	State	Reinforcement Type	Year Installed	Anchorage Type	Prestress (kips)	Corrosion Protection	Comments
Barron Mountain Rock Cut	I-93 NB	NH	Rock bolts—Grade 150 prestressing steel rods and Grade 80 smooth steel rods	1974	Polyester resin grout	40	None	Grouted in bond zone only—bare stressing length
Barron Mountain. Rock Cut	I-93 SB	NH	Rock bolts—Grade 150 prestressing steel rods and Grade 80 smooth steel rods	1974	Polyester resin grout	40	None	Grouted in bond zone only—bare stressing length
Beaucatcher Rock Cut	I-240 W	NC	Rock bolts—Grade 150 prestressing steel rods	1982	Epoxy resin grout	40	Grout	Grouted full-length
Safety Research Coalmine (SRCM)	NIOSH Pittsburgh Research Laboratory	PA	Roof bolts—Grade 60 steel rods	1988	Resin grout, expansion shell or slot and Wedge	N/A	Grout/none	Fully-grouted, or nongrouted roof bolts
Safety Research Coalmine	NIOSH Pittsburgh Research Laboratory	PA	Roof bolts—Grade 60 steel rods	2000	Resin grout	N/A	Grout	Fully-grouted roof bolts
Barron Mtn. Rock Cut	I-93 NB	NH	Rock bolts—Grade 150 prestressing steel rods	1974	Portland cement grout	0	Grout	Fully-grouted passive elements
New Brunswick, Canada	Dams in the Musquash River Basin	N/A	Dam tie-downs—Grade 270 cold drawn steel wire grouted into rock	1964	Portland cement grout	125	Grout	Fully-grouted parallel wire, buttonhead anchorages
17th Street exit ramp	I-99	PA	Reaction blocks—Grade 270 seven wire strand ground anchors grouted into rock.	1992	Portland cement grout	100	Class I—double corrosion protection system	Restressable strands surrounded by grease in trumpet head
17th Street exit ramp	I-99	PA	Reaction blocks—Grade 270 seven wire strand ground anchors grouted into rock	1992	Portland cement grout	100	Class I—double corrosion protection system	Nonrestressable strands surrounded by grout behind the bearing plate

NOTE: NIOSH = National Institute for Occupational Safety and Health.

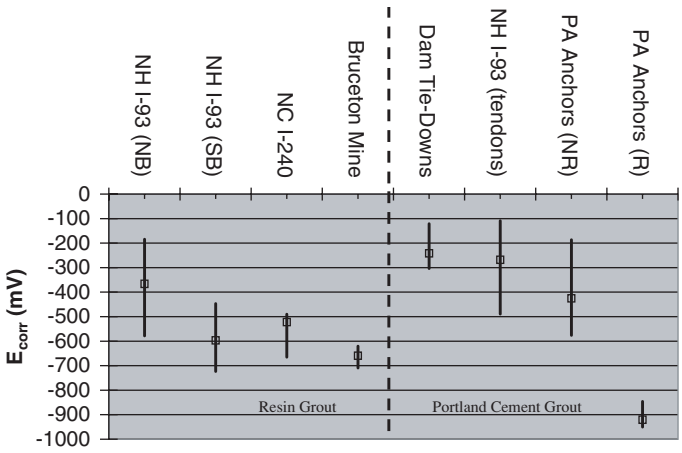

Figure 16. Ranges of half-cell potential measurements for Type II reinforcements.

measurements are also affected by salt concentrations and moisture content of the surrounding rock mass. Higher salt concentrations and dry conditions tend to shift half-cell potentials to more negative values. This is evident from measurements taken at several locations in western New York where monitoring was performed at regular intervals over a 2-year duration (see Appendix C).

Figure 17 presents the means and ranges of corrosion rate measured via the LPR technique at some of the sites listed in Table 24. Corrosion rates for resin-grouted rock bolts at the Barron Mountain and Beaucatcher Rock Cuts are relatively low. However, the LPR measurements only reflect corrosion rates in areas that are in direct contact with the surrounding earth and may not include areas where there is a gap or void separating the steel reinforcement surface from the

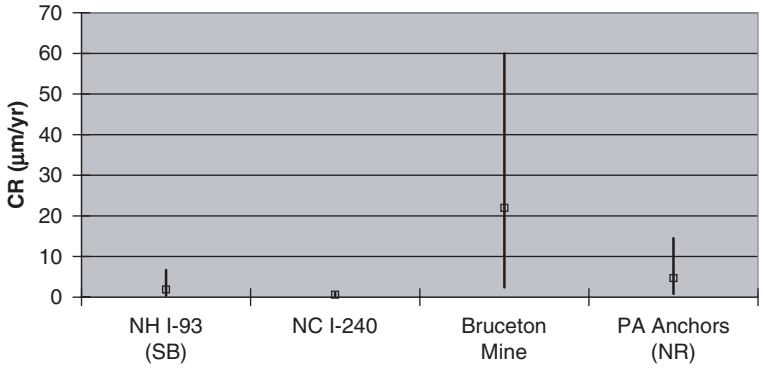

Figure 17. Ranges of corrosion rate measurements for Type II reinforcements.

surrounding rockmass (i.e., the electrolyte). Thus, these measurements demonstrate that resin grout can effectively protect the surface, assuming the surface is adequately covered. Much higher corrosion rates are evident from the NIOSH SRCM. This correlates well with the harsh environmental conditions at this site that includes pH ranging between 2.5 and 3.5 and sulfate concentrations between 800 ppm and 7000 ppm. Also, roof bolts installed at the SRCM may not have a gap behind the anchor plate similar to the rock cut installations such that LPR measurements reflect corrosion rates near the proximal end where moisture and oxygen are more prevalent. Data in Figure 17 also confirm that the non-restressable anchors tested at the I-99 17th Street Exit ramp in Altoona, PA, may not be adequately protected by portland cement grout behind the anchor plate and localized corrosion is occurring at an average rate of 5 µm/yr.

Grout quality and the potential for gaps are indicated from results of sonic echo and ultrasonic testing. These tests indicate that gaps often exist behind the bearing plate, even for fully grouted installations (Withiam et al., 2002). Results from sonic echo testing also provide information on remaining prestress and this may also correlate with conditions along the bonded or anchorage of the reinforcements. Since these conditions may deteriorate with respect to time, these measurements are also useful to interpret service life and durability of rock bolts. Specific details for rock bolt and ground anchor installations, data from condition assessment, data interpretation, and reliability analysis relative to durability and service life, are described in the following sections.

Rock Bolts

Sites with rock bolts described in Table 24 do not incorporate corrosion protection measures other than grout, therefore details of the condition and type of grout are particularly important.

Resin Grout

Although resin grout may provide a barrier from corrosion, there is strong evidence to suggest that areas of the surface may not be covered and vulnerable to corrosion. Even for fully grouted rock bolts it is likely that a gap exists behind the anchor plate that is vulnerable to corrosion. Prestressing tends to cause resin grout to crack, compromising its ability to act as an effective barrier to corrosion. Poor coverage has been observed, both from the results of NDT and direct observations (Fishman et al. 2005; Fishman, 2005). Results from sonic echo testing imply that often the degree of coverage afforded by the grout is relatively low, or grout quality is poor (voids and cracks exist). This is consistent with Compton and Oyler (2005) who reported that the resin grout only covered approximately 60% of the surface for fully grouted roof bolts that were exhumed for observation. Fishman (2005) also reported incomplete coverage in the bonded zone of grouted end-point anchorages exhumed at the site of the Barron Mountain Rock Cut.

Kendorski (2003) estimates the design life of unprotected rock reinforcement systems is approximately 50 years. Results from this study demonstrate that, in instances where the design load of rock reinforcements is based on pullout resistance, the design life may be longer than 50 years, depending on site conditions.

Other factors, such as loss of prestress, may also affect the service life of rock bolts with end-point anchorages. Results from sonic echo tests, that were confirmed from lift-off testing, indicate that a relatively high proportion (approximately 30%) of resin-grouted bolts with end-point anchorages have lost significant levels of prestress at the Barron Mountain Rock Cut (Fishman, 2004; Fishman, 2005). However, this may not be as much of a problem for fully grouted elements. Loss of prestress may be indicative of poor grout cover along the bonded zone, or due to weathering of rock beneath the bearing plate for end-point anchorages.

Knowledge of surface area in electrical contact with earth is required to reconcile corrosion rates from LPR measurements. This surface area is more difficult to determine for rock bolt installations compared to MSE (i.e., Type I) reinforcements. First, the length of the bolt and the grouted length need to be estimated, and then the amount of coverage afforded along the grouted length must be assessed. Installation details for rock bolts are not readily available from construction plans, and details related to bolt length and the length of the bonded zone must be obtained from field notes when available. The length of the bond zone can also be estimated from knowledge of the lock-off load, drill hole diameter, and by estimating the allowable bond stress at the grout/rock interface. However, another utility of sonic echo testing is the confirming or obtaining of missing information about the geometry of the installation. Data from sonic echo tests have been used in this study to verify bolt lengths and bond lengths that may then be used to estimate the surface area of the rock bolts in contact with the surrounding rock in order to reconcile corrosion rates from LPR measurements.

The rock bolts installed at Barron Mountain were only grouted along the bonded length (i.e., end-point anchorages), thus the free/stressing length is more vulnerable to corrosion. This is confirmed by direct visual observations of bolts that were exhumed from the site as reported by Fishman (2005), and is evident in the results from sonic echo tests performed on more than 50 rock bolts from this site. This is useful since direct observations of metal loss from portions of reinforcements that have been retrieved can be compared to corrosion rates measured in situ with LPR. Based on results from sonic echo testing, the bond lengths of rock bolts along the southbound barrel of I-93 at the Barron Mountain Rock-Cut range between 3 and 13 feet. Rock bolts at the Beaucatcher Cut are fully grouted, and results from sonic echo tests indicates that the bolts that were sampled for testing are approximately 10 feet long.

LPR measurements depicted in Figure 17 demonstrate corrosion rates for sections of rock bolts surrounded by grout are relatively low. Although LPR measurements are useful to assess corrosion along grouted areas, more information is needed to assess corrosion rates for exposed sections (i.e., not surrounded by grout) of the reinforcements. Direct observations of exposed portions of exhumed reinforcements indicate that corrosion in these vulnerable areas is much higher than that indicated via LPR measurements. Thus, critical locations that may control design life include the gap behind the anchor plate or other exposed areas.

Metal loss of exposed portions of the reinforcement behind the anchor plate, or other areas, may be expressed using the Romanoff equation as

$$X\left(\frac{\mu m}{side}\right) = A\left(\frac{\mu m}{yr/side}\right)t^{0.8}(yr) \tag{23}$$

where t is time in years. Table 25 is a summary of metal loss measurements obtained from rock reinforcements that have been exhumed from sites located in the United States, Sweden, Finland, and England. These data are useful to assess the variability associated with the constant A that appears in Equation (23).

Based on the data in Table 25, A in Equation (23) has a mean value of 60 μm/yr, a standard deviation of 40 μm/yr, and can be approximated with a lognormal distribution. The data in Table 25 represent site averages. However, data from six reinforcements retrieved from the Barron Mountain Rock Cut were analyzed and rendered a mean of 66 μm/yr for A. Also,

Table 25. Summary of metal loss measurements from rock bolts and ground anchors.

Site	Country	Type	Age (yrs.)	X (μm)	A (μm/yr)
Barron Mountain Rock Cut, I-93 NB[1]	USA	Resin-grouted bar	32	880	55
Barron Mountain Rock Cut, I-93 SB[2]	USA	Resin-grouted bar	33	1498	91
State Route 52, Ellenville, NY[3]	USA	Expansion shell	20	1690	154
Pyhasalmi[4]	Finland	Split set	1.5	63	46
Pyhasalmi[4]	Finland	Split set	1	28	28
Hemmaslahti[4]	Finland	Split set	2	43	25
Hemmaslahti[4]	Finland	Swellex	1.5	90	65
Kerretti[4]	Finland	Swellex	2	56	32
FIP Case 4[5]	Sweden	Ground anchor	26	445	33
Dovenport Royal Dockyard[6]	England	Ground anchor	22	750	63

[1]Fishman (2005).
[2]NCHRP 24-28.
[3]Withiam et al. (2002).
[4]Lokse (1992).
[5]FIP (1986).
[6]Weerasinghe and Adams (1997).

measurements of metal loss from steel elements embedded in fills with resistivity between 3,000 Ω-cm and 10,000 Ω-cm as discussed in the resistance factor calibrations for Type I reinforcements render a value for A equal to 54 μm/yr. Furthermore the statistics generated from Table 25 are relatively close to the nominal metal loss expressed by Eq. (3), which applies to plain steel buried in a wide range of environments. Thus, the statistics rendered from the data in Table 25 appear to be reasonable. The statistical variation of metal loss represented by these parameters can be used to calibrate resistance factors for LRFD similar to that for Type I (MSE) reinforcements. However, there are some notable differences as described in the following example:

The example resistance factor calibration considers that Type II reinforcements are not redundant and failure of a single element could mean that a block of rock is loosened, leading to a system failure. For the purpose of this example a target reliability index, β_T, equal to 3.1 corresponding to $p_f \approx 0.001$ is adopted. This is consistent with past geotechnical design practice for foundations as described by Withiam et al. (1998).

The load bias, λ_Q, used in the resistance factor calibration presumes that rock bolts are actively loaded and prestressed during installation; and prestress is verified via lift-off testing as described by PTI (2004). Thus, the uncertainty relative to the design load is much less compared to Type I reinforcements, whereby the loads are passive and transferred to reinforcements as the system deforms. Design loads are enforced upon the reinforcements during installation, and PTI (2004) recommends that verified lock-off loads be within 5% of design specifications. For the purpose of this example, $\lambda_R = 1$ and COV = 10% are used, and considered to be conservative estimates.

The resistance bias is computed as follows:

$$\lambda_R = \frac{F_{ult}^* A_c^*}{T_{nominal}} \tag{24}$$

$$A_c^* = \frac{\pi D^{*2}}{4} \tag{25}$$

$$D^{*2} = D_i - 2X^* \text{ for } 2X^* < D_i$$
$$D^{*2} = 0 \text{ for } 2X^* \geq D_i \tag{26}$$

For this example, it is assumed that the design capacity of the rock bolt is based on the resistance mobilized along the bonded length and not the structural capacity of the bolt. The structural resistance (tensile strength) remaining at the end of the design life must equal the design load enforced on the system during installation. If the difference between the lock-off load and the original structural capacity of the bolt is high enough, then enough structural capacity may be available at the end of the design life to sustain the design loads even though metal loss may not be explicitly considered during design. A nominal resistance, $T_{nominal}$, equal to 40 kips, is used in this example similar to the Barron Mountain and Beaucatcher Rock Cuts described in Table 24. The reinforcements are assumed to be solid bars made from Grade 150 steel that has a guaranteed ultimate tensile strength (GUTS) of 150 ksi. The GUTS is considered as the nominal strength and F_{ult}^* (the statistical variable for ultimate strength of steel) is considered to have a normal distribution equal to 1.05 times the nominal and COV equal to 0.1 similar to that described by Bounopane et al. (2003) and the statistics used to describe the variation of yield strength for Type I reinforcements. Equation (23) is used to compute metal loss, X^*, where the parameter A is varied statistically according to a lognormal distribution with $\mu_A = 60$ μm and $\sigma_A = 40$ μm.

The calibration is performed considering bolts with a 1-inch initial diameter, D_i, and 50-, 75- and 100-year design lives. Table 26 is a summary of the computed bias, resistance factor, and probability of occurrence for each design life. These results indicate that for this example metal loss does not have a significant impact on performance for design lives of 50 and 75 years, but should be taken into account for service lives in excess of 75 years. The results from this example depend on the selected values for $T_{nominal}$, D_i, and F_{ult}. If these inputs vary then the results depicted in Table 26 do not apply. The purpose of this example is to demonstrate the approach and identify the input needed for a complete calibration. More data are needed to assess typical design scenarios before a more complete calibration can be performed.

Current AASHTO specifications specify $\phi = 0.8$ relative to rupture resistance for high-strength steel reinforcements. Assuming that metal loss is not considered in design but using the same statistical properties for the remaining variables renders $p_f < 0.0001$. The 75-year case shown in Table 26,

Table 26. Results from reliability-based calibration considering the yield limit state for rock bolts.

t_f (years)	λ_R			ϕ	p_f
	μ	σ	Distribution		
50	2.36	0.33	Weibull	1.0	< 0.0001
75	2.22	0.42	Weibull	1.0/0.80	≈0.001/0.0001
100	2.14	0.55	Weibull	0.55	≈0.001

but with $\phi = 0.8$ renders $p_f \approx 0.0001$. This implies that the current AASHTO specifications imply a service life of approximately 75 years for the selected example.

Portland Cement Grout

Based on results from NDT and direct observations, portland cement grout quality generally appears to be good for the rock bolts inspected at the sites listed in Table 24 and depicted in Figure 16. Half-cell potential measurements indicate that the presence of a passive film layer protects the rock bolts from corrosion. However, passivation of the steel may be compromised by the presence of chlorides or acidic conditions. Chlorides may be present along the rock face as a residue from salt spray produced from deicing of the highway. There is some evidence of this from the testing of fully grouted tendons at the Barron Mountain Rock Cut (Fishman, 2004). LPR measurements indicate very low average rates of metal loss and significant metal loss was not observed from several elements that were exhumed for inspection (Fishman, 2005). In general, for installations where lower half-cell potentials (less than −200 mV) are realized corrosion monitoring should be performed to assess the rate of metal loss. Very high rates of corrosion are possible when the passive film layer is locally compromised. Grout cracking may also occur at the beginning of the bonded zone due to the application of prestress. However, the surface is still protected via the alkaline environment until crack widths exceed a minimum value (e.g., 1 mm).

Grout and return tubes are used to install portland cement-grouted rock bolts such that the grout quantity can be adjusted as needed when grout is lost from the drill hole. This is in contrast to resin-grouted bolts for which a fixed quantity of grout is inserted into the drill hole. Thus, the coverage from portland cement grout is expected to be better when compared to resin-grouted installations. Also, prestressed rock bolts require a stressing length that is often protected by grease and a plastic sheath. However, a gap behind the anchor plate is still possible unless a trumpet head assembly is employed. Thus, the main concern with portland cement-grouted rock bolts is with respect to a gap behind the anchor plate. This may be remedied with a trumpet head assembly filled with grease. Alternatively, metal losses need to be considered using Equation (23), similar to those for resin-grouted installations.

Ground Anchors

If the ground anchor system is protected with an adequate corrosion protection system [e.g., meeting the requirements of PTI Class I (PTI, 2004)], then corrosion is generally not a problem. Observations from NDT indicate that, generally, grout quality along the bonded zone appears to be good and no defects or anomalies were encountered along the stressing lengths. The main concern for ground anchorages is near the anchor head assembly and the fact that high-strength, prestressed steel elements may be vulnerable to hydrogen embrittlement and SCC. Hydrogen embrittlement and SCC tend to occur in acidic or chloride-rich environments, and, without proper detailing and workmanship at the anchor head assembly, the service life of the elements is severely compromised by these environments. Time to failure for hydrogen embrittlement and SCC can be relatively short, and the previously cited models describing rate of metal loss for uniform corrosion or incursion of pit depths are not applicable to assess service life. Measurements of half-cell potential and corrosion rate for ground anchors indicate that portland cement grout does not always serve to passivate steel, and the area behind the bearing plate is vulnerable to corrosion. Use of a trumpet head filled with grease appears to be a more effective measure to protect the reinforcements as it is isolated from the surrounding environment by virtue of the dielectric properties of the grease.

Loss of prestress may also affect service life. Current observations in the database do not include sites where this has been observed to be a problem. However, if the anchorage zone is within soil or rock types that creep, then loss of prestress could affect service life. Regular maintenance of lock-off loads could be implemented to achieve a given service life for these conditions.

CHAPTER 4

Conclusions and Recommendations

The main focus of this study is reliability of metal loss modeling and service life estimates for earth reinforcements, including reinforcements for MSE, soil nails, rock bolts, and ground anchors. Reliability analysis is useful for the following:

1. Describing reliability of metal loss models for use in design,
2. Describing effect of deviations in electrochemical properties and site conditions on service life,
3. Calibrating resistance factors for use in LRFD, and
4. Providing tools for asset management that can be used to estimate vulnerability and remaining service life of existing systems.

During Phase II of this research, fieldwork was undertaken to broaden the database describing in situ performance of earth reinforcements compared to what was available at the conclusion of Phase I. Additional data were collected to enhance the geographic distribution of sites included in the monitoring effort and to obtain more information representative of a range of fill conditions including high, good and marginal quality, more sites with LPR measurements providing a better spatial and temporal distribution of measurements at given sites, and more sites with older reinforcements (i.e., older than 25 years). Data were also obtained to further verify the use of LPR measurements to estimate corrosion rate, thus providing a sound basis to use these measurements for statistical analysis of measurements and for reliability analysis of service-life estimates and calibration of resistance factors for use in LRFD.

For MSE reinforcements (Type I), electrochemical properties of the fill were observed to have a significant impact on performance, and the effect of time on corrosion rate is clearly indicated by these data. The spatial distribution of corrosion rates appears to be random, although spatial trends are apparent from data obtained with respect to several of the sites in the database. No significant differences are observed between different climates for galvanized elements, however, marine environments had a detrimental effect on corrosion rates for plain steel (i.e., not galvanized) reinforcements. Also, it was found that seasonal variations affect measured corrosion rates, and considering the climate in the northeastern United States, measurements may vary by a factor of approximately 1.5 throughout a given year.

Data were partitioned considering different fill conditions, reinforcement type and time frames rendering COVs between approximately 40% and 60% within each category. In general, metal loss models available from the existing literature, including the AASHTO model, were found to be conservative. Use of the AASHTO metal loss model is evaluated within the framework of reliability-based design and calibration of resistance factors for LRFD.

Results from LRFD calibrations rendered resistance factors corresponding to a target reliability index of 2.3 and $p_f \approx 0.01$. The following conclusions apply to the resistance factor calibrations for LRFD of MSE walls:

- Computed resistance factors vary depending on the method used to compute reinforcement load, that is, simplified or coherent gravity method.
- Considering galvanized reinforcements in good backfill conditions (i.e., meeting AASHTO criteria for electrochemical parameters) the computed resistance factor is slightly less than what is recommended in the current AASHTO specifications.
- Considering galvanized reinforcements in high quality fill renders resistance factors that are slightly higher than those currently specified by AASHTO for design of MSE walls.
- Data were generated to consider plain steel (i.e., not galvanized) reinforcements with fill materials that meet the AASHTO requirements for electrochemical parameters, a conservative metal loss model, and maximum design life of less than 50 years.
- Data were generated to consider marginal quality fill (i.e., not quite meeting AASHTO criteria) with galvanized reinforcements, a very conservative metal loss model, and maximum design life of less than 50 years.

Type II reinforcements include rock bolts and ground anchors, and their performance is related to the degree of cor-

rosion protection included in the installation. Many rock bolts are only protected by grout and a lack of coverage may occur as a gap behind the anchor plate where grout is lost to the surrounding rock mass during installation, or from remnants of plastic cartridges inherent to resin-grouted installations. However, the design load is often based on the pullout resistance rather than yield of the reinforcement, and metal loss does not appear to be significant for design lives of 50 or 75 years. For a 100-year design life, the rupture limit state likely controls the performance and resistance factors appropriate to this design have been calibrated. The calibration uses approximately 70 observations of metal loss from sites located in the United States, Scandinavia, and the United Kingdom. Compared to MSE reinforcements (Type I), rock bolts are not necessarily redundant so a target reliability index of approximately 3.1 rather than 2.3 was used for the calibration, corresponding to $p_f \approx 0.001$.

Ground anchors for permanent installations generally have a Class I, double corrosion protection system including a trumpet head assembly to protect the area behind the anchor head. There have not been any observations of poor performance when Class I corrosion protection measures are incorporated with proper detailing and workmanship during installation. If the anchor head does not include a trumpet head assembly that is filled with grease, the area near the anchor head may be vulnerable to corrosion. If acidic conditions or high chloride concentrations prevail, then the service life may be severely compromised from hydrogen embrittlement or SCC along exposed portions of the anchor.

Recommended Resistance Factors for LRFD

Current practice (LRFD) for the design of metallic reinforcements for MSE applications is to ensure that reinforcements maintain enough yield resistance to keep the probability that overstress occurs (i.e., probability of occurrence, p_f) below acceptable limits throughout the design life of the facility. Galvanized reinforcements are recommended and sacrificial steel is included in the cross section to compensate for the expected loss of steel subsequent to depletion of the zinc coating along the surface. Provided that the reinforced fill material meets AASHTO criteria for electrochemical parameters, the metal loss model for galvanized metallic MSE reinforcements described in the current AASHTO specifications is recommended for computing the nominal amount of sacrificial steel. This recommendation is based upon approximately 1,000 measurements of metal loss and corrosion rate from samples of galvanized reinforcements and coupons, calculation of the resistance bias and corresponding statistics, and reliability-based calibration of the resistance factor for LRFD considering the yield limit state. The current AASHTO model is necessarily conservative, and corresponding resistance factors correlate to an acceptably low probability of occurrence for a 75- or 100-year design life. The resistance factors listed in Table 27 are recommended for use with LRFD considering the yield limit state, and using the AASHTO metal loss model to compute the nominal resistance at the end of the design life. Different resistance factors are recommended for good versus high quality fill, strip or grid reinforcements. The protocol for sampling and electrochemical testing of wall fill, described in Table 4, is recommended to assess fill quality and if the materials meet the criteria for good or high quality fills.

Although the calibrations resulted in different resistance factors depending on use of the simplified or coherent gravity methods for computing nominal load, use of the same resistance factor is recommended for either method. This is based on the fact that the difference is relatively small, and similar designs are rendered when the same resistance factors are applied as described from the results of the example problem described in Appendix F. Also, the simplified method was originally calibrated to render similar results compared to the coherent gravity approach with the traditional allowable stress methods of design. Furthermore, the load bias associated with the coherent gravity method (D'Appolonia, 2007) may not consider the effect of reinforcement depth, and the calibration appears to favor reinforcements placed within the top 20 feet of the wall. The bias factor for reinforcements located below this depth is expected to be less, corresponding to calibrated resistance factors that are higher and closer to those obtained with respect to the simplified method.

The factors recommended for use with good quality fill and galvanized reinforcements are based on results presented in Table 17 from calibrations performed with respect to the simplified method of analysis. The recommended value of 0.65 corresponds well with values of ϕ computed considering a 75-year design life. Designs considering a 100-year design life are likely to result in relatively thicker reinforcements,

Table 27. Summary of recommended LRFD strength reduction factors for galvanized reinforcements.

Metal Type	Backfill Quality	Metal Loss Model	Design Life (Years)	Resistance Factors (ϕ)	
				Strip	Grid
Galvanized	Good	AASHTO	75 or 100	0.65	0.55
Galvanized	High	AASHTO	75 or 100	0.80	0.70

therefore, the lower resistance factors of 0.55 and 0.60 computed for thinner reinforcements are not recommended; $\phi = 0.65$ corresponds to thicker reinforcements with $S = 6$ mm. For galvanized grid-type reinforcements embedded within good quality fill the recommended value of $\phi = 0.55$ corresponds to most of the values presented in Table 17, and is lower than the maximum of $\phi = 0.6$ computed for W7 and W9 size wires and a 75-year design life.

The factors recommended for use with high quality fill and galvanized reinforcements are based on results presented in Table 18 from calibrations performed with respect to the simplified method of analysis. The recommended value of 0.80 for strip-type reinforcements corresponds well with the value computed for 4-mm-thick reinforcements and a 75-year design life, and is generally less than the values computed considering a 100-year design life, although it is a little higher (by 0.05) than the value of 0.75 computed for the thicker reinforcements ($S =$ 6 mm). The recommended value of $\phi = 0.8$ is considered reasonable because using higher quality fill results in designs with relatively thinner reinforcements, and will most likely be considered in conjunction with longer design lives. For galvanized grid-type reinforcements embedded within high quality fill, the recommended value of $\phi = 0.70$ is equal to or lower than most of the values presented in Table 18, but is 0.05 higher than the values of 0.65 computed for W11 and W14 size wires and design lives of 75 years. However, this is not considered to be a significant difference, so use of $\phi = 0.70$ is considered to be a reasonable representation of the results presented in Table 18.

Current AASHTO specifications prescribe resistance factors of 0.75 for strip-type reinforcements and 0.65 for grid-type reinforcements with rigid facing units (see Chapter 1, Table 7). These resistance factors apply with respect to use of either the simplified or coherent gravity methods to compute reinforcement loads. The resistance factors recommended in Table 27 are similar to these in the current AASHTO specifications for walls constructed with higher quality reinforced fill materials. Based on the information shown in Table 27, resistance factors should be reduced by 0.15 for fills that meet current AASHTO criteria for electrochemical parameters, but not by a very wide margin (i.e., good fill). Alternatively, the same resistance factors could be used with the understanding that the probability of occurrence for the case of good fill conditions is greater compared to when high quality fills are used in construction.

Use of plain steel (i.e., not galvanized) reinforcements is not recommended. However, data on the performance of plain steel reinforcements were analyzed, statistics on metal loss were generated, and resistance factors for use in LRFD were calibrated. The objectives of the study are to present differences with respect to design with galvanized reinforcements. Only fill materials that meet current AASHTO criteria for electrochemical parameters were considered, however, the performance of steel reinforcements depends on whether good or high quality fills are used during construction. The following equations are recommended to estimate nominal sacrificial steel requirements for good and high quality fills:

For good quality fill:

$$X\left(\frac{\mu m}{side}\right) = 80\frac{\mu m}{yr/side} \times t^{0.8}\left(yr\right) \tag{27}$$

For high quality fill:

$$X\left(\frac{\mu m}{side}\right) = 13\frac{\mu m}{yr/side} \times t\left(yr\right) \tag{28}$$

For good quality fill, only a 50-year design life is considered corresponding to a nominal sacrificial steel requirement of 1,829 μm per side according to Equation (27). Thus, a total of 3.66 mm of sacrificial steel is required considering metal loss from all surfaces (additional diameter for round elements and additional thickness for strip-type elements). This is considerably higher than the current AASHTO requirement of 0.82 mm for a 50-year design life with galvanized reinforcements.

A 75-year design life is considered when high quality fill is used in construction corresponding to a nominal sacrificial steel requirement of 975 μm per side according to Equation (28), or approximately 1.95 mm added to the diameter or thickness of an element. This is also higher than the current AASHTO requirement of 1.42 mm for a 75-year design life with galvanized reinforcements. For both cases, calibrated resistance factors of approximately 0.35 were computed considering use of the simplified or coherent gravity methods. Design efficiency factors for the case of plain steel reinforcements are less than half of those realized for the case of galvanized steel reinforcements (efficiency factor 0.2 compared to 0.5).

Use of materials for reinforced fill that do not meet current AASHTO requirements is not recommended. However, data exist in the literature from several sites in which special studies were conducted to access the condition and remaining service life at sites where marginal quality fill was used, often inadvertently. These data are used to assess the conservatism inherent to existing models for computing nominal sacrificial steel requirements and to calibrate resistance factors for the yield limit state. Marginal quality fills are described herein as having $5 < pH < 10$ and $1{,}000\ \Omega\text{-cm} < \rho_{min} < 3{,}000\ \Omega\text{-cm}$. Only the use of galvanized reinforcements and design lives (t_f) less than 50 years are considered with respect to use of marginal fills. The following equation is recommended for computing nominal sacrificial steel requirements:

$$X\left(\frac{\mu m}{side}\right) = \left(t_f - 10\,yrs\right) \times 28\left(\frac{\mu m}{yr/side}\right) \tag{29}$$

Application of Equation (29) presumes that zinc coating with a minimum required thickness of 86 μm per side will be

consumed within 10 years, and the base steel will be consumed at a rate of 28 μm/yr per side thereafter. Although the zinc life is relatively short, the main purpose of the zinc is to mitigate the development of macrocells and promote more uniform corrosion. For t_f of 50 years, the nominal sacrificial steel requirement according to Equation (29) is 2.24 mm (i.e., X = 1120 μm/side). If Equation (29) is the basis for computing the nominal sacrificial steel requirements, a resistance factor of 0.30 is recommended for LRFD and the yield limit state.

Type II reinforcements include rock bolts and ground anchors. Due to the fact that these reinforcements are often surrounded by grout or protected via a single (Class II) or double (Class I) corrosion protection system, only the portions of the assembly that are exposed and in contact with the surrounding environment are vulnerable to corrosion. Due to fundamental differences in the materials, installation details, and workmanship applied to rock bolts versus ground anchors, the reliability inherent to service life estimates of these installations is described separately.

For rock-bolt installations, the most vulnerable locations are behind the bearing plate, which often includes a gap, or other locations where the reinforcement is not completely surrounded by grout or is otherwise left unprotected. Metal loss is a concern at these locations, and previous design guidance has not directly considered metal loss in the consideration of service life. However, resistance to pullout, rather than rupture resistance, often controls the lock-off load for rock-bolt installations; therefore the resistance of the reinforcement section may not be fully mobilized at any time during the service life. Chapter 3 includes an example from a site where pullout resistance controls the lock-off loads and data on metal loss of Type II reinforcements, available from the literature, are used to assess the resistance bias at the end of the design life. The example demonstrates that for the selected site, metal loss is not a significant concern for service lives less than 75 years. A resistance factor for the rupture limit state and a 100-year design life is computed as 0.55, corresponding to a target reliability index of 3.12 and $p_f \approx 0.001$. This example demonstrates how the statistics generated from metal loss measurements can be used to calibrate resistance factors for LRFD of Type II reinforcements. However, the computed resistance factor is sensitive to the lock-off load, and depends on the sizes and steel types of the reinforcements.

If lock-off loads are controlled by rupture (rather than pullout resistance), then sacrificial steel requirements must be considered explicitly. Equation (27) is recommended to compute nominal sacrificial steel requirements. Resistance factors can then be calibrated using the statistics describing metal loss measurements from Type II reinforcements cited in Chapter 3.

Ground anchor systems that use high-strength steels with GUTS in excess of 150 ksi are vulnerable to other forms of corrosion that may include hydrogen embrittlement and SCC. Use of Equation (27) does not apply to degradation from hydrogen embrittlement or SCC. In these cases, service lives are severely compromised if the reinforcements are exposed and in contact with the surrounding soil or rock mass, particularly for environments that are acidic or high in chlorides. Therefore, high-strength steel reinforcements must be isolated from the environment via a corrosion protection system. In these cases, a double corrosion protection system (Class I) is recommended and the service life is governed by the quality and detailing inherent to the double corrosion protection system. Data were collected during this research from one site with high-strength steel reinforcements and a double corrosion protection system. These data indicate that the corrosion protection system at this site is intact and performing well; a grease-filled trumpet head is included with the anchor head assembly.

Recommendations for Asset Management

Asset management is an important issue facing highway operations, and forecasting the needs for maintenance, retrofit, or replacement of existing facilities is an important component of transportation asset management (TAM). Earth-retaining structures should be included in a TAM program along with pavements, bridges, ancillary structures, and so on, to help ensure optimal usage of limited available funding (FHWA, 2008). Properly defining the existing inventory and the development of a performance database are important components of asset management. Relatively rapid, nonintrusive, and nondestructive test techniques are needed to collect data necessary for corrosion monitoring and condition assessment of earth-retaining structures. Results from condition assessment and corrosion monitoring indicate when, or if, accelerated corrosion is occurring and can help transportation agencies decide on the most appropriate course of action when subsurface conditions are unfavorable and service life is uncertain. Agencies can also use these data to evaluate the variance associated with the performance of an inventory; this is valuable information for those with an interest in making reliability-based decisions. This report describes the framework of a performance database useful for asset management, test techniques and protocols that are being employed to collect performance data for earth reinforcements, data interpretation, and preliminary information available from data that has been collected to date.

Performance Data

The performance database includes thousands of measurements of element conditions and corrosion rates from more than 150 sites distributed throughout the United States and Europe. The large sample domain allows evaluation of sample statistics, distributions of element conditions and

corrosion rates, and corresponding probability and reliability analyses. These issues are related to reliability of metal loss modeling, quantification of the effect of construction practice on performance, and understanding the cost benefits of using different materials. All of these are important components of asset management. For example, the database can be used to

- Study the mean and variance of corrosion rates for data sets grouped according to different climate, site conditions, and reinforced fill conditions;
- Quantify performance for marginal reinforced fills; and
- Evaluate the performance of different materials (e.g., steel vs. zinc, other forms of metallization, and the use of polymeric coatings).

These applications will lead to better estimates of service life and can help to quantity the benefits of selecting higher quality backfill for construction or the costs associated with using marginal quality fill. Performance data can also facilitate evaluation of alternative materials, including use of galvanized versus plain steel, or other corrosion protection measures that may include epoxy or polymer coatings. Practices that may lead to poor performance may also be identified and quantified, including the impact that poorly maintained drainage inlets may have on service life, or the effect of fill contamination during service. The database needs to be continuously updated and should include performance data from sites where good practice has been followed as well as from sites with questionable conditions.

Maintenance, Rehabilitation, and Replacement

Issues that can address future needs for maintenance, rehabilitation, retrofit, or replacement include

- Spatial variations of element condition and corrosion rate (e.g., top vs. bottom of wall),
- Special areas that may deserve increased maintenance (e.g., in proximity to drainage inlets), and
- Effects of different climates, use of deicing agents, and so forth.

Improved knowledge of spatial variations and special problems can lead to improved allocation of resources. For example, in some cases, extended service life may be best achieved by retrofitting areas surrounding drainage inlets, or the benefits of improved maintenance of drainage inlets may be realized in terms of increased service life. In areas where deicing salts are used, corrosion monitoring can demonstrate the need to maintain pavements, improve drainage, or install and maintain impervious barriers.

Update Experience with Different Reinforced Fills

An example of the experience gained from collecting and analyzing data relates to the use of reinforced fills that may or may not meet AASHTO specifications for electrochemical properties. The database was divided into two primary groups including data from reinforced fill conforming to AASHTO criteria and from reinforced fill not conforming to AASHTO criteria. The AASHTO corrosion model was applied to estimate reinforcement corrosion rates and to compare them to measured corrosion rates. The observations below were made from the existing database. These observations may be updated as more data become available.

- For reinforced fills conforming to AASHTO criteria, the AASHTO corrosion model overestimates steel corrosion rates for 98% of the data. It should be noted that most of the data in this group are associated with reinforced fills that meet AASHTO requirements by a wide margin.
- For reinforced fills conforming to AASHTO criteria, marine environments have minor to no effect on measured corrosion rates of galvanized reinforcements, but marine environments accelerate corrosion rates of plain steel reinforcements.
- For reinforced fills that do not satisfy AASHTO criteria, marine environments are associated with relatively high corrosion rates.
- Reinforced fills that do not meet AASHTO criteria (i.e., soil resistivity values $\rho < 3{,}000\ \Omega$-cm and pH values < 5) can significantly affect steel corrosion rates, which tend to dramatically increase beyond rates estimated by the AASHTO corrosion model.
- Based on available data, organics content, chlorides, sulfates, and relatively high values of pH have much less effect on measured corrosion than do relatively low resistivity and low pH.
- Review of the latest research information confirms the safety of the electrochemical requirements for fill and associated metal loss rates in the current AASHTO standards.

Recommendations for Future Research

NCHRP Project 24-28 assessed and improved the predictive capabilities of existing computational models for corrosion potential, metal loss, and service life of metal-reinforced systems used in retaining walls and highway cuts and fills. Methodology was developed that incorporates the improved predictive models into an LRFD approach for the design of metal-reinforced systems. Recommended additions and revisions were prepared to incorporate the improved models and methodology in the *AASHTO (2009) LRFD Bridge Design Specifications*.

Additional research is recommended to further validate the predictive models for corrosion potential, metal loss, and service life of metal-reinforced systems from Project 24-28. The validation will require measurements at an independent set of field sites across the United States, supplemented with results from laboratory measurements. Field sites should include rock-bolt installations and MSE walls. Testing of the metal-reinforced systems at each field site will require both (1) NDT techniques (e.g., ultrasonic testing, sonic echo, impulse response, and electrochemical testing) and (2) direct measurement after exhumation of in situ reinforcements or installation of dummy elements by state DOTs or other agencies. The direct measurements will validate the NDT methods as well as the predictive models based upon these methods.

Type I Reinforcements

The following objectives apply to Type I reinforcements and the need for data to validate the performance models and address limitations inherent to the database compiled as part of NCHRP Project 24-28:

- Evaluate effect of marginal fills on performance and service life,
- Study bias inherent to LPR measurements of corrosion rate, and
- Assess the corrosion rate of steel after zinc has been consumed from galvanized elements.

To accomplish these objectives:

1. Develop a relationship between fill resistance (measured as part of the LPR test) and fill resistivity. This relationship depends upon the geometries of the test electrodes, electrode spacing, fill characteristics, and method of measuring fill resistance. If this relationship can be established, it will then be possible to develop much better correlations between measured corrosion rates and the electrochemical properties of the fill.
2. Compare measurements of corrosion rates with direct observations of metal loss from reinforcements that have been exhumed subsequent to LPR measurements. These data will be very useful, particularly to relate loss of tensile strength to LPR measurements, as loss of strength is often from metal loss that has occurred over localized areas.
3. Collect data from sites with galvanized reinforcements where base steel is corroding after zinc has been consumed. Different assumptions regarding corrosion of the base steel have a significant impact on resistance factor calibrations for LRFD.

Further research could also be pursued to further demonstrate applications of performance data. In particular, if the need for rehabilitation or retrofit is identified, cost-effective methods for rehabilitation and retrofit should be selected. Guidance will target improvements to areas where they are most needed, which may be close to sources of fill contamination or otherwise based on the spatial distribution of corrosion or loss of service observed at a particular site. A well-maintained and populated database will facilitate development of site-specific guidance based on the experiences that have been documented from other sites. Guidance needs to be developed for sampling and evaluating backfill and performance of in-service reinforcements. The recommended sampling is likely a hybrid between stratified and random sampling. Representative sample locations are stratified with respect to the vertical direction and stations are randomly located along the length of the wall. A cluster of measurements at each sample point should be averaged to render the corrosion rate at that location.

The sensitivity of designs generated from the recommendations provided in the report need to be evaluated. Typical designs should be executed using recommended resistance factors for LRFD considering use of galvanized or plain steel reinforcements and various fill materials (i.e., high quality, good, and marginal). In this way the impact of these factors on design parameters, including the size and spacing of reinforcements, can be evaluated.

Type II Reinforcements

The following objectives apply to Type II reinforcements and the need to (1) substantiate use of electrochemical test techniques for corrosion monitoring and integrity testing of corrosion protection systems and (2) extract more information on existing conditions from the results of dynamic testing (e.g., sonic echo and impulse response). More data from sites with double corrosion protection systems are required to generate statistics describing the reliability of these installations.

- Study application of corrosion monitoring with LPR techniques. Seek measurements and observations that can characterize the surface area in contact with the surrounding earth material, and knowledge of the influence of grout and other components of the corrosion protection system.
- Refine data analysis techniques for dynamic tests (wave propagation techniques). Verify results obtained with these techniques, and evaluate the limitations of these NDTs for probing earth reinforcements.
- Collect more data to document the performance of corrosion protection systems.

References

AASHTO, 2002a, *Standard Specifications for Transportation Materials and Methods of Sampling and Testing,* 20th ed. American Association of State Highway and Transportation Officials, Washington, D.C.

AASHTO, 2002b, *Standard Specifications for Highway Bridges, Division I,* 17th ed. American Association for Transportation and Highway and Transportation Officials, Washington, D.C.

AASHTO, 2009, *LRFD Bridge Design Specifications,* 4th ed. with Interims, American Association of State Highway and Transportation Officials, Washington, D.C.

Allen, T., Christopher, B., Elias, V., and DiMaggio, J., 2001, *Development of the Simplified Method for Internal Stability of Mechanically Stabilized Earth Walls,* Report No. WA-RD 513.1, Washington State Transportation Center, Seattle, 108 p.

Allen, T. M., A. S. Nowak, and R. J. Bathurst, 2005, *Transportation Research Circular E-C079: Calibration to Determine Load and Resistance Factors for Geotechnical and Structural Design,* Transportation Research Board of the National Academies, Washington, D.C., 83 p.

Anderson, S. A., Alzamora, D., and DeMarco, M. J., 2009, Asset Management Systems for Retaining Walls, *GEO-Velopment: The Role of Geological and Geotechnical Engineering in New and Redevelopment Projects,* ASCE Geo Institute, Reston, Virginia, pp. 162–177.

Association for Metallically Stabilized Earth (AMSE), 2006, Reduced Zinc Loss Rate for Design of MSE Structures, White Paper, AMSE, McLean, Virginia, http://www.amsewalls.org.

Baecher, G. B., and Christian, J. T., 2003, *Reliability and Statistics in Geotechnical Engineering,* John Wiley & Sons, Ltd., West Sussex, England.

Beckham, T. L., Sun, L., and Hopkins, T. C., 2005, *Corrosion Evaluation of Mechanically Stabilized Earth Walls,* Report No. KTC-05-28/SPR 239-02-1F, Kentucky Transportation Cabinet, Frankfort, Kentucky.

Berg, R. R., Christopher, B. R., and Samtani, N. C., 2009, *Design of Mechanically Stabilized Earth Walls and Reinforced Slopes,* Report No. FHWA-NHI-09-xxx, National Highway Institute, Washington, DC, 694 p.

Berke, B. S., and Sagues, A. A., 2009, *Update on Condition of Reinforced Earthwall Straps,* Report No, BD544-32, Florida Department of Transportation, Tallahassee. http://www.dot.state.fl.us/researchcenter/Completed_StateMaterials.shtm.

Berkovitz, B. C., and Healy, E. A., 1997, A Rational Process for Corrosion Evaluation of Mechanically Stabilized Earth Walls, *Mechanically Stabilized Backfill,* J. T. Wu, Ed., Balkema, Rotterdam, the Netherlands, pp. 259–287.

Berkovitz, B. C., 1999, Field Monitoring for Corrosion of Metallic Reinforcements in MSE Structures, *Proc. 34th Symposium of Engineering Geology and Geotechnical Engineering,* Logan, Utah, pp. 144–169.

Bounopane, S. G., Schafer, B. W., and Igusa, T., 2003, Reliability Implications of Advanced Analysis in Design of Steel Frames, Proceedings ASSCCA. 2003, Sydney, Australia.

Briaud, J. L., Griffin, R., Young, A., Soto, A., Suroor, A., and Park, H., 1998, *Long Term Behavior of Ground Anchors and Tieback Walls,* Report FHWA/TX-99/1391-1, Federal Highway Administration, U.S. Department of Transportation, Washington, D.C.

Caltrans, 2009, *Special Standard Specification 19-600: Earth Retaining Structures,* California Department of Transportation, Sacramento, California.

Coats, D. M., Tkacheff, W., and Parks, D. M., 1990, *Corrosion Monitoring System for a Mechanically Stabilized Embankment,* Report No. CA/TL-89/14, NTIS, Springfield, Virginia, 49 p.

Coats, D. M., Castanon, D. R., and Parks, D. M., 2003, *Needs Assessment for Maintenance Monitoring Program for Mechanically Stabilized Embankment Structures,* Draft Report, State of California, Department of Transportation, Division of Engineering Services, Materials Engineering and Testing Services, Corrosion Technology Branch, 251 p.

Compton, C., and Oyler, D., 2005, Investigation of Fully Grouted Roof Bolts Installed Under In Situ Conditions, *Proc. 24th International Conference On Ground Control in Mining,* Morgantown, West Virginia, pp. 302–312.

Darbin, M., Jailloux, J. M., and Montuelle, J., 1988, Durability of Reinforced Earth Structures: The Results of a Long-term Study Conducted on Galvanized Steel, *Proc. Institution of Civil Engineers,* Institution of Civil Engineers, Part 1, Volume 84, pp. 1029–1057.

D'Appolonia Consulting Engineers, McMahon & Mann Consulting Engineers, P.C., and the State University of New York at Buffalo, 2001, *NCHRP Web Document 27: Evaluation of Metal-Tensioned Systems in Geotechnical Applications, Phase I,* Interim Report, Transportation Research Board, National Research Council, Washington, D.C.

D'Appolonia Consulting Engineers, 2007, LRFD Calibration of Coherent Gravity Method for Metallically Stabilized Earth Walls, Association for Metallically Stabilized Earth, http://www.amsewalls.org.

Deaver, R., 1992, *Mechanically Stabilized Earth Wall Study,* Final Report, GDOT Research Project No. 9001, Office of Materials and Research, Georgia Department of Transportation, Forest Park, Georgia.

Elias, V., 1990, *Durability/Corrosion of Soil Reinforced Structures,* Report No. FHWA-RD-89-186, Office of Engineering and Highway Operations, R&D, McLean, Virginia, 173 p.

Elias, V., 1997, *Corrosion/Degradation of Soil Reinforcements for Mechanically Stabilized Earth Walls and Reinforced Slopes,* FHWA Report No. FHWA-SA-96-072, NTIS, Springfield, Virginia, 105 p.

Elias, V., Fishman, K. L., Christopher, B. R., and Berg, R. R., 2009, *Corrosion/Degradation of Soil Reinforcements for Mechanically Stabilized Earth Walls and Reinforced Soil Slopes,* FHWA Report No. FHWA-NHI-09-087, NTIS, Springfield, Virginia.

Fédération Internationale de la Précontrainte (FIP) (International Federation for Prestressing), 1986, *Corrosion and Corrosion Protection of Prestressed Ground Anchorages,* State of the Art Report, Thomas Telford, London, United Kingdom.

FHWA, 1993, *Recommendations Clouterre 1991,* English Translation, report on the French National Project Clouterre, FHWA Report No. FHWA-SA-93-026, Washington, D.C., 321 p.

FHWA, 2008, *Earth Retaining Structures and Asset Management,* Publication No. FHWA-IF-08-014, Federal Highway Administration, Washington D.C.

Fishman, K. L., Gaus, M. P., Withiam, J. L., and Bontea, M., 2002, Condition Assessment of Buried Metal-Tensioned Elements, *Transportation Research Record: Journal of the Transportation Research Board, No. 1786,* Transportation Research Board of the National Academies, Washington, D.C., pp. 85–95.

Fishman, K. L., 2004, *Phase I: Condition Assessment and Evaluation of Rock Reinforcements Along I-93 Barron Mountain Rock Cut, Woodstock, NH,* Report No. FHWA-NH-RD-13733L, NTIS, Springfield, Virginia, 21 p.

Fishman, K. L., Withiam, J. L., and Jackson, B. H., 2005, A Recommended Practice for Condition Assessment of Ground Anchors and Soil Nails, *GEO Construction Quality Assurance/Quality Control, Proceedings of the Conference Sponsored by ADSC: The International Association of Foundation Drilling,* D. A. Bruce and A. W. Cadden, Eds., ADSC, Dallas, Texas.

Fishman, K. L., 2005, *Phase II: Condition Assessment and Evaluation of Rock Reinforcements Along I-93 Barron Mountain Rock Cut, Woodstock, NH,* Report No. FHWA-NH-RD-14282C, NTIS, Springfield, Virginia, 263 p.

Fishman, K. L., Salazar, J. M., and Hilfiker, H. K., 2006, Corrosion in an Arid Environment and Condition Assessment of 20-Year Old Mechanically Stabilized Earth Walls, Presented at 85th Annual Meeting of the Transportation Research Board, Washington, D.C.

Fontana, M. G., 1986. *Corrosion Engineering,* 3rd ed., McGraw Hill, New York, 555 p.

Galambos, T. V., and Ravindra, M. K., 1978, Properties of Steel for Use in LRFD, *Journal of the Structural Engineering Division,* ASCE, 104(9), 1459–1468.

Gladstone, R. A., Anderson, P. L., Fishman, K. L., and Withiam, J. L., 2006, Durability of Galvanized Soil Reinforcement: More Than 30 Years of Experience with Mechanically Stabilized Earth, *Transportation Research Record: Journal of the Transportation Research Board, No. 1975,* Transportation Research Board of the National Academies, Washington, D.C., pp. 49–59.

Gong, J., Jayawickrama, P., and Tinkey, Y., 2005, Nondestructive Evaluation of Installed Soil Nails, *Transportation Research Record: Journal of the Transportation Research Board, No. 1796,* Transportation Research Board of the National Academies, Washington, D.C.

Hearn, G., Abu-Hejleh, N., and Koucherik, J., 2004, Inventory System for Retaining Walls and Sound Barriers, *Transportation Research Record: Journal of the Transportation Research Board, No. 1866,* Transportation Research Board of the National Academies, pp. 85–96.

Hegazy, Y. A., Withiam J. L., and Fishman, K. L., 2003, A Practical Semi-Objective Sampling Criterion—How Many Samples Do We Need? *Soil and Rock America 2003, Proceedings, 12th Pan-American Conference on Soil Mechanics and Geotechnical Engineering,* P. J. Culligan, H. H. Einstein and A. J. Whittle, eds., Vol. 2, pp. 2771–2776.

Jackura, J. A., Garofalo, G., and Beddard, D., 1987, *Investigation of Corrosion at 14 Mechanically Stabilized Embankment Sites,* Report No. CA/TL-87/12, California Department of Transportation, Sacramento.

Kendorski, F. S., 2003, Rock Reinforcement Longevity, *Geostrata,* American Society of Civil Engineers, Reston, Virginia, October, pp. 9–12.

King, R. A., 1978, Corrosion in Reinforced Soil Structures, *Proc. ASCE Symposium on Earth Reinforcement,* Pittsburgh, Pennsylvania.

Lawson, K. M., Thompson, N. G., Islam, M., and Schofield, M. J., 1993, Monitoring Corrosion of Reinforced Soil Structures, *British Journal of NDT,* British Institute of Nondestructive Testing, Liverpool, England, 35(6), pp. 319–324.

Liao, S. T., Huang, C. K., and Wang, C. Y., 2008, Sonic Echo and Impulse Response Tests for Length Evaluation of Soil Nails in Various Bonding Mediums, *Canadian Geotechnical Journal,* Vol. 45, pp. 1025–1035.

Lokse, A., 1992, Durability and Long-Term Performance of Rock Bolts, Ph.D. Dissertation, Norwegian Institute of Technology, University of Trondiem.

Lumenaut, 2007, Software Manual, Version 3.4.21, http://www.lumenaut.com.

McGee, P., 1985, *Reinforced Earth Wall Strip Serviceability Study,* Final Report: Study No. 8405, Georgia Department of Transportation, Atlanta, GA, 24 p.

McVay, M., Birgisson, B., Zhang, L., Perez, A., and Putcha, A., 2000, Load and Resistance Factor Design (LRFD) for Driven Piles Using Dynamic Methods—A Florida Perspective, *Geotechnical Testing Journal,* 23(1), pp. 55–66.

Medford, W. M., 1999, *Monitoring Corrosion of Galvanized Earth Wall Reinforcement,* Presented at 78th Annual Meeting of the Transportation Research Board, Washington, D.C.

Paikowski, S. G., 2004, *NCHRP Report 507: Load and Resistance Factor Design (LRFD) for Deep Foundations,* Transportation Research Board of the National Academies, Washington, D.C., 87 p.

Post Tensioning Institute (PTI), 2004, *Recommendations for Prestressed Rock and Soil Anchors,* 4th Edition, Phoenix, Arizona.

Raeburn, C. L., Monkul, M. M., and Pyles, M. R., 2008, *Evaluation of Corrosion of Metallic Reinforcements and Connections in MSE Retaining Walls,* Report No. FHWA-OR-RD-08-10, Oregon Department of Transportation, Salem, http://www.oregon.gov/ODOT/TD/TP_ERS/, 24 p.

Rehm, G., 1980, *The Service Life of Reinforced Earth Structures from a Corrosion Technology Standpoint,* Expert Report, The Reinforced Earth Company, Vienna, Virginia.

Rodger, A. A., Milne, G. D., and Littlejohn, G. S., 1997. Condition Monitoring & Integrity Assessment of Rock Anchorages, *Ground Anchorages and Anchored Structures,* S. Littlejohn, ed., Thomas Telford, London, England, pp. 343–352.

Romanoff, M., 1957, Underground Corrosion, *National Bureau of Standards, Circular 579,* U.S. Department of Commerce, Washington, D.C.

Rossi, J. P., 1996, *The Corrosion Behavior of Galvanized Steel in Mechanically Stabilized Earth Structures,* MS Thesis, Department of Civil and Environmental Engineering, University of South Florida, Tampa.

Sabatini, P. J., Pass, D. G., and Bachus, R. C., 1999, Ground Anchors and Anchored Systems, *Geotechnical Engineering Circular No. 4,* Federal Highway Administration, U.S. Department of Transportation, Washington, D.C.

Sagues, A. A., Rossi, J., Scott, R. J., Pena, J. A., and Simmons, T., 1998. *Influence of Corrosive Inundation on the Corrosion Rates of Galvanized Tie Straps in Mechanically Stabilized Earth Walls,* Final Report WPI0510686, Florida Department of Transportation Research Center, Tallahassee.

Sagues, A. A., Scott, R., Rossi, J., Pena, J. A., and Powers, R., 2000, Corrosion of Galvanized Strips in Florida Reinforced Earth Walls, *Journal of Materials in Civil Engineering,* ASCE, Reston, Virginia.

Smith, A., Jailloux, J. M., and Segrestin, P., 1996, Durability of Galvanized Steel Reinforcements as a Function of their Shape, *Earth Reinforcement,* Ochiai, Yasufuku, and Omine, eds., Balkema, Rotterdam, pp. 55–60.

Stern, M., and Geary, A. L., 1957, Electrochemical Polarization, *Journal of the Electrochemical Society,* 104(1), p. 56.

Task Force 27—AASHTO-AGC-ARBTA, 1990, *Ground Modification Techniques for Transportation Applications.*

Terre Armée Internationale (TAI), 1977, *Durability of Reinforcing Strips,* Report R50, Paris, France.

Timmerman, D. H., 1990, *Evaluation of Mechanically Stabilized Embankments as Support for Bridge Structures,* Interim Research Report, Ohio Department of Transportation.

USACOE, 1980, *Engineering and Design of Rock Reinforcement,* EM 1110-1-2907, Department of the Army Corps of Engineers, Office of the Chief of Engineers, Washington, D.C.

Vardeman, S. B., 1994, *Statistics for Engineering Problem Solving,* PES Publishing Co., Boston, Massachusetts, 712 p.

Weatherby, D. E., 1982, *Tiebacks,* FHWA/RD-82/047, NTIS, Springfield, Virginia.

Weerasinghe, R. B., and Adams, D., 1997, A Technical Review of Rock Anchorage Practice 1976-1996, *Ground Anchorages and Anchored Structures,* Edited by G. S. Littlejohn, Thomas Telford, London, England, pp. 481–491.

Wheeler, J. J., 1999, *NYSDOT, MSES Corrosion Evaluation Program, End of the Year Report for 1998,* NYSDOT Geotechnical Engineering Bureau, Albany, New York.

Wheeler, J. J., 2000, *NYSDOT, MSES Corrosion Evaluation Program, End of the Year Report for 1999,* NYSDOT Geotechnical Engineering Bureau, Albany, New York.

Wheeler, J. J., 2001, *NYSDOT, MSES Corrosion Evaluation Program, End of the Year Report for 2000,* NYSDOT Geotechnical Engineering Bureau, Albany, New York.

Wheeler, J. J., 2002(a), New York's Mechanically Stabilized Earth Corrosion Evaluation Program, Presented at 81st Annual Meeting of the Transportation Research Board, Washington, D.C.

Wheeler, J. J., 2002(b), *NYSDOT, MSES Corrosion Evaluation Program, End of the Year Report for 2001,* NYSDOT Geotechnical Engineering Bureau, Albany, New York.

Withiam, J. L., Voytko, E. P., Barker, R. M., Duncan, J. M., Kelly, B. C., Musser, S. C., and Elias, V., 1998, *Load and Resistance Factor Design (LRFD) for Highway Bridge Substructures,* FHWA HI-98-032, Federal Highway Administration, Washington, D.C.

Withiam, J. L., Fishman, K. L., and Gaus, M. P., 2002, *NCHRP Report 477: Recommended Practice for Evaluation of Metal-Tensioned Systems in Geotechnical Applications,* TRB, National Research Council, Washington, D.C., 93 p.

Whiting, D., 1986, *Corrosion Susceptibility of Reinforced Earth Systems: Field Surveys, Corrosion Effect of Stray Currents and the Techniques for Evaluating Corrosion of Rebars in Concrete,* ASTM STP 906, V. Chaker, ed., American Society for Testing and Materials, Philadelphia, pp. 64–77.

APPENDIX A

Details of Metal Loss Models

This appendix describes the history and pertinent details of metal loss models that have been proposed for estimating sacrificial steel requirements for MSE reinforcements. Most state highway agencies use some form of the AASHTO specifications for the design of MSE walls. Therefore, the AASHTO metal loss model is used in this study to compute nominal sacrificial steel requirements that serve as a basis for calibration of resistance factors for LRFD. This appendix will describe earlier metal loss models and corresponding data sources leading to the development and adoption of the AASHTO model. These models include the Darbin/Romanoff Models and the Stuttgart Model.

Galvanized steel reinforcements are most often employed for the construction of MSE walls, particularly with respect to transportation-related projects. However, the behavior of plain steel is also of interest, as this is compared or related to the loss of steel after the zinc is depleted from the surface. Furthermore, the AASHTO metal loss model only considers the use of galvanized reinforcements, and other models need to be identified to consider the behavior of plain steel (i.e., not galvanized).

Metal loss models used to estimate sacrificial steel requirements for MSE are empirical, and therefore it is important to describe the data sources considered in their development. Although fill characteristics are important considerations, these models do not explicitly relate fill characteristics in terms of their electrochemical properties to corrosion rates. In general, the models consider the effects of time on corrosion rates and apply to particular ranges of fill characteristics. Care must be exercised when using these models to be sure that fill materials have electrochemical properties within the range for which the models are intended. Metal loss models that may be applied to fill materials, that do not necessarily meet AASHTO requirements, are also identified.

Darbin/Romanoff Model

Romanoff (1957) describes 47 years of data collected by the U.S. National Bureau of Standards (NBS) from extensive monitoring of metal samples buried in situ. In general, the corrosion rate was observed to be greatest during the first few years of burial, subsequently decaying to a steady but significantly lower rate. Romanoff suggested the following exponential equation to predict the amount of general corrosion at some time (t) after burial:

$$x = Kt^n \tag{A-1}$$

In Equation (A-1) x is the loss of thickness in the material at time, t, and K and n are parameters that are soil and site dependent. In Equation (A-1) lower case "x" describes metal loss that may include zinc and steel for galvanized elements. Capital "X" is used for other metal loss equations in this appendix to denote loss of steel subsequent to depletion of zinc.

Comprehensive as it was, less than 10% of those data from the NBS study came from free-draining granular soils such as those used in MSE walls, and even less of these data came from galvanized steels. Darbin et al. (1988) addressed this shortcoming during a 20-year study not only to evaluate the corrosion of metallic earth reinforcements in typical MSE wall backfill, but also to identify the soil parameters that determine the kinetics of the corrosion process. Using the form of Equation (A-1), Darbin et al. (1988) proposed that metal loss of galvanized steel could be described with a constant exponent "n" equal to 0.65, and coefficient "K" depending on soil aggressiveness ($K = 25$ μm/year for soils with resistivity $\rho \geq 1{,}000$ Ω-cm and $K = 20$ μm/year for soils with $\rho \geq 3{,}000$ Ω-cm).

Maximum corrosion rates and loss of reinforcement tensile strength from corrosion may be estimated by multiplying the general corrosion rate obtained from Equation (A-1) by a factor of 2 (Elias, 1990). This factor is applied to the metal

loss of base steel subsequent to depletion of zinc from the surface. Thus, a factor of 2 is applied to the Darbin Model to consider strength loss as follows:

for galvanized elements:

$$\text{if } t_f > \left(\frac{z_i}{25}\right)^{1.54} \text{ then } \quad X(\mu\text{m}) = 50\left(\frac{\mu\text{m}}{yr}\right) \times t_f^{0.65}(yr) - 2 \times z_i(\mu\text{m}) \tag{A-2}$$

$$\text{if } t_f \le \left(\frac{z_i}{25}\right)^{1.54} \text{ then } \quad X(\mu\text{m}) = 0$$

In Equation (A-2), X is loss of steel (base metal) in units of μm, and t_f is service life in years. Loss of base steel occurs subsequent to depletion of the zinc coating, and z_i is the initial zinc thickness. Equation (A-2) is applicable to the range of fill conditions representative of MSE wall construction that exhibit ρ_{min} greater than 1,000 Ω-cm.

Elias (1990) proposed the following model for plain steel reinforcements which also has the same form as the original equation proposed by Romanoff [Eq. (A-1)]:

$$X(\mu\text{m}) = 80\frac{\mu\text{m}}{yr} \times t_f^{0.8} \tag{A-3}$$

Data reviewed for Equation (A-3) are based on the NBS data set for plain steel and include a wide range of fill conditions, many not meeting the stringent electrochemical requirements for MSE fills. However, given the scatter inherent to measurements of fill properties and corrosion rates for plain steel, Equation (A-3) is used as a conservative estimate of metal loss in fills that meet MSE fill requirements, but not by a wide margin. Equation (A-3) also includes a factor of 2 to consider the maximum metal loss.

Although corrosion rates for both galvanized steel and carbon steel clearly vary exponentially with respect to time, simple models involving linear extrapolation have been proposed and are considered valid (Elias, 1990) over the limited time frame from which metal loss measurements of earth reinforcements were available (<20 years). Given this limited time frame, most observations of metal loss for galvanized reinforcements are observations of the loss of the zinc coating, not the carbon steel (i.e., steel was not exposed during the monitoring period). The following models, including the Stuttgart, Caltrans, and AASHTO models, are linearized forms of the Romanoff/Darbin equation.

Stuttgart Model

Rehm (1980) proposed an alternative piecewise linear model for describing metal loss. The longevity of the zinc coating is considered using a bilinear model such that the rate of zinc consumption is greatest during the first 2 to 4 years, followed by a significantly reduced rate. Therefore, the reduced rate considers passivation of zinc that occurs in backfill soils typical of MSE wall construction. Steel consumption is considered to begin after the zinc layer is consumed, but at a rate observed from samples of plain steel appropriate to the age of the reinforcements (i.e., rate of corrosion for steel that has been in service for more than 2 years). This model was the basis for the sacrificial steel requirements for galvanized reinforcements recommended by Task Force 27 (1990); AASHTO (2002a) later adopted a different, more conservative, piecewise linear model as described later in this appendix.

Metal loss models are proposed considering galvanized or plain steel reinforcements and fill materials with low and high salt contents. Low salt contents are described as materials with 4.5<pH<9.5, ρ > 1,000 Ω-cm, chloride content less than 50 ppm, and sulfate content less than 200 ppm. For this condition, the Stuttgart model is as follows:

for galvanized elements:

$$X(\mu\text{m}) = 9\frac{\mu\text{m}}{yr} \times \left(t_f - 2yr - \frac{(z_i - 12\mu\text{m})}{2\frac{\mu\text{m}}{yr}} \right) yr \tag{A-4}$$

for plain steel elements:

$$X(\mu\text{m}) = 45\frac{\mu\text{m}}{yr} \times 2yr + (t_f - 2yr) \times 9\frac{\mu\text{m}}{yr} \tag{A-5}$$

For fill materials that are saturated with chloride or sulfate concentrations greater than the threshold values, the Stuttgart model is as follows:

for galvanized elements:

$$X(\mu\text{m}) = 12\frac{\mu\text{m}}{yr} \times \left(t_f - 3yr - \frac{(z_i - 51\mu\text{m})}{2\frac{\mu\text{m}}{yr}} \right) yr \tag{A-6}$$

for plain steel:

$$X(\mu\text{m}) = 80\frac{\mu\text{m}}{yr} \times 2yr + (t_f - 2yr) \times 12\frac{\mu\text{m}}{yr} \tag{A-7}$$

AASHTO Model

According to AASHTO, MSE fill must comply with the following electrochemical criteria:

- pH = 5 to 10
- Resistivity ≥ 3,000 Ω-cm,

Table A-1. Summary of data sources for metal loss models for MSE reinforcements.

MODEL	DATA SOURCE	MAXIMUM
Stuttgart	NBS	NO
Darbin	Controlled conditions - electrochemical test specimens & samples buried in soil box	YES
AASHTO	Stuttgart & Darbin	YES

- Chlorides ≤ 100 ppm,
- Sulfates ≤ 200 ppm, and
- Organic content ≤ 1%.

The fill requirements are intended to control corrosion potential with fills that are between noncorrosive and "mildly" corrosive. The AASHTO metal loss model defines the following rates at which first zinc, then steel, will be lost from the MSE reinforcement section:

- Loss of zinc (first 2 years): 15 μm/yr;
- Loss of zinc (to depletion): 4 μm/yr; and
- Loss of steel (after zinc depletion): 12 μm/yr.

Using the AASHTO Model the steel loss per side (X) in μm/yr for a given service life, t_f, and initial thickness of zinc coating, z_i, is computed as

$$X(\mu m) = 12\frac{\mu m}{yr} \times \left(t_f - 2yr - \frac{(z_i - 30\mu m)}{4\frac{\mu m}{yr}} \right) yr \qquad \text{(A-8)}$$

Both the Darbin/Romanoff and the Stuttgart Models contribute to the basis of the AASHTO Model. Table A-1 identifies sources of data associated with each. These data sources include the NBS studies from metal samples that were buried within a wide range of fill conditions at sites located throughout the United States; and from carefully controlled laboratory tests conducted in France, specifically with regards to MSE reinforcements. Laboratory studies included electrochemical test cells and burial boxes. The electrochemical test cells were assembled using relatively small (compared to burial boxes) plastic tubes containing specimens of reinforcement surrounded by soil. Electrodes were sealed into the ends of the tubes, serving as reference and counter electrodes, to facilitate measurements of corrosion rates at frequent intervals. Compared to the electrochemical test cells, burial boxes incorporated representative specimens of MSE reinforcements and conditions that more closely resemble field installations. The burial boxes employed weight loss measurements that could be related to metal loss, and corresponding corrosion rates averaged over longer time intervals.

Thus, the AASHTO model considers a variety of data sources, each with its own set of strengths and limitations. However, results from these different data sources compare reasonably well. The outstanding limitations of each data source involve a lack of data to document the corrosion/metal loss of the base steel subsequent to depletion of zinc from the surface. Thus, similar to the Stuttgart model, the AASHTO model considers steel consumption to begin after the zinc layer is consumed, but at a rate observed from samples of plain steel appropriate to the age of the reinforcements.

Figure A-1 illustrates the comparison between the Stuttgart and AASHTO models. The corrosion rates for the zinc coating during the first 2 years of service and for steel subsequent to depletion of zinc roughly correspond to the Stuttgart model that applies to higher salt contents (e.g., chlorides in excess of 50 ppm). However, the corrosion rate for zinc after 2 years in service of 4 μm/year is twice the value of 2 μm/year from the Stuttgart Model. The rationale for the use of the higher corrosion rate may be understood by examining the comparison with the Darbin model as depicted in Table A-2.

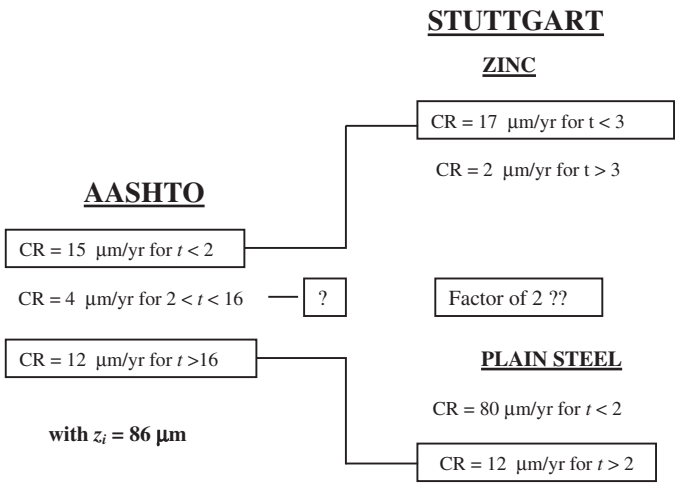

Figure A-1. Comparison of AASHTO and Stuttgart Models.

Table A-2. Comparison of AASHTO and Darbin models.

Darbin Model	$X\ (\mu m) = 50t^{0.65} - 2\ (z_i)$	(Includes Factor of 2)
AASHTO Model	$X\ (\mu m) = (t\text{-}C) \times 12\ (\mu m/yr)$	(C= 16 years with z_i = 86 µm)
Computed Metal Loss X (µm)		
t (yrs)	DARBIN	AASHTO
50	464	408
64	574	576
75	655	708
100	825	1,008

Table A-2 indicates that metal losses computed with the AASHTO model compare reasonably well with the Darbin model. The differences depend on time (service life), and the two models render nearly the same metal loss when t = 64 years. Apparently, using a higher corrosion rate for zinc of 4 µm/year renders metal loss consistent with the Darbin model, which directly considers applying a factor of 2 to consider maximum metal loss. Note that although the AASHTO specifications require fill with ρ > 3,000 Ω-cm, the basis of the models (both Stuttgart and Darbin) are referred to fill with ρ > 1,000 Ω-cm. Thus, the AASHTO model and corresponding specifications for fill are conservative.

Caltrans-Interim Design Guide

Based on the results from limited field studies, Caltrans (Jackura et al., 1987) has proposed design guidance for a wider range of reinforced fill conditions than those considered by AASHTO. Higher rates of metal loss are specified for computing sacrificial steel requirements when reinforced fills that are more aggressive relative to corrosion are considered during design. These metal loss rates are based on limited data collected from MSE wall sites in California (Jackura et al., 1987), and use data available from the earlier NBS studies. Interim design guidance considered fill properties that include minimum resistivity more than 1,000 Ω-cm. However, current specifications used by Caltrans (2009) do not allow use of reinforced fill with minimum resistivity less than 2000 Ω-cm. The steel loss, X, for design life, t_f, is described by the Caltrans interim model as:

$$X(\mu m) = (t_f - C(yrs)) \times K \frac{\mu m}{yr} \quad \text{(A-9)}$$

where C is the time for zinc depletion (years) assuming an initial zinc thickness of 86 µm and K (µm/yr) is the corrosion rate of the base steel. Table A-3 provides values for C and K as functions of fill conditions.

Current specifications used by Caltrans (2009) do not allow use of reinforced fill with minimum resistivity less than 2,000 Ω-cm. Specifically, the current Caltrans specification allows for backfill with a resistivity greater than 2,000 Ω-cm, a pH between 5.5 and 10, and maximum chloride and sulfate concentrations of 250 ppm and 500 ppm, respectively. California considers these conditions by using a higher rate of metal loss in determining sacrificial steel and reducing the design life of the MSE wall to 50 years. Caltrans assumes that the zinc coating provides 10 years of service life for the specified minimum coating thickness of 2 oz/ft² (86 µm per side). This is less than the 16 years of zinc life inherent to the AASHTO metal loss model. A corrosion rate of 1.10 mils/yr (28 µm/yr) is considered to affect the base steel after the zinc has been consumed

Table A-3. Summary of parameters for Caltrans-Interim guidelines (Jackura et al., 1987).

Fill Type	K (µm/yr)	C (years)
Neutral & Alkaline	28	10
Acidic	33	10
Corrosive	71	6
Select Granular	13	30

Notes: Neutral and alkaline: minimum resistivity > 1,000 Ω-cm and pH > 7.
Acidic: minimum resistivity > 1,000 Ω-cm and pH < 7.
Corrosive: minimum resistivity < 1,000 Ω-cm.
Select granular soils are clean, free draining gravels with less than 5% fines and minimum resistivity > 1,000 Ω-cm.

and used to compute the sacrificial steel requirements. These corrosion rates account for the potential for localized corrosion and pitting; that is, a factor of 2 relating the loss of tensile strength to idealized uniform corrosion rates is included.

Caltrans specifications provide incentives to use select granular fill, which is a better quality fill with less than 5% fines and with plasticity index (PI) <6. Caltrans reduces the steel corrosion rate to 13 μm/yr for backfill meeting additional requirements for select granular fill. For select granular fill, lower resistivity and higher salt concentrations are allowed, but the allowable fines content is less compared to current AASHTO requirements.

APPENDIX B

Test Protocols

Proper implementation of test procedures and interpretation of results from condition assessment require information on reinforcement type and geometry, as well as backfill and site conditions. The subsurface environment surrounding the elements must be characterized in terms of soil or rock types, moisture conditions, presence of organics, and electrochemical parameters known to contribute to corrosiveness. Installation details include reinforcement type, metal type, and degree of corrosion protection. Quantitative guidelines are available for assessing the potential aggression posed by an underground environment relative to corrosion (FHWA, 1993). Generally, moisture content, chloride and sulfate ion concentration, resistivity and pH are identified as the factors that most affect corrosion potential of metals underground. Details for collecting, testing, and evaluating soil and groundwater samples are described in the recommended practices prepared by Withiam et al. (2002) and Elias et al. (2009). In what follows sampling and testing protocols for condition assessment and corrosion monitoring reinforcements are described.

Sampling

Selected sites for evaluating the overall performance of earth reinforcements should encompass different reinforcement types, loading, environmental and drainage conditions, backfill, and in-situ soil or rock characteristics representative of installations and construction practices that have been used within the United States over the past 30 to 40 years. Sampling protocols are described for both Type I and Type II reinforcements.

Type I Reinforcements (MSE)

In general, approximately 20 to 30 in-service reinforcements, and 20 to 30 coupons should be monitored at each site. These elements are distributed amongst three or four monitoring stations. The number of monitoring stations depends on the length and geometry of the wall. As a rule of thumb, two locations spaced at least 200 ft (60 m) apart should be considered for mechanically stabilized earth (MSE) structures 800 ft (250 m) or less in length and three locations for longer structures. At each location, corrosion should be monitored at a minimum of two depths from the surface, or preferably, at depth intervals of 10 to 13 ft (3 to 4 m) because differences in oxygen content, moisture content, and salt concentration can produce different corrosion behavior. One critical location (center of structure) should be selected for establishing test locations at both shallow and deep positions. Higher oxygen and salt content are anticipated near the surface, and higher moisture contents or free water near the base of a structure. Prior field programs have indicated that where groundwater intrudes at the base of the structure, higher corrosion rates should be anticipated. Where this condition is not likely, representative estimates may be obtained from shallow-depth monitoring. The shallow-depth stations should be approximately 5 ft (1.5 m) in depth, and the deep position should be approximately at one-fourth of the structure height from base level.

Each monitoring station incorporates two to three sampling points generally located near the base, middle, and top of the walls. Sampling points include at least two reinforcements wired for monitoring, one steel coupon, one galvanized coupon, possibly a zinc coupon, and an access hole for placement of a reference electrode in contact with the wall fill. Special C-clamps are used to facilitate electrical connection and wiring to existing in-service reinforcements. Soldered connections are preferred for new installations. Photographs 1-8 in Figure B-1, depict installation of a typical corrosion monitoring station for in-service reinforcements.

Ideally, three types of coupons should be placed at each location and depth; zinc, steel, and galvanized. In the case of galvanized reinforcements both plain steel and galvanized coupons, and in some instances pure zinc coupons are installed. For monitoring, it is desirable to have one-zinc, one-steel, and up to four galvanized coupons at each depth. The multiple

1. Coring hole through precast panel to access backfill and soil reinforcements

2. Access holes advanced at station

3. Galvanized coupons prepared for installation

4. C-clamps for wiring reinforcements

5. C-clamp attached to reinforcement

6. C-clamp connection sealed with epoxy

Figure B-1. Typical installation of a corrosion monitoring station.

(continued on next page)

7. Station with junction box

8. Typical junction box

Figure B-1. (Continued).

galvanized coupons can provide opportunities for periodic removal. Coupons each have two leads to provide backup in case one connection fails. Coupons are made from the same or similar material as the in-service reinforcements and are placed within the wall fill to provide baseline measurements during monitoring.

In general, more monitoring locations should be established for structures where poor performance is anticipated or known to exist (Withiam et al, 2002; Hegazy et al, 2003). Particular attention should be given to monitoring near drainage inlets or other areas that may be subject to fluctuations in moisture content, high moisture content, or inundation. However, monitoring at locations with "normal" conditions is still necessary to serve as a baseline and to ensure that the sample statistics are not skewed.

Practices vary among state departments of transportation (DOTs) and not all establish corrosion monitoring stations in the same manner including all the details as described in the section. In particular, Caltrans installs a cluster of 18 inspection rods in a grid pattern that includes six columns and three rows. The inspection rods are spaced at 10-foot intervals vertically and are approximately 25 feet apart in the lateral direction. The inspection rods are made from the same material as the in-service reinforcements. In North Carolina, often only a single monitoring point is established near the base of the wall that includes between two and four in-service reinforcement wires for monitoring and zinc and steel coupons (i.e., galvanized coupons are not installed). Details of the practices from California and North Carolina are described in Appendix C.

Type II Reinforcements

Nondestructive testing (NDT) and condition assessment requires a sampling strategy whereby the appropriate sample size is selected to provide a statistical basis for the test results. Withiam et al. (2002) and Hegazy et al. (2003) describe a simplified sampling criteria based on the probability that the sampled population will represent conditions throughout the site. The recommended sample size is based upon the total number of elements at the site, the importance of the facility relative to the consequences of failure, and a reference, or baseline, condition for comparison to observations. Generally, for a population consisting of 10 to 200 metal-tensioned elements, between 10 and 40 randomly distributed samples are required.

Corrosion Monitoring and Condition Assessment

Type I Reinforcements

Visual Observations

Visual observations can be made on the exposed portions of the earth reinforcements, and readings of half-cell potential and corrosion rate are collected from in-service reinforcements

that are wired for monitoring, and from coupons installed within the wall fill. For older walls that are retrofitted for corrosion monitoring, the condition of the reinforcing strips near the tie-strip may be observed where they are connected to the precast concrete wall-facing after advancing the access holes and exposing the reinforcements. For walls where core holes are not advanced through the wall face, reinforcements may be examined from shallow excavations near the surface along the top of the wall.

Half-Cell Potential Measurement

The half-cell potential, E_{corr}, is the difference in potential between the metal element and a reference electrode. Equipment required for performing measurement of half-cell potential includes a half cell, a high impedance voltmeter, and a set of lead wires. A copper/copper sulfate reference electrode (CSE) was used for this study. Lead wires are attached to the end of the test element and the half cell. The lead from the half-cell is connected to the negative terminal of the voltmeter, and the test element lead is connected to the positive terminal. Results from the test can provide a comparison between metallic elements at different locations at the same site, as well as identify the presence of different metals, (e.g., zinc or iron). Half-cell potentials may be correlated with zinc loss and used to monitor the condition of galvanized reinforcements. Coupons or dummy reinforcements assist in interpretation of half-cell potential measurements. Plain steel, galvanized steel, and zinc coupons may provide baseline measurements for comparison.

Half-cell potentials are useful to assess the condition along the surface of the reinforcements/coupons. Half-cell potentials are affected by the environment, including soil moisture and salt content, as well as by conditions on the surface of the test element, including the presence of a passive film layer and metal oxides. Therefore, care should be taken when interpreting measurements to identify when effects other than corrosion or presence of zinc on the surface are affecting measurements of half-cell potential. Multiple measurements of half-cell potential are necessary (i.e., numerous samples) and reference values for steel and zinc potentials need to be obtained under site-specific conditions (i.e., nominal values for zinc and steel potentials may not reflect site conditions).

Linear Polarization Resistance

Linear polarization resistance (LPR) measurements are used to observe instantaneous corrosion rates. Lawson et al. (1993), Elias et al. (2009), and Berkovitz and Healy (1997) describe the application of the LPR technique to MSE reinforcements. Polarization resistance measurements require an instrument to generate a plot of potential versus applied current (E versus i_{app}) for a range of approximately $E \pm 20$ mV relative to the free corrosion potential of the reinforcement being monitored. Three electrodes are required to perform the test including working, counter, and reference electrodes. The working electrode is the reinforcement being monitored and a nearby reinforcement is used as a counter electrode. The potential at the interface of the working electrode is controlled through current impressed between the working and counter electrodes. A CSE serves as a reference electrode to monitor the changing potential of the working electrode. The measured resistance, PR′, is actually the sum of the interface and soil resistance ($PR' = PR + R_s$) and a correction for soil resistance is often necessary.

The LPR uses polarization resistance measurements to estimate the corrosion rate at an instant in time. The measurement represents an average of the corrosion occurring over the surface area of the test element. LPR measurements are made with the FHWA PR Monitor supplied by CC Technologies (Model # PR 4500) following the protocol described by Elias (1990) and Berkovitz and Healy (1997). A few parameters, including an environmental constant, the surface area of the test element, and the density and valence of the metal species must be known, or assumed, to relate the measured polarization resistance to corrosion rate. Also, the measured polarization resistance is corrected for uncompensated soil resistance inherent to testing within the underground environment. The PR Monitor measures the soil resistance (R_s) via the AC impedance technique and subtracts this from the total polarization resistance to render the corrected polarization resistance. The soil resistance is a function of the specific resistance (ρ), which is related to wall fill properties including moisture and salt content, as well as the geometry of the system, including the surface area of the reinforcement and the distance between the reinforcement and the reference cell.

LPR measurements represent the corrosion rate at the instant of measurement. Corrosion rates may vary, and measurements with respect to time are needed. Thus, initial measurements are often taken after installation of corrosion monitoring stations, followed by measurements at 6-month intervals and thereafter for a 2-year duration, and then measurements at 5- or 10-year intervals.

Type II Reinforcements

Details of the recommended practice for condition assessment of Type II reinforcements are described in Withiam et al. (2002) and Fishman et al. (2005). In general, the protocol is described as follows:

- Collect preliminary information including installation details and site conditions.
- Identify appropriate mathematical models of service life and use these models to estimate metal loss from corrosion and remaining service life.
- Probe the elements with nondestructive tests, supplemented with invasive testing as appropriate, to assess the existing condition of selected elements comprising the metal-tensioned system.

- Compare results of the condition assessment to expectations based on site conditions and estimated metal loss.
- Recommend an action plan based on results from the condition assessment.

Installation details have an effect on the vulnerability of the system to corrosion and on our ability to probe the elements and interpret data from NDT. Relevant details include steel type, corrosion protection measures, drill hole dimensions, bond length, free length, total length, date of installation, level of prestress, grout type, and use of couplings. If the system is protected with an adequate, well constructed corrosion protection system [e.g., meeting the requirements of PTI Class I (PTI, 2004)], then corrosion has not been found to be a problem. However, construction details, element durability, and workmanship associated with the corrosion protection system may affect the service life.

Nondestructive test techniques are used to probe the elements, and the results are analyzed for condition assessment. Four NDTs are commonly applied for condition assessment including measurement of half-cell potential, polarization current, impact, and ultrasonic testing. Half-cell potential and polarization measurements are electrochemical tests and the impact and ultrasonic techniques are mechanical tests involving observations of wave propagation. In general, these NDTs are useful indicators of the following aspects of the condition assessment:

- Half-cell potential tests serve as an indicator of corrosion activity.
- Results from the polarization test are correlated with the surface area of steel that may be in contact with the surrounding rock mass (i.e., indicator of grout quality and degree of corrosion protection) and may be used to estimate an average corrosion rate.
- Impact test results are useful to diagnose loss of prestress, assess grout quality, and indicate if the cross section is compromised from corrosion or from a bend or kink in the element.
- Ultrasonic test results are useful for obtaining more detailed information about the condition of elements within the first meter from the proximal end of the element.

Withiam et al. (2002) and Fishman et al. (2002 and 2005) describe details of NDT including test procedures. Half-cell potential and LPR measurements are similar to those described for Type I reinforcements.

Sonic Echo Measurements

The sonic echo method (impact test) is used for evaluating cracking of grouts, fracture of tendons, and loss of element section. For this test method, the specimen is impacted using a hammer or ball device, which generates elastic compression waves with relatively low frequency content. Equipment required for the impact echo test method includes an impact device, an accelerometer, velocity or displacement transducer for measuring the specimen response, and a data acquisition system. Components of the test are connected with standard coaxial cables and Bayonet Neill-Concelman (BNC) connectors. Generally, an accelerometer is attached to the free end of the element and the impact is also applied to the free end.

Ultrasonic Test

The ultrasonic test method is a good technique for evaluating grout condition, fracture of elements, and abrupt changes in the element cross section. The method has many of the features of the sonic echo technique except that the transmitted signal contains relatively higher frequencies. Ultrasonic waves are radiated when an ultrasonic transducer applies periodic strains on the surface of the test object that propagate as stress waves. Compression waves consisting of alternating regions of compression and dilatation propagate along the axial direction of a rock bolt. Equipment required for the test includes a pulse source/receiver unit, an ultrasonic transducer, and a data acquisition system.

The ultrasonic transducer is acoustically coupled to the exposed end of the anchor rod. Grease is used as an acoustic couplant. The time taken for sound pulses, generated at regular intervals, to pass through the specimen and return, is measured. Return pulses may be either from a single reflection at a discontinuity or from multiple reflections between a discontinuity and the end of the specimen. The patterns of the received pulses can provide valuable information about the nature of a defect, and of the structure of the material being tested. The advantage of the pulse-echo method is that only one side of the specimen needs to be accessed for transducer placement.

Data Interpretation

Impact Tests

Impact (sonic echo) test results are interpreted by plotting time-histories of the responses measured by the accelerometer for each impact test. The maximum responses correspond to the impact, and the responses are normalized with respect to these maximum values. Figure B-2 presents typical time histories designated as Bolt Numbers 1, 3, and 10. The decay of the initial response is shown on the left-hand side of Figure B-2 and is useful to assess the relative level of prestress carried by the elements. A relatively high rate of decay (i.e., highly damped system due to more dispersion) is indicative of high

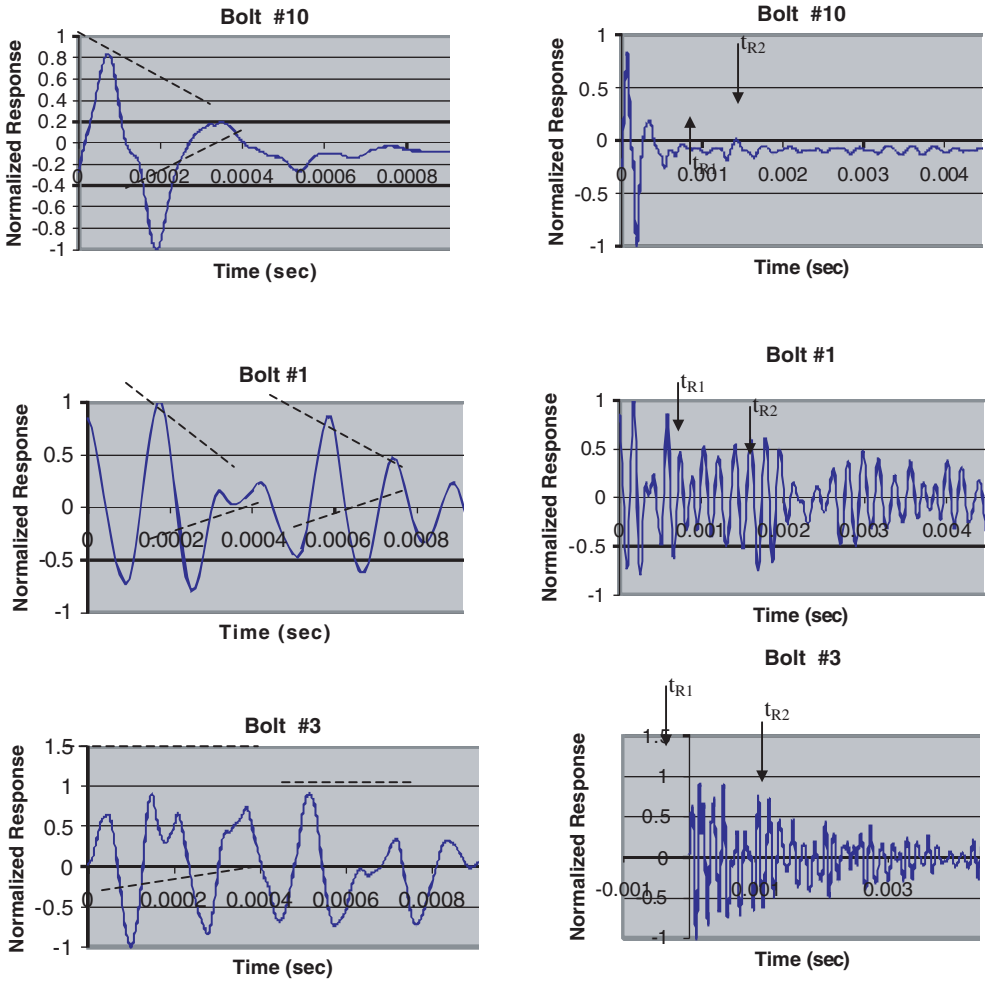

Figure B-2. Typical time histories of responses from impact tests.

remaining prestress, and a low rate of decay is associated with a loss of prestress. Based on past experience, a high rate of decay is indicated if the signal strength decays to less than 20% of the original signal strength within a millisecond. As shown in Figure B-2, Bolt #10 and Bolt #1 are examples of a high rate of decay. A reflection at approximately 0.5 ms is evident from the response of Bolt #1, but the rate of decay subsequent to this reflection is high. The response of Bolt #3 is an example of a low rate of decay.

Responses from impact testing are recognized in terms of relatively strong, versus relatively weak, signal attenuation. If the surrounding grout is very high quality, then strong reflections are not expected beyond a distance of approximately 10 to 15 feet. The plots on the right-hand side of Figure B-2 depict the time history of the response over 5 milliseconds. Based on installation records, and observations from bolts that have been exhumed from this site, we expect that lengths are between 10 and 20 feet, and the elements (rock bolts in this case) are surrounded by grout for approximately 5 feet at the distal end. Assuming that the compression wave velocity of the steel bolt is approximately 18,000 ft/s, the corresponding arrival times for reflected waves is 0.5 to 1.7 milliseconds from the beginning of the grout column and approximately 1 to 2.2 ms from the end of the bolt. Evaluation of these reflections serves two purposes. First, we may assess the difference in grouted lengths from these results to compare with the assumed lengths (corresponding to surface areas) used to interpret the LPR measurements. Second, the strengths of the reflected signals are useful to access grout quality. Good grout quality corresponds to a weak reflected signal from the distal end. If a strong reflection is recognized, then grout quality is considered poor, and the reinforcements may not be completely surrounded by grout in the bonded zone, or the grout may be highly fractured. Based on past experience, strong reflections correspond to reflected signal amplitudes greater than 20%, moderate is between 10% and 20%, and the amplitudes of weak reflections are less than 10% of the maximum response. Using these criteria, the time histories shown in Figure B-2 depict weak reflections for Bolt #10 and strong reflections for Bolts #1 and #3.

Ultrasonic Tests

Due to the higher frequency content of the sound waves compared to the sonic echo test, results from ultrasonic testing provide more resolution and are better suited to detect reflection sources located within the first few feet from the backside of the anchor plate. This region is often associated with a relatively high concentration of oxygen, and subject to cycles of wetting and drying, that promotes corrosion. Often the reinforcement is not in contact with the surrounding rockmass near the anchorage, so corrosion at this location cannot be captured by LPR measurements, and the ultrasonic test is an alternative method to detect a potential loss of cross section from behind the anchorage assembly.

Half-Cell Potentials

The primary purpose of half-cell potential measurements is to establish when significant portions of the galvanized steel reinforcements have lost zinc and steel is exposed to the wall fill. For a given material in a given environment, the potential is an indication of the corrosion activity. The more positive the potential, the greater, in general, is the corrosion. Potential measurements are therefore only qualitative indications of corrosion activity and should only be used to determine the composition of the surface.

Galvanized and plain steel coupons provide baseline measurements for comparison with half-cell potentials of galvanized in-service reinforcements. Typical values of E_{corr} with respect to a CSE are between −1,000 mV to −800 mV for pristine galvanized steel or zinc, and −700 mV to −400 mV for plain carbon steel. If the potential of the reinforcing element is close to that of a recently placed galvanized coupon, it is inferred that the zinc is still present along the length of the reinforcement. As the potential becomes more positive and begins to approach that of the steel coupons, the zinc coating is being lost as steel is exposed on the surface.

The interpretation of potential measurements for galvanized reinforcements considers that four distinguishable layers of zinc coating are formed as a result of the hot-dip process used to galvanize MSE reinforcements. The outside layer is nearly pure zinc, and the succeeding inner layers are essentially zinc-iron alloys. Progressively higher iron contents prevail as the interface with the base steel is approached. Therefore, as zinc consumption progresses towards the base steel interface, the half-cell potential is consistently shifted toward values inherent to iron. Ultimately, measurements of the half-cell potential reflect the presence of steel after all four layers of the zinc coating are exhausted and bare steel is exposed, at least in some areas.

For Type II reinforcements, or soil nails that may be surrounded by grout, half-cell potentials can indicate if an element is effectively passivated or can indicate if the grout is a resin type. Elements passivated by portland cement grout will have half-cell potential greater than −200 mV. Limits recommended by ASTM C-876 suggest that half-cell potentials more positive than −200 mV indicate a low likelihood that corrosion is occurring, while values more negative than −300 mV indicate a high likelihood that corrosion is occurring. For resin-grouted systems and steel reinforcements, half-cell potentials are generally more negative than −500 mV.

Corrosion Rates from LPR Measurements

The corrosion current density is the current within the corrosion cell in the absence of any external sources. Stern and Geary (1957) showed that for small deviations from the free corrosion potential (±20 mV), the corrosion current density is inversely proportional to polarization resistance as:

$$R_p = \left[\frac{d\epsilon}{di_{app}}\right]_{\epsilon\to 0} = \left[\frac{\Delta\epsilon}{\Delta i_{app}}\right]_{\epsilon\to 0} = \frac{\beta_a\beta_c}{2.3\times i_{corr}\left(\beta_a+\beta_c\right)} = \frac{B}{i_{corr}} \quad \text{(B-1)}$$

where

ϵ = the shift of the half-cell potential from the open circuit potential (volts);
i_{app} = applied current (amperes/cm^2);
i_{corr} = corrosion current density (amperes/cm^2);
β_a = anodic Tafel constant (volts/decade);
β_c = cathodic Tafel constant (volts/decade);
B = environmental constant ($B \approx 0.035$ V for galvanized steel and $B \approx 0.026$ V for steel); and
R_p = polarization resistance normalized for area that involves multiplying the polarization resistance (PR) by the reinforcement surface area (A_s) in contact with backfill; that is, R_p (Ω-cm^2) = PR × A_s.

The LPR measurement technique involves scanning or stepping the potential from (−5 to −20 mV) to (+5 to +20 mV) around the free corrosion potential, while simultaneously measuring the applied current. Polarization resistance is determined from the slope of this plot (i.e., $R_p = \epsilon/i_{app}$). If the surface area of the working electrode is known, corrosion current density may be determined from the measured polarization resistance and, ultimately, related to corrosion rate.

Elias (1990) and Lawson et al. (1993) discussed the need to correct the measurement of R_p for soil resistance. If the soil resistance is relatively large, the measured PR′ can be much greater than the true value for PR, and the estimated corrosion rate may be significantly less than the actual corrosion rate occurring at the surface. To correct for the effect of soil resistance, an AC signal is applied to the working electrode at the end of the standard polarization measurement cycle. During a high frequency measurement, the AC voltages reverse magnitude and polarity so rapidly that the interface capacitance does not impede polarization, and PR is short-circuited. This

permits independent measurement of R_s, allowing PR to be calculated as $PR' - R_s$.

Based on Faraday's Law, corrosion rate (CR) can be estimated from i_{corr} as follows:

$$CR\left(\frac{\mu m}{yr}\right) = (3.27\times10^6)\times\frac{i_{corr}\times W}{\rho\times n} \quad \text{(B-2)}$$

where

W = atomic weight (e.g., 55.84 for steel and 65.37 for zinc),
n = valence (e.g., 2 for steel or zinc), and
ρ = density in g/cm^3 (e.g., 7.87 for steel and 7.14 for zinc).

Quantification, or estimation, of errors inherent to measurement of corrosion rate involves an assessment of (1) parameters that are often assumed and used to relate polarization resistance (measured) to corrosion rate and (2) the accuracy of the polarization resistance measurement. Errors in measurement include those associated with measuring polarization resistance and solution resistance, and errors computing the corrosion rate arise from the selection or assumption of the parameters and constants used for Equations (B-1) and (B-2).

Parameters for Computing Corrosion Rate from LPR Measurements

An environmental constant (B) relating polarization resistance to corrosion current density (i_{corr}), and the constants relating i_{corr} to corrosion rate need to be known or assumed to compute corrosion rate from measurement of polarization resistance. These inputs depend upon metal type and the physicochemical properties of the backfill. In general, the B parameter is assumed as 0.026 V for steel elements and 0.05 V for zinc elements embedded in soil. The selection of B for galvanized elements is more ambiguous because it is not known a priori if zinc, steel, or a mixture of zinc and iron is exposed on the surface of the element. However, a value of B equal to 0.035 V is often used to consider galvanized elements. Similarly, the constant relating i_{corr} to corrosion rate may vary by a factor of approximately 1.3, which can be realized by comparing the atomic weights, densities, and valances of steel and zinc for use in Equations (B-1) and (B-2).

The environmental constant is related to the tafel slopes, which define the slopes of the anodic and cathodic branches of the overpotential where they become linear in a plot of overpotential versus the logarithm of applied current. Tafel slopes were measured at 11 sites, included as part of Task 6, using special equipment that applies overpotential (±250 mV), which exceeds what is needed for LPR measurements (±20 mV). Results from these measurements are presented in Table B-1. Direct measurement of tafel slopes is limited because of the need for special equipment and because imparting this level of overpotential can have a lasting effect on the electrochemical properties on the surface of the reinforcement (i.e., future measurements of corrosion rate may be affected by test history).

The means and ranges of the environmental constant, B, that were measured at selected sites are:

Material	Mean (V)	Range (V)
Steel	0.024	0.010–0.030
Galvanized	0.035	0.010–0.058
Zinc	0.040	0.030–0.050

The means of the measurements are very close to the assumed values used in Equations (B-1) and (B-2) to reconcile corrosion rate from LPR measurements.

Table B-1. Summary of observed environmental constants.

State	Site	Element	*B* (V)		
			Steel	Galvanized	Zinc
NH	I-93 Southbound, Barron Mtn.	A	0.033	-	-
		B	0.024	-	-
		C	check	-	-
		D	0.023	-	-
NC	I540 Exit 26B	-	0.010	0.040	0.030
	I540 & TTC	-	0.020	0.050	0.030
	I64 MP 423	-	0.020	0.020	0.050
	I77 at Tyvola	-	0.023	0.034	0.050
NY	SHR Northwest Abutment	1	-	0.042	-
	SHR Southwest Abutment	1	-	0.056	-
	SHR Southwest Abutment	2	-	0.058	-
CA	Site No. 532819	R 15	-	0.010	-
	Site No. 532819	R 8	-	0.010	-
	Site No. 532822	R 1	-	0.037	-
	Site No. 532823	R 12	-	0.010	-
	Site No. 541093	12	-		-
NY	MMCE Lab	-	0.020	0.054	-

NOTE: TTC = Triangle Town Center, SHR = Sweet Home Road, MMCE = McMahon & Mann Consulting Engineers, and - = not applicable.

Comparison of Device Performance

Results obtained with a commercially available general-purpose, corrosion monitoring device (GAMRY G600) are compared with those from a unit built specifically for the FHWA (PR Monitor) for monitoring the performance of MSE reinforcements. The hardware (Potentiostat/Galvanostat/Zero Resistance Ammeter) incorporated into each unit is similar. However, the general-purpose equipment allows user flexibility in terms of data processing and interpretation, and, in contrast, the user cannot alter the protocols programmed into the FHWA unit. Both the GAMRY G600 and the FHWA PR Monitor correct for uncompensated solution resistance (soil resistance) as part of the LPR measurement. Both units measure the soil resistance via an AC input and subtract this from the measured polarization resistance to render the corrected polarization resistance.

The PR Monitor supplied by CC Technologies, Inc. utilizes a potential control stepping sequence that is completely flexible and programmable by the operator. The PR Monitor also presents the coefficient of linear regression used to calculate the value of PR′ from the ϵ vs. i_{app} plot. A regression coefficient of 0.9 or greater indicates a reasonably good fit of the data. The corrosion current density is determined from Equation (B-1) using the measured value of PR, A_s, and the appropriate environmental constant. Finally, Equation (B-2) is used to estimate corrosion rate.

McMahon & Mann Consulting Engineers (MMCE) and Caltrans performed redundant tests with the GAMRY and FHWA PR monitors. Data were collected from sites in northern and southern California during the periods from July 14, 2007 to August 24, 2007 and April 9, 2008 to May 1, 2008. The data set includes 61 individual measurements of polarization resistance from 10 different locations. Corrosion rates are computed using the polarization resistance with the correction for R_s. Once the uncompensated solution resistance is obtained, different operators will compute the same corrosion rate using Equations (B-1) and (B-2); assuming they use the same parameters for surface area, environmental constant (B) and metal valance, density, and atomic weight. Therefore, differences in results from these devices are with respect to the manner in which PR′ and R_s are rendered.

Results of LPR measurements performed with the GAMRY equipment and operated by Caltrans, and measurements made by MMCE using the FHWA PR Monitor are compared in Figure B-3. Figure B-3(a) depicts measurements of PR′ that are not corrected for the uncompensated solution resistance (R_s), and Figure B-3(b) is the independent measurement of R_s. Measurements of PR′ correlate very well ($\rho_{xy} = 0.98$). One data point falls outside the trend line corresponding to a measurement with the GAMRY G600 that is approximately one half of that obtained with the PR Monitor. Some of the GAMRY data were processed and analyzed by both Caltrans and MMCE using a different protocol. Caltrans determined the polarization resistance from the slope of the overpotential versus impressed current for a selected linear region in the vicinity and symmetric with zero applied current (i.e., at the open circuit potential). MMCE determined the polarization resistance at the slope within a region ±10 mV from the open circuit potential. The latter is similar to the protocol employed by the FHWA PR Monitor. Figure B-3(a) shows that the GAMRY data as reconciled by MMCE are closer to the measurements from the FHWA PR Monitor. This is expected, but the comparison serves to demonstrate that there is a small component of measurement variability that is operator dependent, and related to data processing.

Figure B-3(b) demonstrates that measurements of R_s include more variation compared to measurements of PR′. The coefficient of correlation between measurements using the PR Monitor and the GAMRY G600 is 0.87 when considering the entire data set. However, five of the data points that lie above the trend line in Figure B-3(b) are from the same site located in San Bernardino, California. One of these data points also corresponds to the one outlying data point identified in Figure B-3(a). If the five data points from San Bernardino are removed, a coefficient of correlation equal to 0.94 is obtained. Measurements of R_s from the GAMRY G600 (with the San Bernardino data points removed) are on average 15% higher than those measured with the PR Monitor.

The reason for the difference in measurements may be related to the manner in which the measurements are made. Both units use an impressed AC current to make the measurements. The PR Monitor measures R_s with a square wave signal at a frequency of 270 Hz. The GAMRY G600 considers a broad spectrum of response using electrochemical impedance spectrometry (EIS) and renders the value of R_s by plotting the total impedance versus frequency (Bode plot). The latter measurements are theoretically more robust, but EIS measurements are more sensitive to noise and interference and may become unstable; and are also more difficult to interpret if different metals (e.g. zinc and iron) are present on the surface and/or if oxide film layers are present on the surface.

LPR Compared to Tensile Strength Loss

Caltrans tested specimens identified with pitting from inspection rods retrieved from sites in Northern California during the period from July 14, 2007 to August 24, 2007. Each data point presented in Table B-2 involves measurement of tensile strength at two locations: one including the pitted cross section (T_{pitted}) and another from a nearby intact location (T_{intact}) that serves as a reference measurement. The strength loss expressed as a percentage of the intact strength is computed as:

$$\%\ \text{Strength Loss} = \frac{T_{intact} - T_{pitted}}{T_{intact}} \times 100 \qquad \text{(B-3)}$$

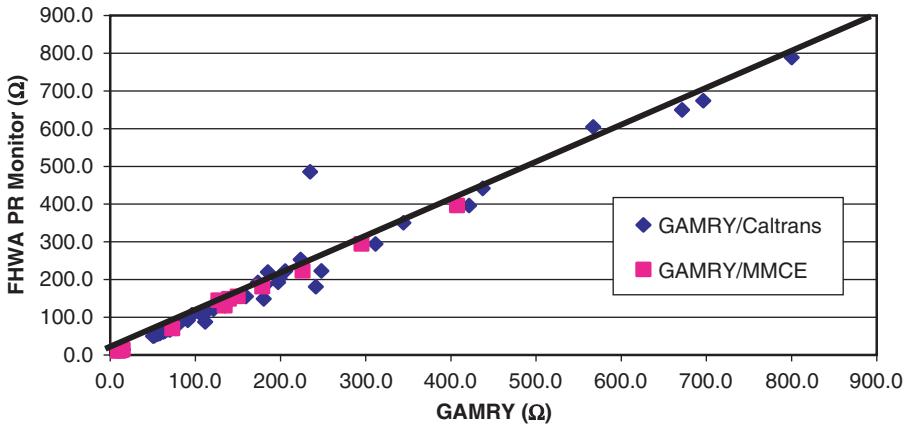

(a) measured ($PR' = PR + R_s$) polarization resistance

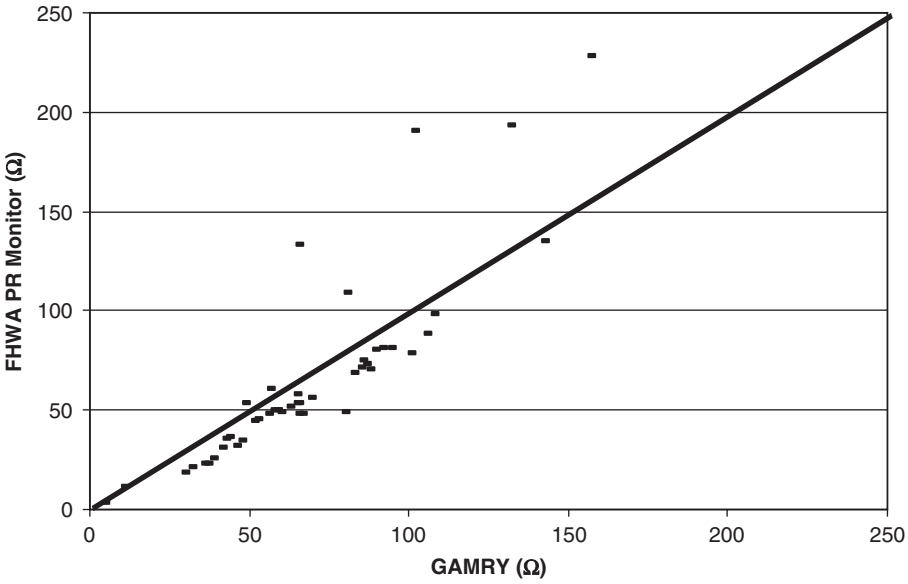

(b) backfill resistance (R_s)

Figure B-3. Polarization resistance measurements with the FHWA PR Monitor and the GAMRY G600.

Strength losses less than 4% are not considered to be significant and may reflect strength variation inherent to the material, rather than from loss of section. The average of the strength variation shown in Table B-2 is 5.2%, with a maximum of 15.8% and minimum 0.3%. The maximum of 15.8% was recorded for plain steel reinforcements (i.e., not galvanized) and all of the measurements were from specimens that had been exposed to the backfill for approximately 20 years and are for rod shaped specimens made from cold-drawn steel wire (ASTM A-82).

The observed loss of tensile strength is compared to the loss anticipated based on metal loss models proposed by Darbin et al. (1988) and the Caltrans-Interim design strength loss model (Jackura et al., 1987). The AASHTO metal loss model was not considered here because the backfills do not meet corresponding AASHTO criteria. The loss of strength of the Darbin and Caltrans-Interim metal loss models is computed as follows:

For the Darbin model:

$$X(\text{in.}) = (25\,\mu\text{m} \times t^{0.65} - 86\,\mu\text{m}) \times 2 \times \frac{1}{25,400}\left(\frac{\text{in.}}{\mu\text{m}}\right) \qquad \text{(B-4)}$$

where X is the loss of base steel in inches after the zinc (assumed to be 86 μm thick) is consumed, and t is time in years. This equation includes a factor of 2 to consider the effect of localized corrosion activity (i.e., pitting).

The diameter after t years of service is then computed as:

$$d_f = d_i - 2 \times (X) \qquad \text{(B-5)}$$

where d_f is the diameter after t years and d_i is the initial diameter of the specimen prior to being galvanized; both

Table B-2. Results from tensile strength testing of pitted specimens from sites in northern California.

Site Details				Sample Details			Observed Strength	Anticipated Strength	
Bridge #	Locale	Age (yr)	ρ (Ω-cm)	Sample[1] Location	Specimen Location (ft)[2]	d_i (in.)	% Loss	Darbin % Loss	Caltrans Interim % Loss
10-0284	Redwood Valley	18	2527	B/13	6-10	0.371	4.5	6.5	9.3
10-0284	Redwood Valley	18	2527	B/14	6-10	0.369	7.8	6.5	9.3
10-0284	Redwood Valley	18	2527	M/8	6-10	0.372	8.8	6.5	9.2
20-0269	Preston	20	2821	T/2	6-10	0.373	2.0	7.4	11.4
20-0269	Preston	20	2821	M/8	5-9	0.374	5.5	7.4	11.4
28-0303	Richmond/Castro	18	1434	T/2	6-10	0.498	13.3	4.8	6.9
28-0303	Richmond/Castro	18	1434	M/8	6-10	0.499	0.3	4.8	6.9
28-0303	Richmond/Castro	18	1434	B/15	6-10	0.499	2.5	4.8	6.9
28-0303	Richmond/Castro	18	1434	M/7	5-9	0.499	1.2	4.8	6.9
28-0294[3]	Richmond/Regatta	19	1600	B/17	6-9	0.421	15.8	29.1[3]	18.9
10-0279	Hopland	18	NA	T/3	6-10	0.375	4.3	6.4	9.2
10-0279	Hopland	18	NA	T/2	6-10	0.375	1.5	6.4	9.2
10-0277	Hopland	18	NA	T/1	6-10	0.374	1.1	6.4	9.2

[1] T, M, and B = top, middle, & bottom; ## inspection rod number location in cluster (elements of 1–18) based on field identification form.
[2] Distance into fill from wall face.
[3] Plain steel specimen (i.e., not galvanized) and
$X\,(\text{in.}) = (40\mu m \times t^{0.8} - 86\mu m) \times 2 \times \frac{1}{25{,}400}(\frac{\text{in.}}{\mu m})$.

diameters are in units of inches. The corresponding loss of strength is:

$$\%\ \text{Loss} = \left(1 - \frac{d_f^2}{d_i^2} \times 100\right) \tag{B-6}$$

Alternatively, according to the Caltrans-Interim design guidelines:

$$A = \frac{\left[d_i - 2 \times k \times (t - C)\right]^2}{d_i^2} \times 100 \tag{B-7}$$

where A is the percentage of the original diameter that remains after t years, C is the life of the zinc protecting the surface of the steel (assumed by Caltrans as 10 years for these backfill conditions), and k is the metal loss per year considering the effect of localized corrosion (assumed by Caltrans as 0.0011 in./yr for these backfill conditions). The corresponding loss of strength is:

$$\%\ \text{Loss} = 100 - A \tag{B-8}$$

The equations for estimating loss of strength appear to be an upper bound with respect to the observed strength loss. With one exception, the Caltrans-Interim design equation estimates greater loss of strength compared to the observed strength loss displayed in Table B-2. The strength losses estimated with the Darbin model are approximately 65% to 70% of those estimated with the Caltrans-Interim design equations, but, in general, these estimates still represent an upper bound to the observed strength losses.

The highest measured corrosion rate of 5.7 μm/yr compares well with the rate predicted via the Darbin model considering 20-year-old reinforcements. However, corrosion rates measured with the LPR technique do not always correlate well with respect to pitting (i.e., the specimen with the deepest pit is not the same specimen with the highest corrosion rate measured via the LPR technique).

LPR Compared to Weight Loss/Thickness Loss

Mild to moderate corrosion was observed from sites in northern California. Caltrans measured the pit depth at sixteen locations along selected inspection elements as summarized in Table B-3. Appendix C includes photographs depicting the locations where pitting was observed. All of these data are from rod-type elements and, generally, pitting does not result in a uniform loss of radius but rather affects a limited portion of the cross section. Pit depths were measured by subtracting the remaining thickness (remaining diameter) from the initial diameter determined from measurements of a nearby section that appeared to be intact. Table B-3 also includes the estimated uniform loss based on the Darbin model (Darbin, 1988) for galvanized elements and Elias (1990) for plain steel elements. The ratio of maximum section loss to estimated uniform loss ranges from 1.2 to 4.8 with an average loss ratio of 2.4.

The estimated uniform rate of metal loss is compared to the corrosion rate measured at an instant in time via the LPR technique. The corrosion rate computed via measurement of LPR may be in error by a factor of 2 considering the selection of parameters needed to relate the measurement of polarization resistance to corrosion rate.

Moderate to severe corrosion was observed from sites in southern California. Table B-4 is a summary (Caltrans

Table B-3. Summary of section loss observed from inspection rods exhumed by Caltrans.

Bridge #	Age Years	Backfill ρ Ω-cm	Elev.[2]	Distance from face (ft)	Pit Depth (μm)	Est. Uniform Loss (μm)	Loss Ratio	Est. Uniform Rate (μm/yr)	LPR Meas. Rate (μm/yr)
28-0297	19	NA[3]	T	6	647.7	169.5	3.8	5.8	4.9
28-0306	17	533	T	2.5	304.8	157.7	1.9	6.0	2.3
28-0306	17	533	B	1	419.1	157.7	2.7	6.0	1.3
10-0286	18	2522	M	1	254.0	163.6	1.6	5.9	1.4
10-0284	18	2522	B	8	342.9	163.6	2.1	5.9	1.4
10-0284	18	2522	B	4	139.7	163.6	-	5.9	2.9
10-0284	18	2522	B	7	584.2	163.6	3.6	5.9	2.9
20-0269	20	2821	M	8	317.5	175.2	1.8	5.7	2.3
28-0303	18	1434	B	4	203.2	163.6	1.2	5.9	2.9
28-0303	18	1434	T	9	520.7	163.6	3.2	5.9	1.9
28-0303	18	1434	M	5	406.4	163.6	2.5	5.9	2.3
28-0303	18	1434	M	6.5	355.6	163.6	2.2	5.9	2.8
28-0294[1]	19	1600	B	5.5	304.8	421.8	-	17.8	25.0
28-0294[1]	19	1600	B	7.7	1155.7	421.8	2.7	17.8	25.0
28-0294[1]	19	1600	M	2.5	508	421.8	1.2	17.8	28.0
10-0278	18	NA	T	4.5	787.4	163.6	4.8	5.9	1.7

[1]Bare steel, i.e. not galvanized
[2]B=bottom, M=middle, T=top
[3]NA = not available

Table B-4. Summary of laboratory data from Caltrans and comparison with field observations.

Inspection Element			Backfill		Condition			CR (μm/yr)	
Bridge No.	Locale	Location, Type	*w* %	ρ_{min} (Ω-cm)	E_{corr} (mV)	Zinc (oz/ft^2)	Pitting	Loss	LPR
53-2819	07-LA-47	R13, Rod	-	1610	-793	1.5	N	-	0.4
53-2821	07-LA-47	L14, Rod	8.4	1763	-474	-	Y	47	179
53-2821	07-LA-47	L16, Rod	8.1	1389	-484	-	Y	26	32
53-2822	07-LA-47	L13, Rod	8.5	3580	-740	1.4	N	-	0.9
53-2822	07-LA-47	L14, Rod	9.1	2072	-537	-	Y	26	104
53-2822	07-LA-47	L15, Rod	10.7	5849	-714	1.5	N	-	1.0
53-2823	07-LA-47	L17, Rod	8.8	1763	-511		Y	99	42
53-2823	07-LA-47	L15, Rod	9.1	2223	-475		Y	99	25
54-1093	08-SBD-30/215	L2, Strip	2.9	6223	-540	5.5	Y	9.5[1]	0.7
54-1093	08-SBD-30/215	L12, Strip	2.1	12705	-594	4.7	N	-	0.7
54-1094	08-SBD-30/215	L8, Strip	-	-	-581	4.8	Y	6.0[1]	1.2
54-1094	08-SBD-30/215	L14, Strip	-	-	-610	1.3	Y	7.5[1]	1.3
56-0794	08-Riv-10	L7, Strip	-	-	-356		Y	NA	80
56-0794	08-Riv-10	L 11, Strip	-	-	-567		Y	40	50
56-0794	08-Riv-10	L 13, Strip	0.4	377	-550	5.2	Y	28[1]	3.7
10-0279	01-Men-101	L15, Rod	3.2	-	-612	4.7	N	-	0.30
10-0279	01-Men-101	L17, Rod	1.8	8414	-	-	-	-	-
LV	09-Men-395	L9, Strip	0.5	11375	-	7.0	N	-	-

[1] pit involves a small surface area on strip
High moisture content, low ρ_{min}, and corresponding higher corrosion
NOTE: NA = data not available. Corroded strip broke during extraction.

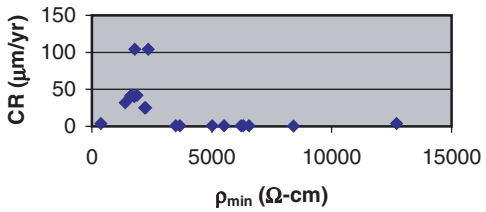

Figure B-4. Minimum resistivity (ρ_{min}) vs. corrosion rate (CR) for corresponding backfill and inspection rod locations.

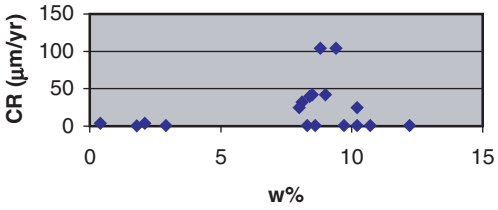

Figure B-5. Moisture content (w%) vs. corrosion rate (CR) for corresponding backfill and inspection rod locations.

southern sites) that provides a comparison of backfill and inspection rod conditions, and corrosion rates measured via direct observation and from LPR measurements.

Corrosion rates computed from observations of remaining diameter/pit depth shown in Table B-4 compare qualitatively with measurements from LPR. In cases where relatively high corrosion rates were measured via LPR (> 20 μm/yr), pitting and corresponding loss of section were also observed along the inspection rods. The corrosion rates at the point of maximum section loss may be four times higher than the average rates measured via LPR, which is consistent with expectations considering the geometry of the rod shaped inspections elements (Smith et al., 1996). In a couple of instances, corrosion rates measured via LPR are higher than direct observations, however, these LPR measurements are anomalous, and when repeated with different equipment (GAMRY vs FHWA PR Monitor) such high values of corrosion rate are not consistently observed. Pitting observed for strip-type reinforcements covered small areas that did not have a significant impact on tensile strength, and relatively low corrosion rates are indicated via LPR.

Correlations of corrosion rate and loss of zinc are particularly interesting because the backfill samples were retrieved from the same locations as the inspection elements. This is not usually the case, and most often backfill data is derived from samples taken at stockpiles or from random locations within the backfill. Higher corrosion rates and lower and remaining zinc (<2 oz/ft^2) measurements are consistently correlated with backfill samples that simultaneously exhibit relatively low minimum resistivity (ρ_{min}) and high moisture content. This trend is illustrated in Figures B-4 and B-5. Higher corrosion rates are not always observed in Figure B-4 when ρ_{min} is low, or in Figure B-5 when moisture contents are higher. However, a comparison of points with CR > 20 μm/yr reveals that both of these conditions are met in these instances. This comparison demonstrates the value of obtaining backfill samples and corrosion rate measurements at the same location and at similar times. The data shown in Figures B-4 and B-5 help to explain why higher corrosion rates are not always observed from sites with poor quality backfill (e.g., low ρ_{min}) and can be useful to reconcile some of the variation apparent from our performance database.

Inspection elements that exhibited high corrosion rates appeared to break at a reduced cross section during extraction. Therefore, a lot of the data on remaining tensile strength do not correspond to the locations with the most severe section loss. Tensile strength data are useful to document the remaining strength of less corroded sections (that did not break upon extraction), and to study inherent variation of material strength.

Data obtained from extraction of inspection elements during field work for Task 6, performed in cooperation with Caltrans, demonstrate that the ratio of maximum metal loss (i.e., loss of tensile strength) to average corrosion rate or metal loss ranges from 1.2 to 4.8 with a mean of 2.4. This factor appears to be inversely proportional to severity of corrosion and tends to range between 2 and 3 when more severe loss of cross section is observed.

LPR measurements are particularly effective to discern the occurrence of relatively mild, moderate, or severe corrosion. For galvanized elements, corrosion rates via LPR correlate best with the percentage of zinc remaining on the surface. When more than 70% of the surface is covered by zinc, corrosion rates measured via LPR reflect the rate of zinc loss. However, there may be instances where localized corrosion of steel may not be reflected in the LPR measurement of corrosion rate. This is more of an issue at sites with relatively poor or marginal quality fill materials where metal loss is less uniform and localized loss of zinc is observed. In general, corrosion rates from LPR measurements are consistent with observations of maximum metal loss considering a factor between 2 and 3 relating the average to the maximum metal loss.

APPENDICES C THROUGH E

Appendices C through E to the contractor's final report for NCHRP Project 24-28 are not published herein but are available on the project web site at http://apps.trb.org/cmsfeed/TRBNetProjectDisplay.asp?ProjectID=727. Note that while the Appendix numbers have been changed to letters in the main report to reflect CRP house style, Appendices C–E, as posted to the site above, retain the contractor's original labeling as Appendices III–V.

- Appendix C (III): Performance Database
- Appendix D (IV): Data Analysis
- Appendix E (V): Details of Monte Carlo Simulations and Reliability Analyses

APPENDIX F

Example

Introduction

This example problem demonstrates analysis and design of a MSE wall using LRFD and the corresponding metal loss models and resistance factors based on recommendations described in this report. The example is adapted from Berg et al. (2009), Appendix E.3. Various designs are executed employing ribbed-steel-strip- or steel-grid-type reinforcements, that may be plain steel or galvanized, and construction that may incorporate high quality, good quality, or marginal quality fills. Both the simplified and the coherent gravity methods will be used to compute reinforcement tension. Results from this example illustrate the effects that these parameters have on the amount of reinforcement needed to meet the demand (i.e., the applicable load case). For the purpose of this illustration it is assumed that fill quality refers to electrochemical properties, and the mechanical properties of the fill (e.g., unit weight, shear strength) are the same for all of the fill qualities considered.

The MSE wall has a sloping backfill surcharge and includes a segmental precast concrete panel face as shown in Figure F-1. The analysis is based on principles of MSE design described by Berg et al. (2009). Table F-1 presents a summary of steps involved in the analysis. This appendix describes details related to evaluation of the internal stability of the wall as this bears on the calculation of tension (yield) resistance and the corresponding reinforcement cross-section. Berg et al. (2009), Appendix E-3, also describes details of the external stability analysis, design of facing elements, overall and compound stability analysis at the service limit state, and design of the wall drainage system.

Step 1. Establish Project Requirements

- Exposed wall height, $H_e = 28$ ft.
- Length of wall = 850 ft.
- Design life = 75 years or 50 years as appropriate in consideration of fill quality and whether or not reinforcements are galvanized.
- No seismic considerations.
- Precast panel units: 5-ft wide × 5-ft tall × 0.5-ft thick.
- Type of reinforcement: Grade 65 (F_y = 65 ksi) with zinc coating of 86 μm for galvanized reinforcements. Nine cases are considered in this example with reinforcement types and sizes summarized as follows:

Case	Fill Quality	Galvanized	Type of Reinforcement
1	High	Yes	50-mm wide × 4-mm thick ribbed strips
2	High	Yes	W11 × W11 (longitudinal × transverse, welded wire fabric)
3	Good	Yes	50-mm wide × 4-mm thick ribbed strips
4	Good	Yes	W11 × W11 (longitudinal × transverse, welded wire fabric)
5	Marginal	Yes	W20 × W11 (longitudinal × transverse, welded wire fabric)
6	High	No	50-mm wide × 6-mm thick ribbed strips
7	High	No	W20 × W11 (longitudinal × transverse, welded wire fabric)
8	Good	No	50-mm wide × 8-mm thick ribbed strips
9	Good	No	W20 × W11 (longitudinal × transverse, welded wire fabric)

Step 2. Evaluate Project Parameters

- Reinforced backfill, $\phi'_r = 34°$, $\gamma_r = 125$ pcf, coefficient of uniformity, $C_u = 7.0$.
- Retained backfill, $\phi'_f = 30°$, $\gamma_f = 125$ pcf.

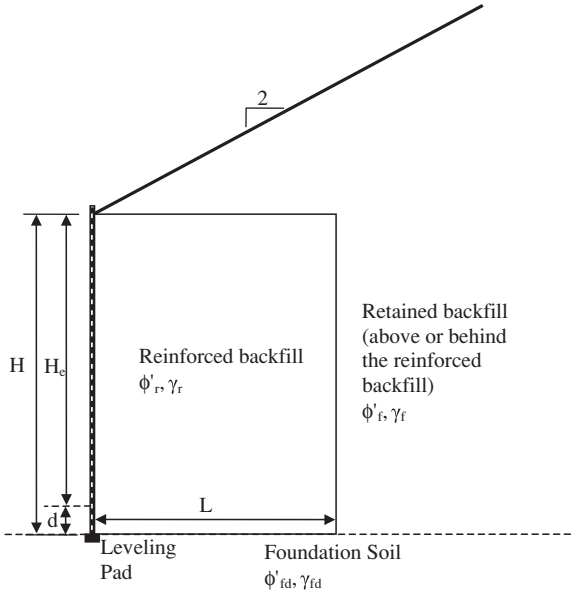

Figure F-1. Configuration showing various parameters for analysis of an MSE wall with sloping backfill (not-to-scale).

Step 3. Estimate Depth of Embedment and Length of Reinforcement

Based on Table C.11.10.2.2.-1 of AASHTO (2009), the minimum embedment depth = H/20 for walls with horizontal ground in front of wall, in other words, 1.4 ft for exposed wall height of 28 ft. For this design, assume embedment, d = 2.0 ft. Thus, design height of the wall, H = H_e + d = 28 ft + 2.0 ft = 30 ft.

Due to the 2H:1V backslope, the initial length of reinforcement is assumed to be 0.8 H or 24 ft. The length of the reinforcement is assumed to be constant throughout the height to limit differential settlements across the reinforced zone because differential settlements could overstress the reinforcements.

Step 4. Estimate Unfactored Loads

To compute the numerical values of various forces and moments, the parameters provided in Step 2 are used. Earth pressures transferred from the retained fill are not considered for internal stability analysis with the simplified method, but are related to reinforcement tension with the Coherent Gravity method. Using the values of the various friction angles, the coefficients of lateral earth pressure for the retained fill are computed as follows:

Coefficient of active earth pressure per Eq. 3.11.5.3-1 of AASHTO (2009) is

$$K_a = \frac{\sin^2(\theta + \phi'_f)}{\Gamma \sin^2\theta \sin(\theta - \delta)}$$

Where, per Eq. 3.11.5.3-2 of AASHTO (2009), the various parameters in above equation are as follows:

$$\Gamma = \left[1 + \sqrt{\frac{\sin(\phi'_f + \delta)\sin(\phi'_f - \beta)}{\sin(\theta - \delta)\sin(\theta + \beta)}}\right]^2$$

δ = friction angle between fill and wall taken as specified,
β = angle (nominal) of fill to horizontal,
θ = angle of back face of wall to horizontal, and
ϕ'_f = effective angle of internal friction of retained backfill.

Table F-1. Summary of steps in analysis of MSE wall with sloping backfill.

Step	Item
1	Establish project requirements
2	Establish project parameters
3	Estimate wall embedment depth and length of reinforcement
4	Estimate unfactored loads
5	Summarize applicable load and resistance factors
6	Evaluate external stability of MSE wall—not discussed, see Berg et al. (2009) 6.1 Evaluation of sliding resistance 6.2 Evaluation of limiting eccentricity 6.3 Evaluation of bearing resistance 6.4 Settlement analysis
7	Evaluate internal stability of MSE wall 7.1 Estimate critical failure surface, variation of K_r and F^* for internal stability 7.2 Establish vertical layout of soil reinforcements 7.3 Calculate horizontal stress and maximum tension at each reinforcement level 7.4 Establish nominal and factored long-term tensile resistance of soil reinforcement 7.5 Establish nominal and factored pullout resistance of soil reinforcement 7.6 Establish number of soil reinforcing strips at each level of reinforcement
8	Design of facing elements—not discussed, see Berg et al. (2009)
9	Check overall and compound stability at the service limit state—not discussed, see Berg et al. (2009)
10	Design wall drainage system—not discussed, see Berg et al. (2009)

Table F-5.1. Summary of applicable load factors.

Load Combination	Load Factors (after AASHTO, 2009, Tables 3.4.1-1 and 3.4.1-2)	
	EV	EH
Strength I (maximum)	1.35	1.5
Strength I (minimum)	1.00	0.9
Service I	1.00	1.0

Note: EV and EH = vertical earth load and horizontal earth load, respectively.

For this example problem, compute the coefficient of active earth pressure for the retained fill, K_{af}, using $\beta = 26.56°$ (for the 2:1 backslope), vertical backface, $\theta = 90°$, and $\delta = \beta$ as follows:

$$\Gamma = \left[1 + \sqrt{\frac{\sin(30° + 26.56°)\sin(30° - 26.56°)}{\sin(90° - 26.56°)\sin(90° + 26.56°)}}\right]^2$$

$$= \left[1 + \sqrt{\frac{(0.834)(0.060)}{(0.894)(0.894)}}\right]^2 = 1.563$$

$$K_{af} = \frac{\sin^2(\theta + \phi'_f)}{\Gamma \sin^2\theta \sin(\theta - \delta)} = \frac{\sin^2(90° + 30°)}{1.563(\sin 90°)^2\left[\sin(90° - 26.56°)\right]}$$

$$= \frac{0.750}{(1.563)(1.0)(0.894)} = 0.537$$

Step 5. Summarize Applicable Load and Resistance Factors

Table F-5.1 summarizes the load factors applied to calculations of reinforcement load using the Simplified Method. For the internal stability analysis using the Simplified Method only the maximum values of the load factors for the Strength I load case apply. However the coherent gravity method requires consideration as to whether maximum or minimum values render the most critical loading conditions. In most cases, the proper choice can be readily identified by inspection at the onset.

Appropriate resistance factors have to be used for computation of factored resistances during evaluation of strength limits states. Based on Table 11.5.5-1 from AASHTO (2009) a resistance factor, $\phi_p = 0.9$ is applied to the nominal pullout resistance. Table F-5.2 summarizes the applicable resistance factors for tensile resistance, ϕ_t, for galvanized, or plain steel, strip and grid reinforcements with different fill conditions as recommended in this report. These resistance factors apply to design lives (t_{design}) up to 100 years unless otherwise noted.

Step 6. Evaluate External Stability of MSE Wall

Not included because metal loss is not relevant to these calculations. See Berg et al. (2009), Appendix E.3.

Step 7. Evaluate Internal Stability Analysis of MSE Wall

7.1 Estimate critical failure surface, variation of K_r, and F for internal stability*

For the simplified method the variation of K_r depends on the stiffness of the reinforcements and is different for strip- or grid-type reinforcements. For the case of inextensible steel ribbed strips, the profile of the critical failure surface, the variation of internal lateral horizontal stress coefficient, K_r, and the variation of the pullout resistance factor, F*, are as shown in Figure F-2 wherein other definitions, such as measurement of depths Z and Z_p as well as heights H and H_1 are also shown. The variation of K_r and F* are with respect to depth Z that is measured from the top of the reinforced soil zone. For the computation of K_r, the value of K_a is based on the angle of internal friction of the reinforced backfill, ϕ_r, and the assumption that the backslope angle $\beta = 0$; thus, $K_a = \tan^2(45° - 34°/2)$

Table F-5.2. Summary of applicable resistance factors for evaluation of tensile resistances.

Reinforcement	Fill Quality		
	High	Good	Marginal
Galvanized Strips	0.80	0.65	NA
Galvanized Grids	0.70	0.55	0.30[1]
Plain Steel Strips	0.45[2]	0.45[1]	NA
Plain Steel Grids	0.35[2]	0.35[1]	NA

[1] t_{design} = 50 yrs
[2] t_{design} = 75 yrs

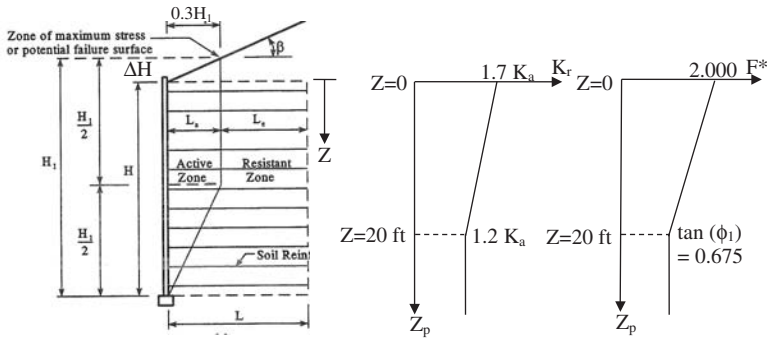

$$\Delta H = \frac{(\tan\beta)(0.3H)}{1-0.3\tan\beta} \qquad H_1 = H + \Delta H$$

Z_p at start of resistant zone, $Z_{p\text{-}s} = Z + L_a\tan\beta$

Z_p at end of resistant zone, $Z_{p\text{-}e} = Z + L\tan\beta$

Use average Z_p over the resistance zone, $Z_{p\text{-}ave}$, for computing pullout resistance

$Z_{p\text{-}ave} = Z + 0.5(L_a\tan\beta + L\tan\beta) = Z + 0.5\tan\beta\,(L_a + L)$

K_a is computed assuming that the backslope angle is zero, i.e., $\beta = 0$ per Article C11.10.6.2.1 of AASHTO (2009)

Figure F-2. Geometry definition, location of critical failure surface, and variation of K_r and F* parameters for steel ribbed strips.

= 0.283. Hence, the value of K_r varies from 1.7(0.283) = 0.481 at Z = 0 ft to 1.2(0.283) = 0.340 at Z = 20 ft. For steel strips, F* = 1.2+$\log_{10}C_u$. Using C_u = 7.0 as given in Step 2, F* = 1.2 + $\log_{10}$(7.0) = 2.045 > 2.000. Therefore, use F* = 2.000.

For the case of inextensible grids (i.e. welded wire fabric) the value of K_r varies from 2.5K_a at Z = 0 (2.5(0.283) = 0.707) to 1.2*K_a at Z = 20 ft. (1.2(0.283)=0.34). For grid-type reinforcements, the value of F* varies from 20(t/S_t) at Z = 0 ft to 10(t/S_t) at Z ≥ 20 ft, where t is the diameter of the transverse wires and S_t is the transverse wire spacing.

The coherent gravity method uses $K_r = K_0$ for the top 20 feet (Z ≤ 20 ft), where K_0 is the coefficient of lateral earth pressure at-rest, approximated as 1− sin ϕ_r = 1 − sin 34° = 0.441 in this example. At depths Z > 20 ft $K_r = K_a$ = 0.283 (in this example).

7.2 Establish vertical layout of soil reinforcements

Using the definition of depth *Z* as shown in Figure F-2 the following vertical layout of the soil reinforcements is chosen:

Z = 1.25 ft, 3.75 ft, 6.25 ft, 8.75 ft, 11.25 ft, 13.75 ft, 16.25 ft,

18.75 ft, 21.25 ft, 23.75 ft, 26.25 ft, and 28.75 ft.

The above layout leads to 12 levels of reinforcements. The vertical spacing was chosen based on a typical vertical spacing, S_v, of approximately 2.5 ft that is commonly used in the industry for steel ribbed strip- or grid-type reinforcement. The vertical spacing near the top and bottom of the walls is locally adjusted as necessary to fit the height of the wall.

For internal stability computations, each layer of reinforcement is assigned a tributary area, A_{trib} as follows:

$$A_{trib} = (w_p)(S_{vt})$$

where w_p is the panel width of the precast facing element, and S_{vt} is the vertical tributary spacing of the reinforcements based on the location of the reinforcements above and below the level of the reinforcement under consideration. The computation of S_{vt} is summarized in Table F-7.1 wherein $S_{vt} = Z^+ - Z^-$. Note that w_p = 5.00 ft per Step 1.

7.3 Calculate horizontal stress and maximum tension at each reinforcement level

The horizontal spacing of the reinforcements is based on the maximum tension (T_{max}) at each level of reinforcements, which requires computation of the horizontal stress, σ_H, at each reinforcement level. The reinforcement tensile and pullout resistances are then compared with T_{max} and an appropriate reinforcement pattern is adopted. This section demonstrates the calculation of horizontal stress, σ_H, and maximum tension, T_{max}.

For the Simplified Method the horizontal stress, σ_H, at any depth within the MSE wall is based on only the soil load as summarized in Table F-7.2.

$$\sigma_H = \sigma_{H\text{-soil}} + \sigma_{H\text{-surcharge}}$$

Table F-7.1. Summary of computations for S_{vt}.

Level	Z (ft)	Z^- (ft)	Z^+ (ft)	S_{vt} (ft)
1	1.25	0	1.25+0.5(3.75–1.25)=2.50	2.50
2	3.75	3.75-0.5(3.75–1.25)=2.50	3.75+0.5(6.25-3.75)=5.00	2.50
3	6.25	6.25-0.5(6.25-3.75)=5.00	6.25+0.5(8.75-6.25)=7.50	2.50
4	8.75	8.75-0.5(8.75-6.25)=7.50	8.75+0.5(11.25-8.75)=10.00	2.50
5	11.25	11.25-0.5(11.25-8.75)=10.00	11.25+0.5(13.75-11.25)=12.50	2.50
6	13.75	13.75-0.5(13.75-11.25)=12.50	13.75+0.5(16.25-13.75)=15.00	2.50
7	16.25	16.25-0.5(16.25-13.75)=15.00	16.25+0.5(18.75-16.25)=17.50	2.50
8	18.75	18.76-0.5(18.75-16.25)=17.50	18.75+0.5(21.25-18.75)=20.00	2.50
9	21.25	21.25-0.5(21.25-18.75)=20.00	21.25+0.5(23.75-21.25)=22.50	2.50
10	23.75	23.75-0.5(23.75-21.25)=22.50	23.75+0.5(26.25-23.75)=25.00	2.50
11	26.25	26.25-0.5(26.25-23.75)=25.00	26.25+0.5(28.75-26.25)=27.50	2.50
12	28.75	28.75-0.5(28.75-26.25)=27.50	30.00	2.50

Using the unit weight of the reinforced soil mass and heights Z and S as shown in Figure F-3(b), the equation for horizontal stress at any depth Z within the MSE wall can be written as follows:

$$\sigma_H = K_r(\gamma_r Z)\gamma_{P\text{-}EV} + K_r(\gamma_r S)\gamma_{P\text{-}EV} = K_r[\gamma_r(Z+S)\gamma_{P\text{-}EV}]$$

Once the horizontal stress is computed at any given level of reinforcement, the maximum tension, T_{max}, is computed as follows:

$$T_{max} = (\sigma_H)(A_{trib})$$

where A_{trib} is the tributary area for the soil reinforcement at a given level.

For the coherent gravity method the factored horizontal stress at each reinforcement level is computed as

$$\sigma_H = K_r\sigma_v$$

where σ_v is the pressure due to resultant vertical forces at the reinforcement level being evaluated, determined using a uniform pressure distribution over an effective width (L-2e) as specified in AASHTO (2009), Article 10.6.1.3, where e is the load eccentricity. The vertical effective stress at each level of reinforcement shall consider the local equilibrium of all forces at that level only. Forces used to compute σ_v (EV and EH) are factored as described in Table F-5.1.

The computations for T_{max} using the simplified method for Case 1 are illustrated at z = 8.75 ft, which is Level 4 in the assumed vertical layout of reinforcement. Assume Strength I (max) load combination for illustration purposes and use appropriate load factors from Table F-5.1.

- At Z = 8.75 ft, the following depths are computed:
  Z^- = 7.50 ft (from Table F-7.1)
  Z^+ = 10.00 ft (from Table F-7.1)
- Obtain K_r by linear interpolation between $1.7K_a = 0.481$ at $Z = 0.00$ ft and $1.2K_a = 0.340$ at $Z = 20.00$ ft as follows:

  At Z^- = 7.50 ft, $K_{r(Z-)} = 0.340 + (20.00\text{ ft} - 7.50\text{ ft})(0.481-0.340)/20.00\text{ ft} = 0.428$
  At Z^+ = 10.00 ft, $K_{r(Z+)} = 0.340 + (20.00\text{ ft} - 10.00\text{ ft})(0.481-0.340)/20.00\text{ ft} = 0.411$

- Compute $\sigma_{H\text{-}soil} = [K_r\,\sigma_{v\text{-}soil}]\gamma_{P\text{-}EV}$ as follows:
  $\gamma_{P\text{-}EV}$ = 1.35 from Table F-5.1

  At Z^- = 7.50 ft,
  $\sigma_{v\text{-}soil(Z-)} = (0.125\text{ kcf})(7.50\text{ ft}) = 0.94$ ksf
  $\sigma_{H\text{-}soil(Z-)} = [K_{r(Zp-)}\sigma_{v\text{-}soil(z-)}]\gamma_{P\text{-}EV} = (0.428)(0.94\text{ ksf})(1.35) = 0.54$ ksf

  At Z^+ = 10.00 ft,
  $\sigma_{v\text{-}soil(Z+)} = (0.125\text{ kcf})(10.00\text{ ft}) = 1.25$ ksf
  $\sigma_{H\text{-}soil(Z+)} = [K_{r(Zp+)}\sigma_{v\text{-}soil(z+)}]\gamma_{P\text{-}EV} = (0.411)(1.25\text{ ksf})(1.35) = 0.69$ ksf
  $\sigma_{H\text{-}soil} = 0.5(0.54\text{ ksf} + 0.69\text{ ksf}) = 0.62$ ksf

- Compute $\sigma_{H\text{-}surcharge} = [K_r\,\sigma_2]\gamma_{P\text{-}EV}$ as follows:
  $\sigma_2 = (1/2)(0.7H\tan\beta)(\gamma_f)$ (from Figure F-3(b))
  $\sigma_2 = (1/2)(0.7*30\text{ ft})[\tan(26.56°)](0.125\text{ kcf}) = 0.656$ ksf
  $\gamma_{P\text{-}EV}$ = 1.35 from Table F-5.1

  At Z^- = 7.50 ft,
  $\sigma_{H\text{-}surcharge} = [K_{r(Z-)}\,\sigma_2]\gamma_{P\text{-}EV} = (0.428)(0.656\text{ ksf})(1.35) = 0.38$ ksf

Table F-7.2. Summary of load components leading to horizontal stress.

Load Component	Load Type	Horizontal Stress
Soil load from reinforced mass, $\sigma_{v\text{-}soil}$	EV	$\sigma_{H\text{-}soil} = [K_r\sigma_{v\text{-}soil}]\gamma_{P\text{-}EV}$
Surcharge load due to backslope, σ_2	EV	$\sigma_{H\text{-}surcharge} = [K_r\sigma_2]\gamma_{P\text{-}EV}$

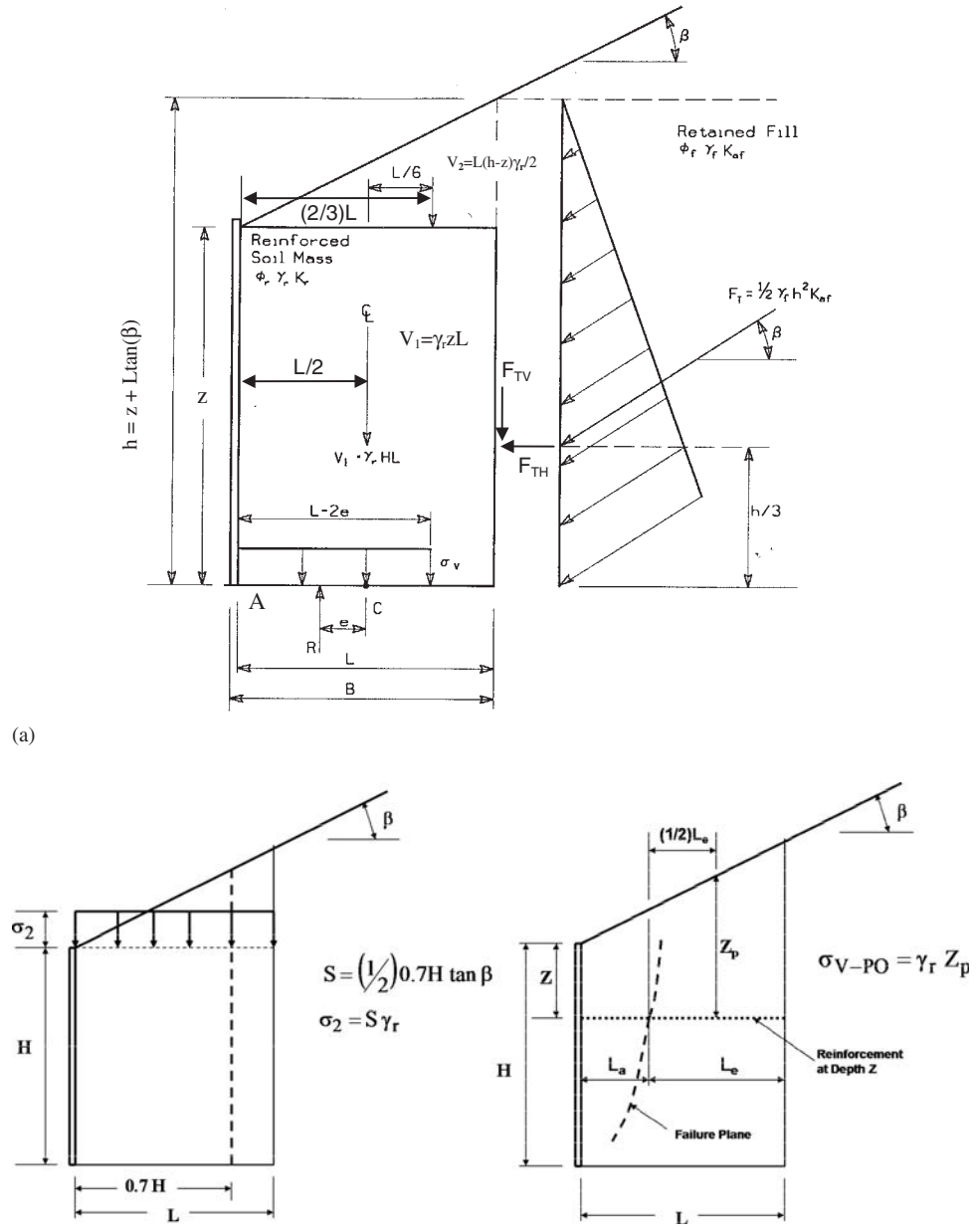

Figure F-3. Legend for computation of forces and moments for (a) internal stability analysis with the coherent gravity method, and (b) internal stability analysis with the simplified method (not-to-scale).

At $Z^+ = 10.00$ ft,

$\sigma_{H\text{-surcharge}} = [K_{r(Z+)}\ \sigma_2]\gamma_{P\text{-}ES} = (0.411)(0.656\ \text{ksf})(1.35)$
$= 0.36$ ksf

$\sigma_{H\text{-surcharge}} = 0.5(0.38\ \text{ksf} + 0.36\ \text{ksf}) = 0.37$ ksf

- Compute $\sigma_H = \sigma_{H\text{-soil}} + \sigma_{H\text{-surcharge}}$ as follows:
  $\sigma_H = 0.62\ \text{ksf} + 0.37\ \text{ksf} = 0.99$ ksf
- Based on Table F-7.1, the vertical tributary spacing at Level 4 is $S_{vt} = 2.50$ ft
- The panel width, w_p, is 5.00 ft (given in Step 1)
- The tributary area, A_{trib}, is computed as follows:
  $A_{trib} = (2.50\ \text{ft})(5.00\ \text{ft}) = 12.50\ \text{ft}^2$
- The maximum tension at Level 4 is computed as follows:
  $T_{max} = (\sigma_H)(A_{trib}) = (0.99\ \text{ksf})(12.50\ \text{ft}^2) = 12.37$ k for panel of 5-ft width

Using similar computations, the various quantities can be developed at other levels of reinforcements and load combinations.

The computations for T_{max} using the coherent method for Case 1 are similar, however σ_v is computed based on the equilibrium of forces and moments using a force diagram similar to Figure F-3(a) for each level of reinforcement. Equations for

unfactored vertical forces and moments for coherent gravity method are as follows:

Force (Force/length units)	LRFD Load Type	Moment arm (Length units) @ Point A
$V_1 = (\gamma_r)(z)(L)$	EV	L/2
$V_2 = \left(\frac{1}{2}\right)(L)(L\tan\beta)(\gamma_f)$	EV	(2/3)L
$F_{TV} = (1/2)(\gamma_r)(h^2)(K_{af})(\sin\beta)$	EH	L
$F_{TH} = (1/2)(\gamma_r)(h^2)(K_{af})(\cos\beta)$	EH	h/3

Note: $h = z + L\tan\beta$

- Compute unfactored vertical forces and moments at Z = 30 ft (about Point A in Figure F-3(a))

$V_1 = 90.00$ k/ft	$MV_1 = 90 \times 12 = 1080.00$ k-ft/ft
$V_2 = 18.00$ k/ft	$MV_2 = 18 \times 16 = 288.00$ k-ft/ft
$F_{TV} = 26.48$ k/ft	$MF_{TV} = 26.48 \times 24 = 635.44$ k-ft/ft
$F_{TH} = 52.95$ k/ft	$MF_{TH} = 52.95 \times 14 = 741.35$ k-ft/ft

- Compute factored moments and forces at Z = 30 ft. (Checks with Strength I maximum and minimum load factors are necessary. Strength I Max was determined to govern for this case and only these calculations are shown here.)

Vertical load @Z = 30 ft, $V_{Ab1} = V_1+V_2$	145.80	k/ft
Vertical load @Z = 30 ft, $V_{Ab2} = F_{TV}$	39.72	k/ft
Total vertical @Z = 30 ft, $\Sigma V = R = V_{Ab1}+V_{Ab2}$	185.52	k/ft
Resisting moments about Point A, $M_{RA1} = MV_1+MV_2$	1846.80	k-ft/ft
Resisting moments about Point A, $M_{RA2} = MF_{TV}$	953.17	k-ft/ft
Total resisting moment @ Point A, $M_{RA} = M_{RA1}+M_{RA2}$	2799.97	k-ft/ft
Overturning moments @ Point A, $M_{OA} = MF_{TH}$	1112.03	k-ft/ft
Net moment at Point A, $M_A = M_{RA} - M_{OA}$	1687.94	k-ft/ft
Location of the resultant from Point A = $(M_{RA} - M_{OA})/V_A$	9.10	ft
Eccentricity of Vertical load @ Z = 30 ft = 0.5*L − a	2.90	ft
Effective width @ Z = 30 ft = $L-2e_L$	18.20	ft
σ_v @t Z = 30 ft = $\Sigma V/(L-2e_L) = \sigma_v$	10.19	ksf

Horizontal stress, σ_H, and tensile force, T_{max}, are computed using K_r appropriate to the coherent gravity method, and tributary area as demonstrated for the simplified method.

7.4 Establish nominal and factored long-term tensile resistance of soil reinforcement

The nominal tensile resistance of soil reinforcements is based on the design life and estimated loss of steel over the design life during corrosion. Table F-7.3 is a summary of the metal loss models recommended in this report and the estimated metal loss per side (i.e., sacrificial steel requirements) for each case considered in this example. For galvanized reinforcements it is assumed that steel corrosion is initiated subsequent to depletion of zinc. For fill materials that meet AASHTO requirements and an initial zinc thickness, $z_i = 86$ μm, zinc life is computed as 16 years using the AASHTO metal loss model described in Table 3 of this report and per Article 11.10.6.4.2a of AASHTO (2009).

Considering Case 1 (described in Step 1) and a design life of 75 years, the anticipated thickness loss is calculated as follows:

$$E_R = 708\ \mu m \times (2\ \text{sides}) = 1416\ \mu m\ (0.056\ \text{in.}),\ \text{and}$$
$$E_C = 4\ \text{mm} - 1.416\ \text{mm} = 2.58\ \text{mm}\ (0.102\ \text{in.})$$

Based on a 50 mm wide strip, the cross-sectional area at the end of 75 years will be equal to (50 mm) × (2.58 mm) = 129 mm^2 (0.2 $in.^2$)

For Grade 65 steel with $F_y = 65$ ksi, the nominal tensile resistance at the end of a 75 year design life will be $T_n = 65$ ksi (0.200 $in.^2$) = 13.00 k/strip. Using the resistance factor, $\phi_t = 0.75$ as listed in Table F-5.2 for galvanized strip-type reinforcements in high quality fill, the factored tensile resistance, $T_r = 13.00$ k/strip (0.75) = 9.75 k/strip.

Table F-7.3. Basis for computing sacrificial steel requirements.

Reinforcement	Fill Quality	Recommended Metal Loss Model	t_{design} (years)	X (t_{design}) (μm)
Galvanized, $z_i = 86$ μm	High	X (μm) = (t_{design} − 16 years) x 12 μm/yr	75	708
Galvanized, $z_i = 86$ μm	Good	X (μm) = (t_{design} − 16 years) x 12 μm/yr	75	708
Galvanized, $z_i = 86$ μm	Marginal	X (μm) = (t_{design} − 10 years) x 28 μm/yr	50	1120
Plain Steel	High	X (μm) = t_{design} x 13 μm/yr	75	975
Plain Steel	Good	X (μm) = 80 x $t_{design}^{0.8}$	50	1829

Considering Case 2, the cross-sectional area at the end of 75 years for a Wll cold drawn wire will be equal to $\pi(0.374$ in (initial diameter of W11) $- 0.056$ in (loss of diameter))$^2/4 = 0.079$ in^2. $T_n = 65$ ksi $(0.079$ in$^2) = 5.14$ k/wire. Using $\phi_t = 0.70$ as listed in Table F-5.2 for galvanized grids in high quality fill, the factored tensile resistance, $T_f = 5.14$ k/wire $(0.70) = 3.61$ k/wire.

7.5 Establish nominal and factored pullout resistance of soil reinforcement

The nominal pullout resistance, P_r, of galvanized steel, ribbed, and strip-type soil reinforcements is computed with the following equation:

$$P_r = \alpha(F^*)(2b)(L_e)[(\sigma_v)(\gamma_{P\text{-}EV})]$$

For Case 1, the following parameters are constant at all levels of reinforcements:

$b = 1.969$ in. $= 0.164$ ft
$\alpha = 1.0$ for inextensible reinforcement per Table 11.10.6.3.2-1 of AASHTO (2009)

The computations for P_r are illustrated for Case 1 at $z = 8.75$ ft which is Level 4 as measured from the top of the wall. Assume Strength I (max) load combination for illustration purposes and use appropriate load factors from Table F-5.1.

- Compute effective (resisting) length, L_e, as follows:

  Since $Z < H_1/2$, active length $L_a = 0.3(H_1)$ and $L_e = L - L_a = L - 0.3(H_1)$
  $H_1 = H + \Delta H$

  $$\Delta H = \frac{(\tan\beta)(0.3\,H)}{1 - 0.3\tan\beta} = \frac{(0.5)(0.3 \times 30\text{ ft})}{1 - 0.3(0.5)} = 5.29\text{ ft}$$

  $H_1 = H + \Delta H = 30.00$ ft $+ 5.29$ ft $= 35.29$ ft
  Active length, $L_a = 0.3(35.29$ ft$) = 10.59$ ft
  Effective (resisting) length, $L_e = 24.00$ ft $- 10.59$ ft $= 13.41$ ft

- Compute $(\sigma_v)(\gamma_{P\text{-}EV})$

  As per Figure F-3(b), $\sigma_v = \gamma_r(Z_{p\text{-}ave})$
  $Z_{p\text{-}ave} = Z + 0.5\tan\beta\,(L_a + L) = 8.75$ ft $+ 0.5[\tan(26.56°)]$ $(10.59$ ft $+ 24.00$ ft$) = 17.40$ ft
  Per Article 11.10.6.3.2 of AASHTO (2009), use unfactored vertical stress for pullout resistance. Thus,
  $\gamma_{P\text{-}EV} = 1.00$
  $\sigma_v(\gamma_{P\text{-}EV}) = (0.125$ kcf$)(17.40$ ft$)\,(1.00) = 2.175$ ksf

- Obtain F* at $Z = 8.75$ ft
  Obtain F* by linear interpolation between 2.000 at $Z = 0$ and 0.675 at $Z = 20.00$ ft as follows:

  $F^* = 0.675 + (20.00\text{ ft} - 8.75\text{ ft})(2.000 - 0.675)/20\text{ ft} = 1.420$

- Compute nominal pullout resistance as follows:

  $P_r = \alpha(F^*)(2)(b)(L_e)[(\sigma_{v\text{-}soil})(\gamma_{P\text{-}EV})]$
  $P_r = (1.0)(1.420)(2)(0.164$ ft$)(13.41$ ft$)(2.175$ ksf$)$
  $= 13.58$ k/strip

- Compute factored pullout resistance as follows:
  $P_{rr} = \phi P_r = (0.90)(13.58$ k/strip$) = 12.23$ k/strip

Using similar computations, the various quantities can be developed at other levels of reinforcements and load combinations. These calculations are similar for grid-type reinforcements but with the appropriate factor for F*. Calculations of pullout resistance are the same using either the simplified or coherent gravity methods.

7.6 Establish number of soil reinforcements at each level of reinforcement

Based on T_{max}, T_r, and P_{rr}, the number of strip reinforcements at any given level of reinforcements can be computed as follows:

- Based on tensile resistance considerations, the number of strip reinforcements, N_t, is computed as follows:

  $$N_t = T_{max}/T_r$$

- Based on pullout resistance considerations, the number of strip reinforcements, N_p, is computed as follows:

  $$N_p = T_{max}/P_{rr}$$

Based on T_{max}, T_r and P_{rr}, the number of longitudinal wires for grid-type reinforcements at any given level of reinforcements can be computed as follows:

- Assume spacing of the longitudinal wires, $S_l = 6$ in. $= 0.5$ ft
- Based on tensile resistance considerations, the number of longitudinal wires, N_t, is computed as follows:

  $$N_t = T_{max}/T_r$$

- Based on pullout resistance considerations, the number of longitudinal wires, N_p, is computed as follows:

  $$N_p = 1 + (T_{max}/P_{rr})/(S_l)$$

Considering Case 1 and the Level 4 reinforcement at $Z = 8.75$ ft, the number of strip reinforcements can be computed as follows:

- $T_{max} = 12.36$ k for panel of 5-ft width, $T_r = 10.41$ k/strip, $P_{rr} = 12.23$ k/strip
- $N_t = T_{max}/T_r = (12.36$ k for panel of 5-ft width$)/(10.41$ k/strip$)$ $= 1.19$ strips for panel of 5-ft width

Table F-7.4 (a). Simplified method—computed reinforcement requirements.

Case	Fill Quality	Galvanized	Reinforcement Type	t_{design} (years)	A_s per 5-ft. wide panel (in.^{2})
1	High	Yes	Strip	75	8.1
2	High	Yes	Grid	75	7.1
3	Good	Yes	Strip	75	9.0
4	Good	Yes	Grid	75	8.9
5	Marginal	Yes	Grid	50	17.0/16.4[1]
6	High	No	Strip	75	13.0
7	High	No	Grid	75	13.8
8	Good	No	Strip	50	16.7
9	Good	No	Grid	50	19.2

Table F-7.4 (b). Coherent gravity method—computed reinforcement requirements.

Case	Fill Quality	Galvanized	Reinforcement Type	t_{design} (years)	A_s per 5 ft. wide panel (in^2)
1	High	Yes	Strip	75	9.0
2	High	Yes	Grid	75	7.3
3	Good	Yes	Strip	75	10.2
4	Good	Yes	Grid	75	8.9
5	Marginal	Yes	Grid	50	17.6/17.0[1]
6	High	No	Strip	75	14.4
7	High	No	Grid	75	14.0
8	Good	No	Strip	50	18.0
9	Good	No	Grid	50	19.6

[1] Model I/Model II— demonstrates that resistance factors are calibrated with respect to different models to render similar designs.

- $N_p = T_{max}/P_{rr}$ = (12.36 k for panel of 5-ft width)/(12.23 k/strip) = 1.01 strips for panel of 5-ft width
- Since $N_t > N_p$, tension breakage is the governing criteria and therefore the governing value, N_g, is 1.19. Round up to select two strips at Level 4 for each panel of 5-ft width.

The computations in Sections 7.4 to 7.6 are repeated at each level of reinforcement. Tables of results from the computations at all levels of reinforcement for Strength I (max) load combination and Cases 1–9 are included at the end of this appendix. The last column of the tables for Cases 1, 3, 6, and 8 provides horizontal spacing of the reinforcing strips, which is obtained by dividing the panel width, w_p, by the governing number of strips, N_g.

Tables F-7.4(a) and (b) summarize the steel requirements computed using the Simplified and Coherent Gravity Methods, respectively, for Cases 1–9 in terms of the steel area (A_s) required for each 5-ft width of the wall (corresponding to the width of the precast concrete facing panel).

Both Models I and II are used to compute nominal steel requirements for Case 5. As described in the report, Model II renders twice the nominal sacrificial steel compared to Model I, but resistance factors are calibrated to render the same probability that reinforcement resistance may fall below acceptable levels before the end of the design life ($p_f = 0.01$). This example demonstrates that the designs executed with Models I or II and corresponding resistance factors are indeed similar.

These results demonstrate the advantages of using galvanized steel to reduce the sacrificial steel requirements. Reinforcement requirements for plain steel are between 1.5 and 2.0 times higher in terms of cross-sectional area (A_s) compared to when galvanized steel reinforcements are used in similar fill conditions (e.g., Case 1 compared to Case 6, Case 2 compared to Case 7, Case 3 compared to Case 8, and Case 4 compared to Case 9). Designs achieved using the simplified method of analysis are close to those rendered with the coherent gravity method when the same resistance factors are applied. This is expected because the simplified method was calibrated to render results similar to the coherent gravity method. However, when comparing details of the designs achieved with the coherent gravity compared to the simplified methods, the distributions of the reinforcements are different. Use of the coherent gravity method results in fewer reinforcements placed near the top of the wall and more reinforcements placed near the bottom compared to designs achieved with the simplified method.

CASE 1

H=	30	ft	K_a=	0.283		ϕ_p=	0.9	X=	708	μm =	0.027874 in
L=	24	ft	$\gamma_{P\text{-}EV}$ =	1.35		ϕ_t=	0.8	t=	75	yrs	
tanβ=	0.5		σ_2=	0.65625	ksf	b=	0.164 ft	z_i=	86	μm	
ΔH=	5.294118	ft	$F^*_{min}=\tan(\phi_r)$=	0.674502089				$CR_{z0\text{-}z2}$=	15	μm/yr	
H_1=	35.29412	ft	F^*_{max}=	2				CR_{z2+}=	4	μm/yr	
L_a=	10.58824	ft						CR_{steel}=	12	μm/yr	
γ_r=	125	pcf						s=	4	mm =	0.15748 in
C_u=	7							F_y=	65	ksi	

GALVANIZED STEEL STRIPS AND HIGH QUALITY FILL (ρ_{min} >10,000 Ω–cm)

SIMPLIFIED METHOD

Level	Z	$Z_{p\text{-}ave}$	σ_H	T_{max}	F*	L_e	$\phi_p P_r$	$\phi_t T_n$	N_p	N_t	N_g	S_h
	(ft)	(ft)	ksf	k/ 5 ft wide panel	dim	(ft)	k/strip	k/strip	-	-	-	(ft)
1	1.25	9.90	0.52	6.45	1.917	13.41	9.39	10.41	0.7	0.6	2	2.50
2	3.75	12.40	0.69	8.61	1.751	13.41	10.75	10.41	0.8	0.8	2	2.50
3	6.25	14.90	0.85	10.57	1.586	13.41	11.69	10.41	0.9	1.0	2	2.50
4	8.75	17.40	0.99	12.36	1.420	13.41	12.23	10.41	1.0	1.2	2	2.50
5	11.25	19.90	1.12	13.95	1.254	13.41	12.35	10.41	1.1	1.3	2	2.50
6	13.75	22.19	1.23	15.36	1.089	14.25	12.70	10.41	1.2	1.5	2	2.50
7	16.25	24.31	1.33	16.58	0.923	15.75	13.04	10.41	1.3	1.6	2	2.50
8	18.75	26.44	1.41	17.62	0.757	17.25	12.74	10.41	1.4	1.7	2	2.50
9	21.25	28.56	1.52	18.98	0.675	18.75	13.33	10.41	1.4	1.8	2	2.50
10	23.75	30.69	1.66	20.77	0.675	20.25	15.47	10.41	1.3	2.0	2	2.50
11	26.25	32.81	1.81	22.56	0.675	21.75	17.76	10.41	1.3	2.2	3	1.67
12	28.75	34.94	1.95	24.36	0.675	23.25	20.22	10.41	1.2	2.3	3	1.67
										A_{sum} =	8.06	

CASE 2

H=	30 ft	K_a=	0.283		ϕ_p=	0.9		X=	708 μm =	0.027874016 in
L=	24 ft	$\gamma_{P\text{-}EV}$ =	1.35		ϕ_t=	0.7		t=	75 yrs	
tanβ=	0.5	σ_2=	0.65625 ksf		S_t=	1 ft		z_i=	86 μm	
ΔH=	5.294118 ft	F^*_{min}=	0.311666667		S_l=	0.5 ft		$CR_{z0\text{-}z2}$=	15 μm/yr	
H_1=	35.29412 ft	F^*_{max}=	0.623333333	**Tranverse**	W11	0.374 in diameter		CR_{z2+}=	4 μm/yr	
L_a=	10.58824 ft							CR_{steel}=	12 μm/yr	
γ_r=	125 pcf						**Longitudinal**	W11	0.374 in diameter	
								F_y=	65 ksi	

GALVANIZED GRIDS AND HIGH QUALITY FILL (ρ_{min} > 10,000 Ω-cm)

SIMPLIFIED METHOD

Level	Z	$Z_{p\text{-}ave}$	σ_H	T_{max}	F*	L_e	$\phi_p P_r$	$\phi_t T_n$	N_p	N_t	N_g	Bar Mat
	(ft)	(ft)	ksf	k/ 5 ft wide panel	dim	(ft)	k/ft	k/wire	-	-	-	-
1	1.25	9.90	0.75	9.32	0.604	13.41	18.03	3.62	2.0	2.6	3	3W11 + W11 x 1.0'
2	3.75	12.40	0.96	12.06	0.565	13.41	21.13	3.62	2.1	3.3	4	4W11 + W11 x 1.0'
3	6.25	14.90	1.15	14.31	0.526	13.41	23.64	3.62	2.2	4.0	4	4W11 + W11 x 1.0'
4	8.75	17.40	1.29	16.08	0.487	13.41	25.57	3.62	2.3	4.4	5	5W11 + W11 x 1.0'
5	11.25	19.90	1.39	17.36	0.448	13.41	26.90	3.62	2.3	4.8	5	5W11 + W11 x 1.0'
6	13.75	22.19	1.45	18.16	0.409	14.25	29.10	3.62	2.2	5.0	6	6W11 + W11 x 1.0'
7	16.25	24.31	1.48	18.47	0.370	15.75	31.89	3.62	2.2	5.1	6	6W11 + W11 x 1.0'
8	18.75	26.44	1.46	18.30	0.331	17.25	33.98	3.62	2.1	5.1	6	6W11 + W11 x 1.0'
9	21.25	28.56	1.52	18.98	0.312	18.75	37.56	3.62	2.0	5.2	6	6W11 + W11 x 1.0'
10	23.75	30.69	1.66	20.77	0.312	20.25	43.58	3.62	2.0	5.7	6	6W11 + W11 x 1.0'
11	26.25	32.81	1.81	22.56	0.312	21.75	50.05	3.62	1.9	6.2	7	7W11 + W11 x 1.0'
12	28.75	34.94	1.95	24.36	0.312	23.25	56.96	3.62	1.9	6.7	7	7W11 + W11 x 1.0'
										A_{sum} =	7.14	

CASE 3

H=	30	ft	K_a=	0.283		ϕ_p=	0.9	X=	708	μm =	0.027874 in
L=	24	ft	$\gamma_{P\text{-}EV}$ =	1.35		ϕ_t=	0.65	t=	75	yrs	
tanβ=	0.5		σ_2=	0.65625	ksf	b=	0.164 ft	z_i=	86	μm	
ΔH=	5.294118	ft	$F^*_{min}=\tan(\phi_r)$=	0.674502089				$CR_{z0\text{-}z2}$=	15	μm/yr	
H_1=	35.29412	ft	F^*_{max}=	2				CR_{z2+}=	4	μm/yr	
L_a=	10.58824	ft						CR_{steel}=	12	μm/yr	
γ_r=	125	pcf						s=	4	mm =	0.15748 in
C_u=	7							F_y=	65	ksi	

GALVANIZED STRIPS AND GOOD QUALITY FILL (3000 Ω-cm< ρ_{min} < 10,000 Ω-cm)

SIMPLIFIED METHOD

Level	Z	$Z_{p\text{-}ave}$	σ_H	T_{max}	F*	L_e	$\phi_p P_r$	$\phi_t T_n$	N_p	N_t	N_g	S_h
	(ft)	(ft)	ksf	k/ 5 ft wide panel	dim	(ft)	k/strip	k/strip	-	-	-	(ft)
1	1.25	9.90	0.52	6.45	1.917	13.41	9.39	8.46	0.7	0.8	2	2.50
2	3.75	12.40	0.69	8.61	1.751	13.41	10.75	8.46	0.8	1.0	2	2.50
3	6.25	14.90	0.85	10.57	1.586	13.41	11.69	8.46	0.9	1.3	2	2.50
4	8.75	17.40	0.99	12.36	1.420	13.41	12.23	8.46	1.0	1.5	2	2.50
5	11.25	19.90	1.12	13.95	1.254	13.41	12.35	8.46	1.1	1.6	2	2.50
6	13.75	22.19	1.23	15.36	1.089	14.25	12.70	8.46	1.2	1.8	2	2.50
7	16.25	24.31	1.33	16.58	0.923	15.75	13.04	8.46	1.3	2.0	2	2.50
8	18.75	26.44	1.41	17.62	0.757	17.25	12.74	8.46	1.4	2.1	3	1.67
9	21.25	28.56	1.52	18.98	0.675	18.75	13.33	8.46	1.4	2.2	3	1.67
10	23.75	30.69	1.66	20.77	0.675	20.25	15.47	8.46	1.3	2.5	3	1.67
11	26.25	32.81	1.81	22.56	0.675	21.75	17.76	8.46	1.3	2.7	3	1.67
12	28.75	34.94	1.95	24.36	0.675	23.25	20.22	8.46	1.2	2.9	3	1.67
										A_{sum} =	8.99	

CASE 4

H=	30 ft	K_a=	0.283		ϕ_p=	0.9		X=	708 μm =	0.027874016 in
L=	24 ft	$\gamma_{P\text{-}EV}$ =	1.35		ϕ_t=	0.55		t=	75 yrs	
tanβ=	0.5	σ_2=	0.65625 ksf		S_t=	1.0 ft		z_i=	86 μm	
ΔH=	5.294118 ft	F^*_{min}=	0.311666667		S_l=	0.5 ft		$CR_{z0\text{-}z2}$=	15 μm/yr	
H_1=	35.29412 ft	F^*_{max}=	0.623333333 **Tranverse**		W11	0.374 in diameter		CR_{z2+}=	4 μm/yr	
L_a=	10.58824 ft							CR_{steel}=	12 μm/yr	
γ_r=	125 pcf						**Longitudinal**	W11	0.374 in diameter	
								F_y=	65 ksi	

GALVANIZED GRIDS AND GOOD QUALITY FILL (3000 Ω-cm< ρ_{min} < 10,000 Ω-cm)

SIMPLIFIED METHOD

Level	Z	$Z_{p\text{-}ave}$	σ_H	T_{max}	F*	L_e	$\phi_p P_r$	$\phi_t T_n$	N_p	N_t	N_g	Bar Mat
	(ft)	(ft)	ksf	k/ 5 ft wide panel	dim	(ft)	k/ft	k/wire	-	-	-	-
1	1.25	9.90	0.75	9.32	0.604	13.41	18.03	2.84	2.0	3.3	4	W11 + W11 x 1.0'
2	3.75	12.40	0.96	12.06	0.565	13.41	21.13	2.84	2.1	4.2	5	W11 + W11 x 1.0'
3	6.25	14.90	1.15	14.31	0.526	13.41	23.64	2.84	2.2	5.0	6	W11 + W11 x 1.0'
4	8.75	17.40	1.29	16.08	0.487	13.41	25.57	2.84	2.3	5.7	6	W11 + W11 x 1.0'
5	11.25	19.90	1.39	17.36	0.448	13.41	26.90	2.84	2.3	6.1	7	W11 + W11 x 1.0'
6	13.75	22.19	1.45	18.16	0.409	14.25	29.10	2.84	2.2	6.4	7	W11 + W11 x 1.0'
7	16.25	24.31	1.48	18.47	0.370	15.75	31.89	2.84	2.2	6.5	7	W11 + W11 x 1.0'
8	18.75	26.44	1.46	18.30	0.331	17.25	33.98	2.84	2.1	6.4	7	W11 + W11 x 1.0'
9	21.25	28.56	1.52	18.98	0.312	18.75	37.56	2.84	2.0	6.7	7	W11 + W11 x 1.0'
10	23.75	30.69	1.66	20.77	0.312	20.25	43.58	2.84	2.0	7.3	8	W11 + W11 x 1.0'
11	26.25	32.81	1.81	22.56	0.312	21.75	50.05	2.84	1.9	7.9	8	W11 + W11 x 1.0'
12	28.75	34.94	1.95	24.36	0.312	23.25	56.96	2.84	1.9	8.6	9	W11 + W11 x 1.0'
										A_{sum} =	8.90	

CASE 5(a) - Model I

H=	30 ft	K_a=	0.283		ϕ_p=	0.9		X=	1120 μm =	0.044094488 in
L=	24 ft	$\gamma_{P\text{-}EV}$ =	1.35		ϕ_t=	0.3		t=	50 yrs	
tanβ=	0.5	σ_2=	0.65625 ksf		S_t=	1.0 ft		z_i=	86 μm	
ΔH=	5.294118 ft	F^*_{min}=	0.311666667		S_l=	0.5 ft		$CR_{z0\text{-}z2}$=	8.6 μm/yr	
H_1=	35.29412 ft	F^*_{max}=	0.623333333	**Tranverse**	W11	0.374 in diameter		CR_{z2+}=	8.6 μm/yr	
L_a=	10.58824 ft							CR_{steel}=	28 μm/yr	
γ_r=	125 pcf						**Longitudinal**	W20	0.505 in diameter	
								F_y=	65 ksi	

GALVANIZED GRIDS AND MARGINAL QUALITY FILL (1000 Ω-cm< ρ_{min} < 3,000 Ω-cm)

SIMPLIFIED METHOD

Level	Z	$Z_{p\text{-}ave}$	σ_H	T_{max}	F*	L_e	$\phi_p P_r$	$\phi_t T_n$	N_p	N_t	N_g	Bar Mat
	(ft)	(ft)	ksf	k/ 5 ft wide panel	dim	(ft)	k/ft	k/wire	-	-	-	-
1	1.25	9.90	0.75	9.32	0.604	13.41	18.03	2.66	2.0	3.5	4	4W20 + W11 x 1.0'
2	3.75	12.40	0.96	12.06	0.565	13.41	21.13	2.66	2.1	4.5	5	5W20 + W11 x 1.0'
3	6.25	14.90	1.15	14.31	0.526	13.41	23.64	2.66	2.2	5.4	6	6W20 + W11 x 1.0'
4	8.75	17.40	1.29	16.08	0.487	13.41	25.57	2.66	2.3	6.0	7	7W20 + W11 x 1.0'
5	11.25	19.90	1.39	17.36	0.448	13.41	26.90	2.66	2.3	6.5	7	7W20 + W11 x 1.0'
6	13.75	22.19	1.45	18.16	0.409	14.25	29.10	2.66	2.2	6.8	7	7W20 + W11 x 1.0'
7	16.25	24.31	1.48	18.47	0.370	15.75	31.89	2.66	2.2	6.9	7	7W20 + W11 x 1.0'
8	18.75	26.44	1.46	18.30	0.331	17.25	33.98	2.66	2.1	6.9	7	7W20 + W11 x 1.0'
9	21.25	28.56	1.52	18.98	0.312	18.75	37.56	2.66	2.0	7.1	8	8W20 + W11 x 1.0'
10	23.75	30.69	1.66	20.77	0.312	20.25	43.58	2.66	2.0	7.8	8	8W20 + W11 x 1.0'
11	26.25	32.81	1.81	22.56	0.312	21.75	50.05	2.66	1.9	8.5	9	9W20 + W11 x 1.0'
12	28.75	34.94	1.95	24.36	0.312	23.25	56.96	2.66	1.9	9.2	10	10W20 + W11 x 1.0'
										A_{sum} =	17.03	

CASE 5(b) - Model II

H=	30 ft	K_a=	0.283		ϕ_p=	0.9		X=	2240 μm =	0.088188976 in
L=	24 ft	$\gamma_{P\text{-}EV}$ =	1.35		ϕ_t=	0.5		t=	50 yrs	
tanβ=	0.5	σ_2=	0.65625 ksf		S_t=	1.0 ft		z_i=	86 μm	
ΔH=	5.294118 ft	F^*_{min}=	0.311666667		S_l=	0.5 ft		$CR_{z0\text{-}z2}$=	8.6 μm/yr	
H_1=	35.29412 ft	F^*_{max}=	0.623333333	**Tranverse**	W11	0.374 in diameter		CR_{z2+}=	8.6 μm/yr	
L_a=	10.58824 ft							CR_{steel}=	56 μm/yr	
γ_f=	125 pcf						**Longitudinal**	W20	0.505 in diameter	
								F_y=	65 ksi	

GALVANIZED GRIDS AND MARGINAL QUALITY FILL (1000 Ω-cm< ρ_{min} < 3,000 Ω-cm)

SIMPLIFIED METHOD

Level	Z	$Z_{p\text{-}ave}$	σ_H	T_{max}	F*	L_e	$\phi_p P_r$	$\phi_t T_n$	N_p	N_t	N_g	Bar Mat
	(ft)	(ft)	ksf	k/ 5 ft wide panel	dim	(ft)	k/ft	k/wire	-	-	-	-
1	1.25	9.90	0.75	9.32	0.604	13.41	18.03	2.76	2.0	3.4	4	4W20 + W11 x 1.0'
2	3.75	12.40	0.96	12.06	0.565	13.41	21.13	2.76	2.1	4.4	5	5W20 + W11 x 1.0'
3	6.25	14.90	1.15	14.31	0.526	13.41	23.64	2.76	2.2	5.2	6	6W20 + W11 x 1.0'
4	8.75	17.40	1.29	16.08	0.487	13.41	25.57	2.76	2.3	5.8	6	6W20 + W11 x 1.0'
5	11.25	19.90	1.39	17.36	0.448	13.41	26.90	2.76	2.3	6.3	7	7W20 + W11 x 1.0'
6	13.75	22.19	1.45	18.16	0.409	14.25	29.10	2.76	2.2	6.6	7	7W20 + W11 x 1.0'
7	16.25	24.31	1.48	18.47	0.370	15.75	31.89	2.76	2.2	6.7	7	7W20 + W11 x 1.0'
8	18.75	26.44	1.46	18.30	0.331	17.25	33.98	2.76	2.1	6.6	7	7W20 + W11 x 1.0'
9	21.25	28.56	1.52	18.98	0.312	18.75	37.56	2.76	2.0	6.9	7	7W20 + W11 x 1.0'
10	23.75	30.69	1.66	20.77	0.312	20.25	43.58	2.76	2.0	7.5	8	8W20 + W11 x 1.0'
11	26.25	32.81	1.81	22.56	0.312	21.75	50.05	2.76	1.9	8.2	9	9W20 + W11 x 1.0'
12	28.75	34.94	1.95	24.36	0.312	23.25	56.96	2.76	1.9	8.8	9	9W20 + W11 x 1.0'
										A_{sum} =	16.42	

CASE 6

H=	30 ft	K_a=	0.283	ϕ_p=	0.9	X=	975 μm =	0.038386 in
L=	24 ft	$\gamma_{P\text{-}EV}$ =	1.35	ϕ_t=	0.45	t=	75 yrs	
tanβ=	0.5	σ_2=	0.65625 ksf	b=	0.164 ft			
ΔH=	5.294118 ft	$F^*_{min}=\tan(\phi_r)$=	0.674502089					
H_1=	35.29412 ft	F^*_{max}=	2					
L_a=	10.58824 ft							
γ_r=	125 pcf					s=	6 mm =	0.23622 in
C_u=	7					F_y=	65 ksi	

PLAIN STEEL STRIPS AND HIGH QUALITY FILL (ρ_{min} >10,000 Ω–cm)

SIMPLIFIED METHOD

Level	Z	$Z_{p\text{-}ave}$	σ_H	T_{max}	F*	L_e	$\phi_p P_r$	$\phi_t T_n$	N_p	N_t	N_g	S_h
	(ft)	(ft)	ksf	k/ 5 ft wide panel	dim	(ft)	k/strip	k/strip	-	-	-	(ft)
1	1.25	9.90	0.52	6.45	1.917	13.41	9.39	9.18	0.7	0.7	2	2.50
2	3.75	12.40	0.69	8.61	1.751	13.41	10.75	9.18	0.8	0.9	2	2.50
3	6.25	14.90	0.85	10.57	1.586	13.41	11.69	9.18	0.9	1.2	2	2.50
4	8.75	17.40	0.99	12.36	1.420	13.41	12.23	9.18	1.0	1.3	2	2.50
5	11.25	19.90	1.12	13.95	1.254	13.41	12.35	9.18	1.1	1.5	2	2.50
6	13.75	22.19	1.23	15.36	1.089	14.25	12.70	9.18	1.2	1.7	2	2.50
7	16.25	24.31	1.33	16.58	0.923	15.75	13.04	9.18	1.3	1.8	2	2.50
8	18.75	26.44	1.41	17.62	0.757	17.25	12.74	9.18	1.4	1.9	2	2.50
9	21.25	28.56	1.52	18.98	0.675	18.75	13.33	9.18	1.4	2.1	3	1.67
10	23.75	30.69	1.66	20.77	0.675	20.25	15.47	9.18	1.3	2.3	3	1.67
11	26.25	32.81	1.81	22.56	0.675	21.75	17.76	9.18	1.3	2.5	3	1.67
12	28.75	34.94	1.95	24.36	0.675	23.25	20.22	9.18	1.2	2.7	3	1.67
										A_{sum} =	13.02	

CASE 7

H=	30 ft	K_a=	0.283		ϕ_p=	0.9		X=	975 μm =	0.038385827 in
L=	24 ft	$\gamma_{P\text{-}EV}$ =	1.35		ϕ_t=	0.35		t=	75 yrs	
tanβ=	0.5	σ_2=	0.65625 ksf		S_t=	1 ft				
ΔH=	5.294118 ft	F^*_{min}=	0.311666667		S_l=	0.5 ft				
H_1=	35.29412 ft	F^*_{max}=	0.623333333	**Tranverse**	W11	0.374 in diameter				
L_a=	10.58824 ft									
γ_r=	125 pcf						**Longitudinal**	W20	0.505 in diameter	
								F_y=	65 ksi	

PLAIN STEEL GRIDS AND HIGH QUALITY FILL (ρ_{min} > 10,000 Ω-cm)

SIMPLIFIED METHOD

Level	Z	$Z_{p\text{-}ave}$	σ_H	T_{max}	F*	L_e	$\phi_p P_r$	$\phi_t T_n$	N_p	N_t	N_g	Bar Mat
	(ft)	(ft)	ksf	k/ 5 ft wide panel	dim	(ft)	k/ft	k/wire	-	-	-	-
1	1.25	9.90	0.75	9.32	0.604	13.41	18.03	3.28	2.0	2.8	3	3W20 + W11x 1.0'
2	3.75	12.40	0.96	12.06	0.565	13.41	21.13	3.28	2.1	3.7	4	4W20 + W11x 1.0'
3	6.25	14.90	1.15	14.31	0.526	13.41	23.64	3.28	2.2	4.4	5	5W20 + W11x 1.0'
4	8.75	17.40	1.29	16.08	0.487	13.41	25.57	3.28	2.3	4.9	5	5W20 + W11x 1.0'
5	11.25	19.90	1.39	17.36	0.448	13.41	26.90	3.28	2.3	5.3	6	6W20 + W11x 1.0'
6	13.75	22.19	1.45	18.16	0.409	14.25	29.10	3.28	2.2	5.5	6	6W20 + W11x 1.0'
7	16.25	24.31	1.48	18.47	0.370	15.75	31.89	3.28	2.2	5.6	6	6W20 + W11x 1.0'
8	18.75	26.44	1.46	18.30	0.331	17.25	33.98	3.28	2.1	5.6	6	6W20 + W11x 1.0'
9	21.25	28.56	1.52	18.98	0.312	18.75	37.56	3.28	2.0	5.8	6	6W20 + W11x 1.0'
10	23.75	30.69	1.66	20.77	0.312	20.25	43.58	3.28	2.0	6.3	7	7W20 + W11x 1.0'
11	26.25	32.81	1.81	22.56	0.312	21.75	50.05	3.28	1.9	6.9	7	7W20 + W11x 1.0'
12	28.75	34.94	1.95	24.36	0.312	23.25	56.96	3.28	1.9	7.4	8	8W20 + W11x 1.0'
										A_{sum} =	13.82	

CASE 8

H=	30 ft	K_a=	0.283	ϕ_p=	0.9	X=	1829.22 μm =	0.072017 in
L=	24 ft	$\gamma_{P\text{-}EV}$ =	1.35	ϕ_t=	0.45	t=	50 yrs	
tanβ=	0.5	σ_2=	0.65625 ksf	b=	0.164 ft			
ΔH=	5.294118 ft	$F^*_{min}=\tan(\phi_r)$=	0.674502089					
H_1=	35.29412 ft	F^*_{max}=	2					
L_a=	10.58824 ft							
γ_r=	125 pcf					s=	8 mm =	0.314961 in
C_u=	7					F_y=	65 ksi	

PLAIN STEEL STRIPS AND GOOD QUALITY FILL (3000 Ω-cm< ρ_{min} < 10,000 Ω-cm)

SIMPLIFIED METHOD

Level	Z	$Z_{p\text{-}ave}$	σ_H	T_{max}	F*	L_e	$\phi_p P_r$	$\phi_t T_n$	N_p	N_t	N_g	S_h
	(ft)	(ft)	ksf	k/ 5 ft wide panel	dim	(ft)	k/strip	k/strip	-	-	-	(ft)
1	1.25	9.90	0.52	6.45	1.917	13.41	9.39	9.84	0.7	0.7	2	2.50
2	3.75	12.40	0.69	8.61	1.751	13.41	10.75	9.84	0.8	0.9	2	2.50
3	6.25	14.90	0.85	10.57	1.586	13.41	11.69	9.84	0.9	1.1	2	2.50
4	8.75	17.40	0.99	12.36	1.420	13.41	12.23	9.84	1.0	1.3	2	2.50
5	11.25	19.90	1.12	13.95	1.254	13.41	12.35	9.84	1.1	1.4	2	2.50
6	13.75	22.19	1.23	15.36	1.089	14.25	12.70	9.84	1.2	1.6	2	2.50
7	16.25	24.31	1.33	16.58	0.923	15.75	13.04	9.84	1.3	1.7	2	2.50
8	18.75	26.44	1.41	17.62	0.757	17.25	12.74	9.84	1.4	1.8	2	2.50
9	21.25	28.56	1.52	18.98	0.675	18.75	13.33	9.84	1.4	1.9	2	2.50
10	23.75	30.69	1.66	20.77	0.675	20.25	15.47	9.84	1.3	2.1	3	1.67
11	26.25	32.81	1.81	22.56	0.675	21.75	17.76	9.84	1.3	2.3	3	1.67
12	28.75	34.94	1.95	24.36	0.675	23.25	20.22	9.84	1.2	2.5	3	1.67
										A_{sum} =	16.74	

CASE 9

H=	30 ft	K_a=	0.283		ϕ_p=	0.9		X=	1829.22 μm =		0.072016544 in
L=	24 ft	$\gamma_{P\text{-}EV}$ =	1.35		ϕ_t=	0.35		t=	50 yrs		
tanβ=	0.5	σ_2=	0.65625 ksf		S_t=	1.0 ft					
ΔH=	5.294118 ft	F^*_{min}=	0.311666667		S_l=	0.5 ft					
H_1=	35.29412 ft	F^*_{max}=	0.623333333	**Tranverse**	W11	0.374 in diameter					
L_a=	10.58824 ft										
γ_r=	125 pcf						**Longitudinal**	W20	0.505 in diameter		
								F_y=	65 ksi		

PLAIN STEEL GRIDS AND GOOD QUALITY FILL (3000 Ω-cm< ρ_{min} < 10,000 Ω-cm)

SIMPLIFIED METHOD

Level	Z	$Z_{p\text{-}ave}$	σ_H	T_{max}	F*	L_e	$\phi_p P_r$	$\phi_t T_n$	N_p	N_t	N_g	Bar Mat
	(ft)	(ft)	ksf	k/ 5 ft wide panel	dim	(ft)	k/ft	k/wire	-	-	-	-
1	1.25	9.90	0.75	9.32	0.604	13.41	18.03	2.33	2.0	4.0	5	5W20 + W11 x 1.0'
2	3.75	12.40	0.96	12.06	0.565	13.41	21.13	2.33	2.1	5.2	6	6W20 + W11 x 1.0'
3	6.25	14.90	1.15	14.31	0.526	13.41	23.64	2.33	2.2	6.1	7	7W20 + W11 x 1.0'
4	8.75	17.40	1.29	16.08	0.487	13.41	25.57	2.33	2.3	6.9	7	7W20 + W11 x 1.0'
5	11.25	19.90	1.39	17.36	0.448	13.41	26.90	2.33	2.3	7.5	8	8W20 + W11 x 1.0'
6	13.75	22.19	1.45	18.16	0.409	14.25	29.10	2.33	2.2	7.8	8	8W20 + W11 x 1.0'
7	16.25	24.31	1.48	18.47	0.370	15.75	31.89	2.33	2.2	7.9	8	8W20 + W11 x 1.0'
8	18.75	26.44	1.46	18.30	0.331	17.25	33.98	2.33	2.1	7.9	8	8W20 + W11 x 1.0'
9	21.25	28.56	1.52	18.98	0.312	18.75	37.56	2.33	2.0	8.2	9	9W20 + W11 x 1.0'
10	23.75	30.69	1.66	20.77	0.312	20.25	43.58	2.33	2.0	8.9	9	9W20 + W11 x 1.0'
11	26.25	32.81	1.81	22.56	0.312	21.75	50.05	2.33	1.9	9.7	10	10W20 + W11 x 1.0'
12	28.75	34.94	1.95	24.36	0.312	23.25	56.96	2.33	1.9	10.5	11	11W20 + W11 x 1.0'
										A_{sum} =	19.23	

CASE 1

H=	30	ft	K_{af}=	0.283		ϕ_p=	0.9	X=	708	μm =	0.027874 in
L=	24	ft	k_{0f}=	0.440807097		ϕ_t=	0.8	t=	75	yrs	
tanβ=	0.5		$\gamma_{P\text{-}EV}$ =	1.35		b=	0.164 ft	z_j=	86	μm	
ΔH=	5.294118	ft	V_2=	18 k/ft				$CR_{z0\text{-}z2}$=	15	μm/yr	
H_1=	35.29412	ft	$F^*_{min}=\tan(\phi_r)$=	0.674502089				CR_{z2+}=	4	μm/yr	
L_a=	10.58824	ft	F^*_{max}=	2				CR_{steel}=	12	μm/yr	
γ_r=	125	pcf	K_{ab} =	0.537				s=	4	mm =	0.15748 in
C_u=	7		γ_b=	125 pcf				F_y=	65	ksi	
			$\gamma_{P\text{-}EH}$ =	1.5							

GALVANIZED STRIPS AND HIGH QUALITY FILL (ρ_{min} > 10,000 Ω-cm)

COHERENT GRAVITY METHOD

Level	Z	$Z_{p\text{-}ave}$	σ_H	T_{max}	F*	L_e	$\phi_p P_r$	$\phi_t T_n$	N_p	N_t	N_g	S_h
	(ft)	(ft)	ksf	k/ 5 ft wide panel	dim	(ft)	k/strip	k/strip	-	-	-	(ft)
1	1.25	9.90	0.47	5.86	1.917	13.41	9.39	10.41	0.6	0.6	2	2.50
2	3.75	12.40	0.65	8.07	1.751	13.41	10.75	10.41	0.8	0.8	2	2.50
3	6.25	14.90	0.82	10.21	1.586	13.41	11.69	10.41	0.9	1.0	2	2.50
4	8.75	17.40	0.98	12.26	1.420	13.41	12.23	10.41	1.0	1.2	2	2.50
5	11.25	19.90	1.14	14.24	1.254	13.41	12.35	10.41	1.2	1.4	2	2.50
6	13.75	22.19	1.29	16.13	1.089	14.25	12.70	10.41	1.3	1.5	2	2.50
7	16.25	24.31	1.44	17.94	0.923	15.75	13.04	10.41	1.4	1.7	2	2.50
8	18.75	26.44	1.57	19.65	0.757	17.25	12.74	10.41	1.5	1.9	2	2.50
9	21.25	28.56	1.77	22.10	0.675	18.75	13.33	10.41	1.7	2.1	3	1.67
10	23.75	30.69	2.04	25.51	0.675	20.25	15.47	10.41	1.6	2.5	3	1.67
11	26.25	32.81	2.35	29.36	0.675	21.75	17.76	10.41	1.7	2.8	3	1.67
12	28.75	34.94	2.70	33.73	0.675	23.25	20.22	10.41	1.7	3.2	4	1.25
										A_{sum} =	8.99	

CASE 2

H=	30 ft	K_{af}=	0.283		ϕ_p=	0.9		X=	708 μm =	0.027874016 in
L=	24 ft	k_{0f}=	0.440807097		ϕ_t=	0.7		t=	75 yrs	
tanβ=	0.5	$\gamma_{P\text{-}EV}$ =	1.35		S_t=	1.0 ft		z_i=	86 μm	
ΔH=	5.294118 ft	V_2=	18 k/ft		S_l=	0.5 ft		$CR_{z0\text{-}z2}$=	15 μm/yr	
H_1=	35.29412 ft	F^*_{min}=	0.311666667	**Tranverse**	W11	0.374 in diameter		CR_{z2+}=	4 μm/yr	
L_a=	10.58824 ft	F^*_{max}=	0.623333333					CR_{steel}=	12 μm/yr	
γ_r=	125 pcf	K_{ab} =	0.537				**Longitudinal**	W11	0.374 in diameter	
		γ_b=	125 pcf					F_y=	65 ksi	
		$\gamma_{P\text{-}EH}$ =	1.5							

GALVANIZED GRIDS AND HIGH QUALITY FILL (ρ_{min} > 10,000 Ω-cm)

COHERENT GRAVITY METHOD

Level	Z	$Z_{p\text{-}ave}$	σ_H	T_{max}	F*	L_e	$\phi_p P_r$	$\phi_t T_n$	N_p	N_t	N_g	S_h
	(ft)	(ft)	ksf	k/ 5 ft wide panel	dim	(ft)	k/ft	k/wire	-	-	-	-
1	1.25	9.90	0.47	5.86	0.604	13.41	18.03	3.62	1.7	1.6	2	2W11 + W11 x 1.0'
2	3.75	12.40	0.65	8.07	0.565	13.41	21.13	3.62	1.8	2.2	3	3W11 + W11 x 1.0'
3	6.25	14.90	0.82	10.21	0.526	13.41	23.64	3.62	1.9	2.8	3	3W11 + W11 x 1.0'
4	8.75	17.40	0.98	12.26	0.487	13.41	25.57	3.62	2.0	3.4	4	4W11 + W11 x 1.0'
5	11.25	19.90	1.14	14.24	0.448	13.41	26.90	3.62	2.1	3.9	4	4W11 + W11 x 1.0'
6	13.75	22.19	1.29	16.13	0.409	14.25	29.10	3.62	2.1	4.5	5	5W11 + W11 x 1.0'
7	16.25	24.31	1.44	17.94	0.370	15.75	31.89	3.62	2.1	5.0	5	5W11 + W11 x 1.0'
8	18.75	26.44	1.57	19.65	0.331	17.25	33.98	3.62	2.2	5.4	6	6W11 + W11 x 1.0'
9	21.25	28.56	1.77	22.10	0.312	18.75	37.56	3.62	2.2	6.1	7	7W11 + W11 x 1.0'
10	23.75	30.69	2.04	25.51	0.312	20.25	43.58	3.62	2.2	7.0	8	8W11 + W11 x 1.0'
11	26.25	32.81	2.35	29.36	0.312	21.75	50.05	3.62	2.2	8.1	9	9W11 + W11 x 1.0'
12	28.75	34.94	2.70	33.73	0.312	23.25	56.96	3.62	2.2	9.3	10	10W11 + W11 x 1.0'
										A_{sum} =	7.25	

CASE 3

H=	30	ft	K_{af}=	0.283		ϕ_p=	0.9		X=	708 μm =	0.027874 in
L=	24	ft	k_{0f}=	0.440807097		ϕ_t=	0.65		t=	75 yrs	
tanβ=	0.5		$\gamma_{P\text{-}EV}$ =	1.35		b=	0.164	ft	z_i=	86 μm	
ΔH=	5.294118	ft	V_2=	18	k/ft				$CR_{z0\text{-}z2}$=	15 μm/yr	
H_1=	35.29412	ft	F^*_{min}=tan(ϕ_r)=	0.674502089					CR_{z2+}=	4 μm/yr	
L_a=	10.58824	ft	F^*_{max}=	2					CR_{steel}=	12 μm/yr	
γ_r=	125	pcf	K_{ab} =	0.537					s=	4 mm =	0.15748 in
C_u=	7		γ_b=	125	pcf				F_y=	65 ksi	
			$\gamma_{P\text{-}EH}$ =	1.5							

GALVANIZED STRIPS AND GOOD QUALITY FILL (3000 Ω-cm< ρ_{min} < 10,000 Ω-cm)

COHERENT GRAVITY METHOD

Level	Z	$Z_{p\text{-}ave}$	σ_H	T_{max}	F*	L_e	$\phi_p P_r$	$\phi_t T_n$	N_p	N_t	N_g	S_h
	(ft)	(ft)	ksf	k/ 5 ft wide panel	dim	(ft)	k/strip	k/strip	-	-	-	(ft)
1	1.25	9.90	0.47	5.86	1.917	13.41	9.39	8.46	0.6	0.7	2	2.50
2	3.75	12.40	0.65	8.07	1.751	13.41	10.75	8.46	0.8	1.0	2	2.50
3	6.25	14.90	0.82	10.21	1.586	13.41	11.69	8.46	0.9	1.2	2	2.50
4	8.75	17.40	0.98	12.26	1.420	13.41	12.23	8.46	1.0	1.4	2	2.50
5	11.25	19.90	1.14	14.24	1.254	13.41	12.35	8.46	1.2	1.7	2	2.50
6	13.75	22.19	1.29	16.13	1.089	14.25	12.70	8.46	1.3	1.9	2	2.50
7	16.25	24.31	1.44	17.94	0.923	15.75	13.04	8.46	1.4	2.1	3	1.67
8	18.75	26.44	1.57	19.65	0.757	17.25	12.74	8.46	1.5	2.3	3	1.67
9	21.25	28.56	1.77	22.10	0.675	18.75	13.33	8.46	1.7	2.6	3	1.67
10	23.75	30.69	2.04	25.51	0.675	20.25	15.47	8.46	1.6	3.0	4	1.25
11	26.25	32.81	2.35	29.36	0.675	21.75	17.76	8.46	1.7	3.5	4	1.25
12	28.75	34.94	2.70	33.73	0.675	23.25	20.22	8.46	1.7	4.0	4	1.25
										A_{sum} =	10.23	

CASE 4

H=	30 ft	K_{af}=	0.283		ϕ_p=	0.9		X=	708 μm =	0.027874016 in
L=	24 ft	k_{0f}=	0.440807097		ϕ_t=	0.55		t=	75 yrs	
tanβ=	0.5	γ_{P-EV} =	1.35		S_t=	1.0 ft		z_i=	86 μm	
ΔH=	5.294118 ft	V_2=	18 k/ft		S_l=	0.5 ft		CR_{z0-z2}=	15 μm/yr	
H_1=	35.29412 ft	F^*_{min}=	0.311666667	**Tranverse**	W11	0.374 in diameter		CR_{z2+}=	4 μm/yr	
L_a=	10.58824 ft	F^*_{max}=	0.623333333					CR_{steel}=	12 μm/yr	
γ_r=	125 pcf	K_{ab} =	0.537				**Longitudinal**	W11	0.374 in diameter	
		γ_b=	125 pcf					F_y=	65 ksi	
		γ_{P-EH} =	1.5							

GALVANIZED GRIDS AND GOOD QUALITY FILL (3000 Ω-cm< ρ_{min} < 10,000 Ω-cm)

COHERENT GRAVITY METHOD

Level	Z	$Z_{p\text{-}ave}$	σ_H	T_{max}	F*	L_e	$\phi_p P_r$	$\phi_t T_n$	N_p	N_t	N_g	S_h
	(ft)	(ft)	ksf	k/ 5 ft wide panel	dim	(ft)	k/ft	k/wire	-	-	-	-
1	1.25	9.90	0.47	5.86	0.604	13.41	18.03	2.84	1.7	2.1	3	3W11 + W11 x 1.0'
2	3.75	12.40	0.65	8.07	0.565	13.41	21.13	2.84	1.8	2.8	3	3W11 + W11 x 1.0'
3	6.25	14.90	0.82	10.21	0.526	13.41	23.64	2.84	1.9	3.6	4	4W11 + W11 x 1.0'
4	8.75	17.40	0.98	12.26	0.487	13.41	25.57	2.84	2.0	4.3	5	5W11 + W11 x 1.0'
5	11.25	19.90	1.14	14.24	0.448	13.41	26.90	2.84	2.1	5.0	6	6W11 + W11 x 1.0'
6	13.75	22.19	1.29	16.13	0.409	14.25	29.10	2.84	2.1	5.7	6	6W11 + W11 x 1.0'
7	16.25	24.31	1.44	17.94	0.370	15.75	31.89	2.84	2.1	6.3	7	7W11 + W11 x 1.0'
8	18.75	26.44	1.57	19.65	0.331	17.25	33.98	2.84	2.2	6.9	7	7W11 + W11 x 1.0'
9	21.25	28.56	1.77	22.10	0.312	18.75	37.56	2.84	2.2	7.8	8	8W11 + W11 x 1.0'
10	23.75	30.69	2.04	25.51	0.312	20.25	43.58	2.84	2.2	9.0	9	9W11 + W11 x 1.0'
11	26.25	32.81	2.35	29.36	0.312	21.75	50.05	2.84	2.2	10.3	11	11W11 + W11 x 1.0'
12	28.75	34.94	2.70	33.73	0.312	23.25	56.96	2.84	2.2	11.9	12	12W11 + W11 x 1.0'
										A_{sum} =	8.90	

CASE 5(a). Model I

H=	30 ft	K_{af}=	0.283		ϕ_p=	0.9		X=	1120 μm =	0.044094488 in
L=	24 ft	k_{0f}=	0.440807097		ϕ_t=	0.3		t=	50 yrs	
tanβ=	0.5	$\gamma_{P\text{-}EV}$ =	1.35		S_t=	1.0 ft		z_i=	86 μm	
ΔH=	5.294118 ft	V_2=	18 k/ft		S_l=	0.5 ft		$CR_{z0\text{-}z2}$=	8.6 μm/yr	
H_1=	35.29412 ft	F^*_{min}=	0.311666667	**Tranverse**	W11	0.374 in diameter		CR_{z2+}=	8.6 μm/yr	
L_a=	10.58824 ft	F^*_{max}=	0.623333333					CR_{steel}=	28 μm/yr	
γ_r=	125 pcf	K_{ab} =	0.537				**Longitudinal**	W20	0.505 in diameter	
		γ_b=	125 pcf					F_y=	65 ksi	
		$\gamma_{P\text{-}EH}$ =	1.5							

GALVANIZED GRIDS AND MARGINAL QUALITY FILL (1,000 Ω-cm< ρ_{min} < 3,000 Ω-cm)

COHERENT GRAVITY METHOD

Level	Z	$Z_{p\text{-}ave}$	σ_H	T_{max}	F*	L_e	$\phi_p P_r$	$\phi_t T_n$	N_p	N_t	N_g	S_h
	(ft)	(ft)	ksf	k/ 5 ft wide panel	dim	(ft)	k/ft	k/wire	-	-	-	-
1	1.25	9.90	0.47	5.86	0.604	13.41	18.03	2.66	1.7	2.2	3	3W20 + W11 x 1.0'
2	3.75	12.40	0.65	8.07	0.565	13.41	21.13	2.66	1.8	3.0	4	4W20 + W11 x 1.0'
3	6.25	14.90	0.82	10.21	0.526	13.41	23.64	2.66	1.9	3.8	4	4W20 + W11 x 1.0'
4	8.75	17.40	0.98	12.26	0.487	13.41	25.57	2.66	2.0	4.6	5	5W20 + W11 x 1.0'
5	11.25	19.90	1.14	14.24	0.448	13.41	26.90	2.66	2.1	5.4	6	6W20 + W11 x 1.0'
6	13.75	22.19	1.29	16.13	0.409	14.25	29.10	2.66	2.1	6.1	7	7W20 + W11 x 1.0'
7	16.25	24.31	1.44	17.94	0.370	15.75	31.89	2.66	2.1	6.7	7	7W20 + W11 x 1.0'
8	18.75	26.44	1.57	19.65	0.331	17.25	33.98	2.66	2.2	7.4	8	8W20 + W11 x 1.0'
9	21.25	28.56	1.77	22.10	0.312	18.75	37.56	2.66	2.2	8.3	9	9W20 + W11 x 1.0'
10	23.75	30.69	2.04	25.51	0.312	20.25	43.58	2.66	2.2	9.6	10	10W20 + W11 x 1.0'
11	26.25	32.81	2.35	29.36	0.312	21.75	50.05	2.66	2.2	11.0	12	12W20 + W11 x 1.0'
12	28.75	34.94	2.70	33.73	0.312	23.25	56.96	2.66	2.2	12.7	13	13W20 + W11 x 1.0'
										A_{sum} =	17.63	

CASE 5(b). Model II

H=	30 ft	K_{af}=	0.283		ϕ_p=	0.9		X=	2240 μm =	0.088188976 in
L=	24 ft	k_{0f}=	0.440807097		ϕ_t=	0.5		t=	50 yrs	
tanβ=	0.5	$\gamma_{P\text{-}EV}$ =	1.35		S_t=	1.0 ft		z_i=	86 μm	
ΔH=	5.294118 ft	V_2=	18 k/ft		S_l=	0.5 ft		$CR_{z0\text{-}z2}$=	8.6 μm/yr	
H_1=	35.29412 ft	F^*_{min}=	0.311666667	**Tranverse**	W11	0.374 in diameter		CR_{z2+}=	8.6 μm/yr	
L_a=	10.58824 ft	F^*_{max}=	0.623333333					CR_{steel}=	56 μm/yr	
γ_r=	125 pcf	K_{ab} =	0.537				**Longitudinal**	W20	0.505 in diameter	
		γ_b=	125 pcf					F_y=	65 ksi	
		$\gamma_{P\text{-}EH}$ =	1.5							

GALVANIZED GRIDS AND MARGINAL QUALITY FILL (1,000 Ω-cm< ρ_{min} < 3,000 Ω-cm)

COHERENT GRAVITY METHOD

Level	Z	$Z_{p\text{-}ave}$	σ_H	T_{max}	F*	L_e	$\phi_p P_r$	$\phi_t T_n$	N_p	N_t	N_g	S_h
	(ft)	(ft)	ksf	k/ 5 ft wide panel	dim	(ft)	k/ft	k/wire	-	-	-	-
1	1.25	9.90	0.47	5.86	0.604	13.41	18.03	2.76	1.7	2.1	3	3W20 + W11 x 1.0'
2	3.75	12.40	0.65	8.07	0.565	13.41	21.13	2.76	1.8	2.9	3	3W20 + W11 x 1.0'
3	6.25	14.90	0.82	10.21	0.526	13.41	23.64	2.76	1.9	3.7	4	4W20 + W11 x 1.0'
4	8.75	17.40	0.98	12.26	0.487	13.41	25.57	2.76	2.0	4.4	5	5W20 + W11 x 1.0'
5	11.25	19.90	1.14	14.24	0.448	13.41	26.90	2.76	2.1	5.2	6	6W20 + W11 x 1.0'
6	13.75	22.19	1.29	16.13	0.409	14.25	29.10	2.76	2.1	5.9	6	6W20 + W11 x 1.0'
7	16.25	24.31	1.44	17.94	0.370	15.75	31.89	2.76	2.1	6.5	7	7W20 + W11 x 1.0'
8	18.75	26.44	1.57	19.65	0.331	17.25	33.98	2.76	2.2	7.1	8	8W20 + W11 x 1.0'
9	21.25	28.56	1.77	22.10	0.312	18.75	37.56	2.76	2.2	8.0	9	9W20 + W11 x 1.0'
10	23.75	30.69	2.04	25.51	0.312	20.25	43.58	2.76	2.2	9.3	10	10W20 + W11 x 1.0'
11	26.25	32.81	2.35	29.36	0.312	21.75	50.05	2.76	2.2	10.7	11	11W20 + W11 x 1.0'
12	28.75	34.94	2.70	33.73	0.312	23.25	56.96	2.76	2.2	12.2	13	13W20 + W11 x 1.0'
										A_{sum} =	17.03	

CASE 6

H=	30 ft	K_{af}=	0.283	ϕ_p=	0.9	X=	975 μm =	0.038386 in
L=	24 ft	k_{0f}=	0.440807097	ϕ_t=	0.45	t=	75 yrs	
tanβ=	0.5	$\gamma_{P\text{-}EV}$ =	1.35	b=	0.164 ft			
ΔH=	5.294118 ft	V_2=	18 k/ft					
H_1=	35.29412 ft	$_{nin}$=tan(ϕ_r)=	0.674502089					
L_a=	10.58824 ft	F^*_{max}=	2					
γ_r=	125 pcf	K_{ab} =	0.537			s=	6 mm =	0.23622 in
C_u=	7	γ_b=	125 pcf			F_y=	65 ksi	
		$\gamma_{P\text{-}EH}$ =	1.5					

PLAIN STEEL STRIPS AND HIGH QUALITY FILL (ρ_{min} > 10,000 Ω-cm)

COHERENT GRAVITY METHOD

Level	Z	$Z_{p\text{-}ave}$	σ_H	T_{max}	F*	L_e	$\phi_p P_r$	$\phi_t T_n$	N_p	N_t	N_g	S_h
	(ft)	(ft)	ksf	k/ 5 ft wide panel	dim	(ft)	k/strip	k/strip	-	-	-	(ft)
1	1.25	9.90	0.47	5.86	1.917	13.41	9.39	9.18	0.6	0.6	2	2.50
2	3.75	12.40	0.65	8.07	1.751	13.41	10.75	9.18	0.8	0.9	2	2.50
3	6.25	14.90	0.82	10.21	1.586	13.41	11.69	9.18	0.9	1.1	2	2.50
4	8.75	17.40	0.98	12.26	1.420	13.41	12.23	9.18	1.0	1.3	2	2.50
5	11.25	19.90	1.14	14.24	1.254	13.41	12.35	9.18	1.2	1.6	2	2.50
6	13.75	22.19	1.29	16.13	1.089	14.25	12.70	9.18	1.3	1.8	2	2.50
7	16.25	24.31	1.44	17.94	0.923	15.75	13.04	9.18	1.4	2.0	2	2.50
8	18.75	26.44	1.57	19.65	0.757	17.25	12.74	9.18	1.5	2.1	3	1.67
9	21.25	28.56	1.77	22.10	0.675	18.75	13.33	9.18	1.7	2.4	3	1.67
10	23.75	30.69	2.04	25.51	0.675	20.25	15.47	9.18	1.6	2.8	3	1.67
11	26.25	32.81	2.35	29.36	0.675	21.75	17.76	9.18	1.7	3.2	4	1.25
12	28.75	34.94	2.70	33.73	0.675	23.25	20.22	9.18	1.7	3.7	4	1.25
										A_{sum} =	14.41	

CASE 7

H=	30 ft	K_{af}=	0.283		ϕ_p=	0.9		X=	975 μm =	0.038385827 in	
L=	24 ft	k_{0f}=	0.440807097		ϕ_t=	0.35		t=	75 yrs		
tanβ=	0.5	$\gamma_{P\text{-}EV}$ =	1.35		S_t=	1.0 ft					
ΔH=	5.294118 ft	V_2=	18 k/ft		S_l=	0.5 ft					
H_1=	35.29412 ft	F^*_{min}=	0.311666667	**Tranverse**	W11	0.374 in diameter					
L_a=	10.58824 ft	F^*_{max}=	0.623333333								
γ_r=	125 pcf	K_{ab} =	0.537				**Longitudinal**	W20	0.505 in diameter		
		γ_b=	125 pcf					F_y=	65 ksi		
		$\gamma_{P\text{-}EH}$ =	1.5								

PLAIN STEEL GRIDS AND HIGH QUALITY FILL (ρ_{min} > 10,000 Ω-cm)

COHERENT GRAVITY METHOD

Level	Z	$Z_{p\text{-}ave}$	σ_H	T_{max}	F*	L_e	$\phi_p P_r$	$\phi_t T_n$	N_p	N_t	N_g	S_h
	(ft)	(ft)	ksf	k/ 5 ft wide panel	dim	(ft)	k/ft	k/wire	-	-	-	-
1	1.25	9.90	0.47	5.86	0.604	13.41	18.03	3.28	1.7	1.8	2	2W20 + W11 x 1.0'
2	3.75	12.40	0.65	8.07	0.565	13.41	21.13	3.28	1.8	2.5	3	3W20 + W11 x 1.0'
3	6.25	14.90	0.82	10.21	0.526	13.41	23.64	3.28	1.9	3.1	4	4W20 + W11 x 1.0'
4	8.75	17.40	0.98	12.26	0.487	13.41	25.57	3.28	2.0	3.7	4	4W20 + W11 x 1.0'
5	11.25	19.90	1.14	14.24	0.448	13.41	26.90	3.28	2.1	4.3	5	5W20 + W11 x 1.0'
6	13.75	22.19	1.29	16.13	0.409	14.25	29.10	3.28	2.1	4.9	5	5W20 + W11 x 1.0'
7	16.25	24.31	1.44	17.94	0.370	15.75	31.89	3.28	2.1	5.5	6	6W20 + W11 x 1.0'
8	18.75	26.44	1.57	19.65	0.331	17.25	33.98	3.28	2.2	6.0	6	6W20 + W11 x 1.0'
9	21.25	28.56	1.77	22.10	0.312	18.75	37.56	3.28	2.2	6.7	7	7W20 + W11 x 1.0'
10	23.75	30.69	2.04	25.51	0.312	20.25	43.58	3.28	2.2	7.8	8	8W20 + W11 x 1.0'
11	26.25	32.81	2.35	29.36	0.312	21.75	50.05	3.28	2.2	9.0	9	9W20 + W11 x 1.0'
12	28.75	34.94	2.70	33.73	0.312	23.25	56.96	3.28	2.2	10.3	11	11W20 + W11 x 1.0'
										A_{sum} =	14.02	

CASE 8

H=	30 ft	K_{af}=	0.283	ϕ_p=	0.9	X=	1829.22 μm =	0.072017 in
L=	24 ft	k_{0f}=	0.440807097	ϕ_t=	0.45	t=	50 yrs	
tanβ=	0.5	$\gamma_{P\text{-}EV}$ =	1.35	b=	0.164 ft			
ΔH=	5.294118 ft	V_2=	18 k/ft					
H_1=	35.29412 ft	$_{min}$=tan(ϕ_r)=	0.674502089					
L_a=	10.58824 ft	F^*_{max}=	2					
γ_r=	125 pcf	K_{ab} =	0.537			s=	8 mm =	0.314961 in
C_u=	7	γ_b=	125 pcf			F_y=	65 ksi	
		$\gamma_{P\text{-}EH}$ =	1.5					

PLAIN STEEL STRIPS AND GOOD QUALITY FILL (3000 Ω-cm< ρ_{min} < 10,000 Ω-cm)

COHERENT GRAVITY METHOD

Level	Z	$Z_{p\text{-}ave}$	σ_H	T_{max}	F*	L_e	$\phi_p P_r$	$\phi_t T_n$	N_p	N_t	N_g	S_h
	(ft)	(ft)	ksf	k/ 5 ft wide panel	dim	(ft)	k/strip	k/strip	-	-	-	(ft)
1	1.25	9.90	0.47	5.86	1.917	13.41	9.39	9.84	0.6	0.6	2	2.50
2	3.75	12.40	0.65	8.07	1.751	13.41	10.75	9.84	0.8	0.8	2	2.50
3	6.25	14.90	0.82	10.21	1.586	13.41	11.69	9.84	0.9	1.0	2	2.50
4	8.75	17.40	0.98	12.26	1.420	13.41	12.23	9.84	1.0	1.2	2	2.50
5	11.25	19.90	1.14	14.24	1.254	13.41	12.35	9.84	1.2	1.4	2	2.50
6	13.75	22.19	1.29	16.13	1.089	14.25	12.70	9.84	1.3	1.6	2	2.50
7	16.25	24.31	1.44	17.94	0.923	15.75	13.04	9.84	1.4	1.8	2	2.50
8	18.75	26.44	1.57	19.65	0.757	17.25	12.74	9.84	1.5	2.0	2	2.50
9	21.25	28.56	1.77	22.10	0.675	18.75	13.33	9.84	1.7	2.2	3	1.67
10	23.75	30.69	2.04	25.51	0.675	20.25	15.47	9.84	1.6	2.6	3	1.67
11	26.25	32.81	2.35	29.36	0.675	21.75	17.76	9.84	1.7	3.0	3	1.67
12	28.75	34.94	2.70	33.73	0.675	23.25	20.22	9.84	1.7	3.4	4	1.25
										A_{sum} =	17.98	

CASE 9

H=	30 ft	K_{af}=	0.283		ϕ_p=	0.9		X=	1829.22 μm =		0.072016544 in
L=	24 ft	k_{0f}=	0.440807097		ϕ_t=	0.35		t=	50 yrs		
tanβ=	0.5	$\gamma_{P\text{-}EV}$ =	1.35		S_t=	1.0 ft					
ΔH=	5.294118 ft	V_2=	18 k/ft		S_l=	0.5 ft					
H_1=	35.29412 ft	F^*_{min}=	0.311666667	**Tranverse**	W11	0.374 in diameter					
L_a=	10.58824 ft	F^*_{max}=	0.623333333								
γ_r=	125 pcf	K_{ab} =	0.537				**Longitudinal**	W20	0.505 in diameter		
		γ_b=	125 pcf					F_y=	65 ksi		
		$\gamma_{P\text{-}EH}$ =	1.5								

PLAIN STEEL GRIDS AND GOOD QUALITY FILL (3000 Ω-cm< ρ_{min} < 10,000 Ω-cm)

COHERENT GRAVITY METHOD

Level	Z	$Z_{p\text{-}ave}$	σ_H	T_{max}	F*	L_e	$\phi_p P_r$	$\phi_t T_n$	N_p	N_t	N_g	S_h
	(ft)	(ft)	ksf	k/ 5 ft wide panel	dim	(ft)	k/ft	k/wire	-	-	-	-
1	1.25	9.90	0.47	5.86	0.604	13.41	18.03	2.33	1.7	2.5	3	3W20 + W11 x 1.0'
2	3.75	12.40	0.65	8.07	0.565	13.41	21.13	2.33	1.8	3.5	4	4W20 + W11 x 1.0'
3	6.25	14.90	0.82	10.21	0.526	13.41	23.64	2.33	1.9	4.4	5	5W20 + W11 x 1.0'
4	8.75	17.40	0.98	12.26	0.487	13.41	25.57	2.33	2.0	5.3	6	6W20 + W11 x 1.0'
5	11.25	19.90	1.14	14.24	0.448	13.41	26.90	2.33	2.1	6.1	7	7W20 + W11 x 1.0'
6	13.75	22.19	1.29	16.13	0.409	14.25	29.10	2.33	2.1	6.9	7	7W20 + W11 x 1.0'
7	16.25	24.31	1.44	17.94	0.370	15.75	31.89	2.33	2.1	7.7	8	8W20 + W11 x 1.0'
8	18.75	26.44	1.57	19.65	0.331	17.25	33.98	2.33	2.2	8.4	9	9W20 + W11 x 1.0'
9	21.25	28.56	1.77	22.10	0.312	18.75	37.56	2.33	2.2	9.5	10	10W20 + W11 x 1.0'
10	23.75	30.69	2.04	25.51	0.312	20.25	43.58	2.33	2.2	11.0	11	11W20 + W11 x 1.0'
11	26.25	32.81	2.35	29.36	0.312	21.75	50.05	2.33	2.2	12.6	13	13W20 + W11 x 1.0'
12	28.75	34.94	2.70	33.73	0.312	23.25	56.96	2.33	2.2	14.5	15	15W20 + W11 x 1.0'
										A_{sum} =	19.63	

APPENDIX G

List of Symbols and Summary of Equations

List of Symbols

A	constant in Equation (23)
A_c	cross sectional area of reinforcement at the end of service
A_c^*	statistical variable for A_c
b	width of strip-type reinforcement
C	time in years for zinc depletion from galvanized reinforcements
COV_Q	coefficient of variation for load bias
COV_R	coefficient of variation for resistance bias
CR	corrosion rate used in Equation (16)
D_i	initial diameter of bars/wires
D^*	diameter of bar or wire corrected for corrosion loss
E_c	strip thickness corrected for corrosion loss
$f_z(r_z)$	pdf representing zinc corrosion rates, r_z in Equation (18)
F_s	cumulative density function representing steel corrosion rates in Equation (18)
F_y	yield strength of steel
F_y^*	statistical variable for F_y
F_{ult}	ultimate strength of steel
F_{ult}^*	statistical variable for F_{ult}
g	random variable representing safety margin
K	coefficient of lateral earth pressure
k	constant in Equation (1)
n	exponent for Equation (1), or number of longitudinal wires in Equation (12)
$\mathrm{p_f}$	probability of occurrence (e.g., probability that yield stress will be exceeded before the end of intended service life)
P[X1|X2]	probability of X1 given X2 in Equation (18)
Q	random variable representing "measured or actual" load
Q_{ni}	nominal (i.e., computed) loads from sources that may include earth loads, surcharge loads, impact loads or live loads
Q_n	nominal load from single source
r_0	the lowest rate of zinc corrosion for which base steel will be consumed within t_f and is equal to z_i/t_f as used in Equation (18)

r_s	mean steel corrosion rate
r_{z1}	mean of the initial rate of zinc corrosion, i.e. until reaching t_1
r_{z2}	mean corrosion rate of zinc subsequent to t_1
r_z	mean zinc corrosion rate [used in Equation (18)]
R	random variable representing "measured or actual" resistance
R_n	nominal (i.e., computed) resistance
S	initial thickness of strip-type reinforcements
ΔS	loss of thickness due to corrosion
S_H	horizontal spacing of reinforcements
S_V	vertical spacing of reinforcements
t	time (years) in Equation (1)
t_1	time for which r_{z1} prevails, usually taken as 2 to 3 years
t_f	service life in years
t_{design}	design life used in Equations (17a) and (17b)
T_{max}	maximum reinforcement tension at a given level per unit width of wall
$T_{nominal}$	nominal tension/prestress applied to rock bolts during installation and used in Eq. (24)
T_{rem}	remaining tensile strength
x	loss of thickness per side or loss of radius as used in Equation (1)
X	loss of steel
X'	given amount of steel loss used in Equation (18)
z_i	initial thickness of zinc coating for galvanized reinforcements
β	reliability index
β_T	target reliability index
ϕ	resistance factor
γ_i	load factor for the ith load source as used in Equation (6)
γ_Q	load factor as used in Equations (21) and (22)
λ_{Ac}	bias of remaining cross section defined as the ratio of measured (actual) to nominal (computed) values
λ_{Fy}	bias of yield stress defined as the ratio of measured (actual) to nominal (computed) values
λ_R	resistance bias defined as the ratio of measured (actual) to nominal (computed) values
λ_Q	load bias defined as the ratio of measured (actual) to nominal (computed) values
ρ	resistivity of fill material
σ_H, σ_v	horizontal and vertical stress, respectively, at depth of interest in the reinforced zone
$\Delta\sigma_H$	supplemental factored horizontal pressure due to external surcharges
σ_s	standard deviation of steel corrosion rate as used in Equation (18)
σ_z	standard deviation of zinc corrosion rate as used in Equation (18)

Summary of Equations

Chapter 1—Background

Durability and Performance Issues for Earth Reinforcements

Romanoff (1957) proposed the following power law to predict rates of corrosion of buried metal elements:

$$x = kt^n \tag{1}$$

Darbin et al. (1988) and Elias (1990) proposed equations, having the same form as Equation (1), to estimate steel loss for plain steel and galvanized elements, respectively. These models are developed using measurements of corrosion from elements buried in fill representative of MSE construction. The following models apply to galvanized and plain steel reinforcements, respectively:

for galvanized elements

$$\begin{aligned} &\text{if } t_f > \left(\frac{z_i}{25}\right)^{1.54} \text{ then} \quad X(\mu\text{m}) = 50\left(\frac{\mu\text{m}}{yr}\right) \times t_f^{0.65}(yr) - 2 \times z_i(\mu\text{m}) \\ &\text{if } t_f \le \left(\frac{z_i}{25}\right)^{1.54} \text{ then} \quad X(\mu\text{m}) = 0 \end{aligned} \tag{2}$$

for plain steel elements

$$X(\mu\text{m}) = 80\frac{\mu\text{m}}{yr} \times t_f^{0.8} \tag{3}$$

For Equation (2) loss of base steel occurs subsequent to depletion of the zinc coating, and z_i is the initial zinc thickness. Equation (2) is applicable to the range of fill conditions representative of MSE wall construction that exhibit ρ_{min} greater than 1,000 Ω-cm. Data reviewed for Equation (3) are based on the NBS data set for plain steel and include a wider range of fill conditions.

Although corrosion rates for both galvanized and plain steel clearly vary exponentially with respect to time, a number of models (including the AASHTO model) approximate loss of steel using linear extrapolation for the purpose of design. Calibration of LRFD resistance factors for galvanized reinforcements assumes that the steel cross section is not consumed before the zinc coating, which serves as the sacrificial anode protecting the base steel. Since the zinc layers do not contribute to the tensile strength of the reinforcements, strength loss is also delayed until the zinc is consumed, and loss of steel section is described according to Equation (4). In general the thickness of steel, X, consumed per side over the design life, t_f, may be computed as

$$X(\mu\text{m}) = (t_f(yrs) - C(yrs)) \times r_s \frac{\mu\text{m}}{yr} \tag{4}$$

where C is the time for zinc depletion ($C = t_1 + \left(C = t_1 + \frac{(z_i - r_{z1} \times t_1)}{r_{z2}}\right)$, which is computed based on the initial zinc thickness, z_i, the initial corrosion rate for zinc, r_{z1}, the subsequent zinc corrosion rate, r_{z2}, and the duration for which r_{z1} prevails (t_1 – usually taken as 2 to 3 years). The corrosion rate of the base steel subsequent to zinc depletion is r_s.

Equation (5) is based on Equation (4) but uses the AASHTO model parameters where the steel loss per side (X) in μm/yr for a given service life, t_f, and initial thickness of zinc coating, z_i, is computed as

$$X(\mu\text{m}) = 12\frac{\mu\text{m}}{yr} \times \left(t_f - 2yr - \frac{(z_i - 30\,\mu\text{m})}{4\frac{\mu\text{m}}{yr}} \right) yr \tag{5}$$

Load and Resistance Factor Design (LRFD)

LRFD is a reliability-based design method by which loads and resistances are factored such that

$$\sum \gamma_i Q_{ni} \le \phi R_n \tag{6}$$

Load and resistance factors are applied such that the associated probability of the load exceeding the resistance is low. The limit state equation corresponding to Equation (6) is:

$$g(R,Q) = R - Q_i = \lambda_R R_n - \sum \lambda_{Qi} Q_{ni} > 0 \tag{7}$$

Chapter 2—Research Approach

Yield Limit State

Reinforcement loads are computed based on the horizontal stress carried by the reinforcements computed as

$$\sigma_H = K\sigma_v + \Delta\sigma_H \tag{8}$$

The maximum reinforcement tension per unit width of wall is computed from σ_H based on the vertical spacing of the reinforcements as

$$T_{\max} = \sigma_H S_V \tag{9}$$

Equations (8) and (9) describe the demand placed on the reinforcements, the capacity is the yield resistance of the reinforcements computed as

$$R = \frac{F_y A_c}{S_H} \tag{10}$$

for strip-type reinforcements

$$\begin{aligned} &A_c = bE_c \\ &E_c = (S - \Delta S) \text{ for } \Delta S < S, \text{ and 0 for } \Delta S \geq S \end{aligned} \tag{11}$$

and for steel grid-type reinforcements

$$A_c = n \times \pi \times \frac{D^{*2}}{4} \tag{12}$$

$$D^* = D_1 - \Delta S \text{ for } \Delta S < D_i, \text{ and 0 for } \Delta S \geq D_i$$

For galvanized reinforcements

$$\begin{aligned} &\Delta S = 2 \times r_s \times (t_f - C) \qquad \text{For } C < t_f \\ &\Delta S = 0 \qquad\qquad\qquad\quad \text{For } C \geq t_f \end{aligned} \tag{13a}$$

$$C = 2\,yrs + \frac{(z_i - 2 \times r_{z1})}{r_{z2}} \tag{13b}$$

For plain steel reinforcements

$$\Delta S = 2 \times r_s \times t_f \tag{14}$$

Using the statistics and observed distribution for measurements of corrosion rate, the bias of the remaining strength is computed and used as input for the reliability-based calibration of resistance factor. The bias is computed as

$$\lambda_R = \frac{F_y^* A_c^*}{F_y A_c} \tag{15}$$

Resistance Factor Calibration

The Monte Carlo analysis for calibration of resistance factor computes values for the limit state function, g = R − Q, considering the uncertainty of R and Q, and renders the probability that g <0. The variables R and Q can be related to nominal value as follows:

$Q = Q_n \times \lambda_Q$, and based on the LRFD equation [Equation 6],

$$R = \lambda_R \times R_n = \frac{\lambda_R \times \gamma_Q \times Q_n}{\phi}$$

Chapter 3—Findings and Applications

Trends

A power law was regressed to achieve the "best fit" with the data describing the relationship between corrosion rates and fill resistivity rendering the following equation, which is limited to galvanized reinforcements that are less than 20 years old:

$$CR \approx 1{,}400\rho^{-0.75} \tag{16}$$

Metal Loss Models and Reliability

Two different metal loss models for computing nominal sacrificial steel requirements with respect to marginal quality fills are studied to illustrate how this impacts the reliability of service life estimates. The first model (Model I) is from Jackura et al. (1987) for "neutral" fill and the second model (Model II) is a similar form, but with double the corrosion rate for steel as follows:

$$\text{Model I}: X(\mu\text{m}) = (t_{design} - 10)\, years \times 28 \frac{\mu\text{m}}{year} \tag{17a}$$

$$\text{Model II}: X(\mu\text{m}) = (t_{design} - 10)\, years \times 56 \frac{\mu\text{m}}{year} \tag{17b}$$

Verification of Monte Carlo Analysis

Sagues Formulation. Equation (18) was proposed by Sagues et al. (2000) to compute the probability that loss of base steel, *X,* from galvanized reinforcements exceeds a given threshold, *X′* as:

$$P[X > X' | t_f, z_i, r_z, \sigma_z, r_s, \sigma_s] = \int_{r_0}^{\infty} f_z(r_z)\left(1 - F_s\left((X')/(t_f - z_i/r_z)\right)\right) dr_z \tag{18}$$

For each value of *X* the bias of the remaining cross section (strip-type reinforcements) is computed as:

$$\lambda_{Ac} = \frac{(S - 2 \times X)}{[S - 2 \times 12 \times (t_f - C)]} \tag{19}$$

wherein the AASHTO metal loss model, Equation (5), is used in the denominator to compute nominal remaining cross section. A mean and standard deviation were determined from the distribution of the computed bias to describe the variation of λ_{Ac}. The bias of the remaining tensile strength was then computed as:

$$\lambda_R = \lambda_{Ac} \times \lambda_{Fy} \tag{20}$$

Closed-form Solutions for Reliability Index. For a specific limit state and a single load source, the reliability index (β) and the resistance factor (ϕ) can be related using the following formula (Allen et al., 2005), which assumes that the load and resistance bias both have normal distributions:

$$\beta = \frac{\left(\frac{\gamma_Q}{\phi_R}\right)\lambda_R - \lambda_Q}{\sqrt{\left(COV_R\left(\frac{\gamma_Q}{\phi_R}\right)\lambda_R\right)^2 + \left(COV_Q\lambda_Q\right)^2}} \tag{21}$$

In the case of lognormal distributions for load and resistance bias:

$$\beta = \frac{\ln\left[\frac{\gamma_Q\lambda_R}{\phi_R\lambda_Q}\sqrt{\left(1+COV_Q^2\right)/\left(1+COV_R^2\right)}\right]}{\sqrt{\ln\left[\left(1+COV_Q^2\right)\left(1+COV_R^2\right)\right]}} \tag{22}$$

For a given load factor, and known load and resistance statistics, Equations (21) and (22) are satisfied for selected values of resistance factor, rendering related pairs of reliability indices and resistance factors. From the computed pairs of β versus ϕ_R, resistance factors can be selected corresponding to the targeted level of reliability.

Type II—Condition Assessment

Rock Bolts

Metal loss of exposed portions of the reinforcement behind the anchor plate, or other areas, may be expressed using the Romanoff equation as

$$X\left(\frac{\mu m}{side}\right) = A\left(\frac{\mu m}{yr/side}\right)t^{0.8}\left(yr\right) \tag{23}$$

The resistance bias is computed as follows:

$$\lambda_R = \frac{F_{ult}^* A_c^*}{T_{nominal}} \tag{24}$$

$$A_c^* = \frac{\pi D^{*2}}{4} \tag{25}$$

$$D^{*2} = D_i - 2X^* \text{ for } 2X^* < D_i$$
$$D^{*2} = 0 \text{ for } 2X^* \geq D_i \tag{26}$$

Chapter 4—Conclusions and Recommendations

Recommended Resistance Factors for LRFD

The following equations are recommended to estimate nominal sacrificial steel requirements for plain steel reinforcements (i.e., not galvanized) for good and high quality fills:

$$\text{Good Quality Fill: } X\left(\frac{\mu m}{side}\right) = 80\frac{\mu m}{yr/side} \times t^{0.8}\left(yr\right) \tag{27}$$

$$\text{High Quality Fill: } X\left(\frac{\mu m}{side}\right) = 13\frac{\mu m}{yr/side} \times t\left(yr\right) \tag{28}$$

The following equation is recommended for computing nominal sacrificial steel requirements for galvanized reinforcements in marginal quality fills:

$$X\left(\frac{\mu m}{side}\right) = \left(t_f - 10\,yrs\right) \times 28\left(\frac{\mu m}{yr/side}\right) \tag{29}$$

Abbreviations and acronyms used without definitions in TRB publications:

AAAE	American Association of Airport Executives
AASHO	American Association of State Highway Officials
AASHTO	American Association of State Highway and Transportation Officials
ACI–NA	Airports Council International–North America
ACRP	Airport Cooperative Research Program
ADA	Americans with Disabilities Act
APTA	American Public Transportation Association
ASCE	American Society of Civil Engineers
ASME	American Society of Mechanical Engineers
ASTM	American Society for Testing and Materials
ATA	Air Transport Association
ATA	American Trucking Associations
CTAA	Community Transportation Association of America
CTBSSP	Commercial Truck and Bus Safety Synthesis Program
DHS	Department of Homeland Security
DOE	Department of Energy
EPA	Environmental Protection Agency
FAA	Federal Aviation Administration
FHWA	Federal Highway Administration
FMCSA	Federal Motor Carrier Safety Administration
FRA	Federal Railroad Administration
FTA	Federal Transit Administration
HMCRP	Hazardous Materials Cooperative Research Program
IEEE	Institute of Electrical and Electronics Engineers
ISTEA	Intermodal Surface Transportation Efficiency Act of 1991
ITE	Institute of Transportation Engineers
NASA	National Aeronautics and Space Administration
NASAO	National Association of State Aviation Officials
NCFRP	National Cooperative Freight Research Program
NCHRP	National Cooperative Highway Research Program
NHTSA	National Highway Traffic Safety Administration
NTSB	National Transportation Safety Board
PHMSA	Pipeline and Hazardous Materials Safety Administration
RITA	Research and Innovative Technology Administration
SAE	Society of Automotive Engineers
SAFETEA-LU	Safe, Accountable, Flexible, Efficient Transportation Equity Act: A Legacy for Users (2005)
TCRP	Transit Cooperative Research Program
TEA-21	Transportation Equity Act for the 21st Century (1998)
TRB	Transportation Research Board
TSA	Transportation Security Administration
U.S.DOT	United States Department of Transportation